# Impacts of Climate Change and Controlled Tile Drainage on Water Quality and Quantity in Southern Ontario, Canada

by
Karlen Hanke

A thesis
presented to the University of Waterloo
in fulfillment of the
thesis requirements for the degree of
Master of Science
in
Geography (Water)

Waterloo, Ontario, Canada, 2018

## Author's Declaration

I hereby declare that I am the sole author of this thesis. This is a true copy of the thesis, including any required final revisions, as accepted by my examiners. I understand that my thesis may be made electronically available to the public.

## Abstract

Within the Great Lakes region, agricultural non-point source nitrogen (N) and phosphorus (P) contamination contribute to algal blooms and decreased water quality, particularly from tile-drained landscapes. These water quality challenges are accompanied by anthropogenically induced increases in greenhouse gases within the atmosphere, which are leading to changes in climate, which may in turn exacerbate water quality issues by changing hydrological and biogeochemical cycling. This may be particularly important during the non-growing season (NGS), during which most of the annual nutrient export and flow occurs in the Great Lakes region. However, hydrologic and biogeochemical processes during the NGS are less well understood compared to the growing season. The implementation of beneficial management practices (BMP) such as controlled tile drainage (CD) have the potential to mitigate both current and future water quality issues. However, there is little information on the potential water quality tradeoffs associated with this particular practice under both contemporary and future climates. Such information is necessary before CD may be widely recommended and adopted as a BMP. In this thesis, the Soil Water Assessment Tool (SWAT) model was used to demonstrate the potential for CD to reduce nutrient losses in midwestern Ontario, under both current and future climates, and to understand the processes affecting nutrient export responses through the analyses of the water balance, flow regimes, and weather patterns, and to examine seasonal differences in these variables. In this study, two Soil Water Assessment Tool (SWAT) models were applied at varying scales. One was generated for the Medway Creek watershed, near London, ON, to understand the impact of climate change on water quality and quantity by forcing the model with a bias corrected general circulation model (GCM) ensemble. The second SWAT model was run at the field scale, for a field site near Londesborough, ON to understand the potential water quality tradeoffs associated with CD for a field with low-sloped clay loam soil. Results indicate that future changes in climate will cause shifts in seasonal water budgets, resulting in much greater nutrient export during the NGS and an overall increase in annual nutrient losses by the 2080-2100 period. These changes will be driven by precipitation quantity, but also changing precipitation characteristics (timing, form, magnitude, and frequency) and temperature, which will influence runoff pathways. The use of CD will not mitigate water quality issues and will instead exacerbate TP losses in runoff by increasing soil moisture and consequently increasing surface runoff. Although reductions of tile flow were greater than the simulated increases in surface runoff, the approximately 10X greater TP concentrations in surface runoff resulted in an overall increase in simulated edge-of-field TP losses. This will be particularly problematic where CD is used both during the NGS and growing season. This thesis has provided an improved understanding of the impacts of climate change on water quality in the MCW, and has demonstrated that CD has little potential to mitigate water quality issues in the present or future. This thesis has also demonstrated that understanding nutrient export processes during the NGS will be increasingly important for increasing BMP efficacy, reducing NPS contamination, and the occurrence of harmful algal blooms.

## Acknowledgements

This thesis was funded by the Quebec-Ontario Cooperation for Agri-Food research.

I would first like to acknowledge Dr. Merrin Macrae for the feedback and support she provided throughout my thesis. I am very thankful for her patience and extensive knowledge while I explored topics involving unaccustomed research methods, allowing me to further my career in the environmental field. Thank you to my committee members Dr. Nandita Basu, Dr. Aubert Michaud, and Dr. Derek Robinson for their valuable feedback on this thesis. Especially, Aubert, thank you for hosting me at your office in Quebec City, Nandita for your educative edits and invaluable experience, and both, thank you for keeping me on track and providing guidance throughout my thesis.

Then I would then like to thank Idhaya Chandhiran Ilampooranan and Dr. Mohamed Abu Niang for the intensive SWAT modeling support they provided throughout my thesis, and Craig Merkley from the UTRCA for his knowledge of the modelled watershed. Whenever I had questions they were very reliable sources an provided very helpful advice. In addition, I would like to thank Steph H. and James C. for their help with edits and the rest of my lab mates/friends for putting up with the modelling talk around the lab and in meetings.

Thank you to my parents Alex Hanke and Karen Coombs, and my girlfriend Sneha Sumanth; without their support and encouragement, this thesis would not have been possible.

Finally, we would acknowledge the World Climate Research Programme's Working Group on Coupled Modelling, which is responsible for CMIP, and we thank the climate modeling groups (listed in Table 2.1 of this paper) for producing and making available their model output. For CMIP the U.S. Department of Energy's Program for Climate Model Diagnosis and Intercomparison provides coordinating support and led development of software infrastructure in partnership with the Global Organization for Earth System Science Portals.

## Table of Contents

## List of Figures

## List of Tables

# Chapter 1 - Introduction and literature review

## 1.1 Introduction, problem statement, and objectives

Phosphorus (P) loading to surface water bodies is a major problem because algae and cyanobacteria in freshwater environments are growth limited by P. Consequently, elevated loads can lead to the eutrophication of lakes, which can lead to harmful algae blooms (HAB) (Heisler et al., 2008) that degrade ecosystem health, create hypoxic zones, (Diaz, 2001; Ludsin et al., 2013) and affect economies that rely on good water quality (Bingham et al., 2015). In Lake Erie, numerous HABs, have been related to eutrophication caused by non-point source (NPS) contamination from agricultural systems (Scavia et al., 2014).

Within the Great Lakes watershed, the majority of nutrients are currently exported in the non-growing season (NGS; Macrae et al., 2007b; Royer et al., 2006; Van Esbroeck et al., 2016; Williams et al., 2018). Therefore, an improved understanding during this period is necessary to help reduce NPS contamination. However, with increased greenhouse gas (GHG) levels in the atmosphere, it is anticipated that there will be an intensification of the climate, which will include increased precipitation, higher intensity precipitation, increased temperatures, and more heat waves (Grillakis et al., 2011; McDermid et al., 2015; Rudra et al., 2015; Wang et al., 2014, 2015b). The resulting shift in the seasonality in southern Ontario may modify the efficacy of current BMPs and exacerbate water quality issues (Bosch et al. 2014). To mitigate the impact of agriculture on nutrient export while maintaining productive crops, BMP recommendations are adjusted as the understanding of these systems is improved. An improved understanding of the timing of runoff and nutrient transfer, and the pathways through which runoff occurs, will assist managers in recommending BMPs that will work both now and in future.

Hydrologic and water quality modeling will be increasingly important for understanding how the seasonality and pathways of nutrient export will change under a warmer climate, enabling targeted watershed and field management plans. After a model is created, it can then be easily altered to predict environmental responses to emerging and current BMPs. To fully understand the impacts of climate change

and BMPs on water quantity and quality, it is imperative to run models at a range of scales. The need for this was demonstrated by Sloan et al. (2017), who demonstrated that both spatial scale and tile drainage distribution modified stream flow regimes. To assist watershed stewards and managers in recommending appropriate BMPs to reduce nutrient loads from watersheds, both now and in future, model simulations are required that will provide insight into potential changes in runoff patterns, nutrient loads and BMP efficacy. Therefore, the objectives of this thesis were to:

1) Use a watershed scale SWAT model to determine the effects of changing precipitation patterns and temperatures on seasonal and annual water balances, flow regimes, total phosphorus, nitrate, and sediment export from an agricultural watershed in southwestern Ontario, Canada.
2) Develop a field scale SWAT model to determine the effects that drainage water management will have on seasonal flow paths and phosphorus export from an agricultural field in southwestern Ontario.

Objective 1 was addressed in "Impacts of climate change on seasonal hydrology and nutrient and sediment loads in the Medway Creek watershed in southern Ontario" (Chapter 2 of this thesis), while objective 2 is addressed in "Controlled tile drainage impacts on field scale runoff pathways and phosphorus losses in southern Ontario" (Chapter 3 of this thesis).

## 1.2 Literature review

### 1.2.1 Agriculture non-point source contamination and its role in eutrophication

Eutrophication occurs when there is an overabundance of nutrients in an aquatic ecosystem. In agricultural systems, P and N application as inorganic fertilizers or manure is necessary for the growth of economically viable crops (Sharpley et al., 2001). Consequently, these sources are significant contributors of NPS contamination and eutrophication (Arbuckle and Downing, 2001; Michalak et al., 2013). Depending on the type of water body receiving nutrients, the limiting nutrient will be different. Within fresh water ecosystems, P is not abundant; therefore, algae growth is uninhibited as long as this nutrient is present.

Conversely, N is the limiting nutrient in more coastal ecosystems (Correll, 1998). Due to the issues in Lake Erie, recently an international agreement (Great Lakes Water Quality Agreement) has been made with the goal to reduce springtime P loads by 40 percent (from 2008 levels) by 2025 (IJC, 2012).

### 1.2.2 Nutrient forms and dominant pathways in agricultural landscapes

Within agricultural systems, nutrient export can vary between nearby watersheds and even fields due to complex interactions between many factors. Climate is one of the major factors influencing hydrological and nutrient export responses, and it drives the other processes occurring in environment. Furthermore, interactions among the landscape, soil characteristics, and management practices can influence hydrologic transport pathways and biogeochemical cycling of nutrients. For example, in agricultural landscapes where soils are slow to drain or receive frequent floods, tile drains are installed within the subsurface to facilitate soil water drainage. This management practice is common in agricultural fields throughout the Lake Erie watershed, particularly in the southwestern end. Tiles benefit crops through earlier planting in spring, excessive plant water stress prevention, improved soil structure, and trafficability (Fraser & Fleming, 2001). Conversely, in tile drained soils, nutrient loss can also be greater because of the enhanced connectivity to streams, increased by soil macropores (Simard et al., 2000; Molder et al., 2015), which are large soil pores created by biological activity, environmental stressors (desiccation and freezing process), plant roots. The following sections will describe the major factors influencing nutrient transport pathways, and the speciation differences between these pathways.

#### *1.2.2.1 Phosphorus dynamics in the environment*

In agricultural systems, P losses in runoff have traditionally been associated with surface runoff and the erosion of P-rich surface soils (Carpenter et al. 1998). However, tile drains have also been shown to increase P losses from fields (King et al., 2015). The potential for tile drains to enhance P loss in runoff has resulted in significant debate regarding the installation of tile drains in fields. This is particularly important in the Lake Erie watershed, where tile drainage has been identified as a major driver of P loss

(Jarvie et al., 2017). However, there is a need for balance between agronomic and environmental impacts as food security is also an important issue.

There are two main fractions of total phosphorus (TP), one is dissolved reactive phosphorus (DRP), which consists of phosphorus forms in solution and is bio-available to algae. Conversely, the other fraction particulate phosphorus (PP) is typically reported as anything greater than 0.45 µm, and not as great a concern because it is not bioavailable (Simard et al., 2000); however, it can become available dependent on the environmental conditions affecting bacterial decomposition and desorption/dissolution processes (Spivakov et al., 1999). Within these two fractions, P can be either inorganic (i.e. orthophosphate or cation bound P) or organic phosphorus (contains carbon and bio-unavailable), each with their own chemical characteristics affecting transport dynamics. A key difference is their interaction with the soil. Organic P tends to have less affinity for the soil solid phase (George et al., 2017) and adsorption to soil particles because orthophosphate can have greater sorption capacity and strength (Bolster & Sistani, 2009; Lilienfein et al., 2004). Furthermore, microbes within the soil increase the dissolved inorganic P pool through mineralization of the organic matter. Conversely, they can also temporally decrease the DRP pool through the assimilation (immobilized) into their cells (Spivakov et al., 1999). This DRP pool is strongly adsorbed to the oxides of clay mineral subsoils resulting in slow percolation through the soil matrix and accumulation (McDowell et al., 2001).

Generally, phosphorus export tends to increase during high stream flow events (Gentry et al. 2007). High flow events are typically a result of rainstorms, or snowmelt events, or both during the NGS, which contribute significantly to the annual water yield (Macrae et al., 2007b); consequently, supplying a large proportion of the annual TP and DRP export to streams (Macrae et al., 2007a; Puustinen et al., 2007; Van Esbroeck et al., 2016). Between events in the NGS, there is variability in the magnitude of peak flows and overall loads that can be greatly influenced by the antecedent soil moisture conditions (Macrae et al., 2010; Vidon et al., 2009) and precipitation event characteristics (Vidon & Cuadra, 2010, 2011).

##### *1.2.2.1.1 Phosphorus transport dynamics and forms in surface runoff*

As noted above, surface runoff has been identified as a primary pathway for P loss from fields. Within surface runoff, PP is the dominant P fraction (Gentry et al. 2007; Hart et al., 2004; Van Esbroeck et al., 2016), and is greatly influenced by soil erosion (Eghbal & Gilley, 2001). Therefore, the proportion of TP as PP and P associated with sediment (typically inorganic P) is affected by factors that control the adsorption capacity such as soil characteristics (texture, mineral content, and organic content) and changing environmental conditions (i.e. redox and pH; Boström et al., 1984; Li et al., 2017; Moazed et al., 2010; Spivakov et al., 1999; Xiao et al., 2017), and field slope/topography. However, this may not always be the case, as manure application can increase the amount of PP that is organic (Leytem et al., 2002).

In tile drained systems, surface runoff is generally decreased due to the amount of flow redistributed to tile drains (Muma et al., 2016), and this helps to decrease the TP loads leaving in runoff (Ball Coelho et al., 2012; Bengtson et al., 1995). However, this pathway can still account for a large proportion of annual P loads to streams, since TP concentrations are typically higher in surface runoff (Haygarth et al., 1998; Sharpley et al., 2001). Although P losses are usually reduced in a tiled setting, P transport risk can be increased in surface runoff due to the connectivity of the field to streams, precipitation intensity, variable source areas, and lack of BMPs such as nutrient management (4Rs) and soil erosion control practices (Chapi et al., 2015; Reid, et al., 2012; Sharpley et al., 1999, 2008, 2011; Van Esbroeck et al., 2017; Uusi-Kämppä et al., 1998). For example, nutrient management influences the amount of P that accumulates in the near soil surface (0-5 cm). Fields with high nutrient inputs will have a greater risk of transporting increased P in surface runoff (Sharpley et al., 2001), especially as DRP with inorganic nutrient applications (i.e. fertilizer) before rainfall (Haygarth et al., 1998). Furthermore, no-tillage, which maximizes crop residue and reduces soil erosion can cause a subsequent increase of DRP in surface runoff (Ulén et al., 2010).

##### *1.2.2.1.2 Phosphorus transport dynamics and forms in the subsurface: percolation and lateral movement*

In the subsurface, P can take two pathways to streams: groundwater flow and tile flow. Groundwater flow will occur in all systems, and the transport of water is slow due to the long residence time in soils, which enables the adsorption of P (Sharpley et al., 2014). Generally, in tile drained landscapes, the annual water yield will increase because tiles drain the water typically stored in the subsurface and increase the infiltration capacity (King et al., 2015). This causes increased P availability and a decrease in P residence times, making tiles the dominant lateral pathway for P in the subsurface.

Within a tiled landscape, soil properties can control the impact on stream flow responses, P export magnitudes, and speciation. Through tile drain installation, typically in natural ecosystems they increase peak runoff rates, and in existing agricultural landscapes may cause a decrease in peak flows (Blann et al., 2009). However, this is not always the case and it is believed that soil texture will play a key role. For example, in sandy soils peak flows will increase with tile installation due to greater seepage rates through the soil matrix, to tiles. While clay soils, the increased infiltration combined slower seepage rates to tiles will attenuate the higher magnitude surface runoff events and decrease peak flows (Robinson, 1990; Robinson & Rycroft, 1999; Skaggs et al., 1994; Sloan et al., 2017).

In addition to matrix flow, macropores are another flow pathway and can form in all soils, but clay is of particular concern because large and deep desiccation and freeze thaw cracks can form (Peron et al., 2009). Consequently, agricultural landscapes with clay soils and macropores can also have greater peak flows after tile installation (Robinson & Rycroft, 1999; Schwab et al., 1985). However, exact quantification of the connectivity is difficult (Luo et al., 2010) and peak flows are dependent on many other factors such as management practices, slopes, and climate (Skaggs et al., 1994; Sloan et al., 2017; Wiskow & Van Der Ploeg, 2003). In other soils (i.e. sandy), macropores do not have the same issue with surface connectivity, only earthworm passages and roots are likely, and these will not increase infiltration and percolation rates as substantially.

Generally, depending on the degree of connectivity, macropore flow can account for the majority of the contaminants initially transported through tile drains because of a precipitation event (Kung et al., 2000). Typically, this results in clay soils having greater P loads exported via tiles due to greater macropore connectivity , (Beauchemin et al., 1998; King et al., 2015), and in most cases PP will be the dominant form of P in drains due to the macropores direct connection of the surface to tiles (Vidon, & Cuadra, 2011; Simard et al., 2000). This suggests that macropores are present since greater DRP proportion would be expected with matrix flow. Sandy soils have been shown to have a larger proportion of TP as DRP in tile flow (Eastman et al., 2010). This can mostly be attributed to the soil texture and macropore characteristics, as more subsurface flow will be routed through the soil matrix, which also has a lower sorption capacity (Daly et al., 2001; Dils & Heathwaite, 1999; Fox & Kamprath, 1970).

In addition to soil factors, some management practices interact with the soil macropores to further influence the P export and flow response in tiles. For example, tillage that disrupts the soil surface (i.e. conventional tillage) has been shown to decrease macropore flow (Andreini & Steenhuis, 1990). Consequently, tillage that cause minimal disruption to the soil surface (i.e. no-till or conservation tillage) has been associated with higher TP loads in tiles (Geohring et al., 2001) and increased DRP loads in runoff (Gaynor & Findlay, 1995). Although this is the case, depending on climate and biological activity macropores can be quick to reform (weeks to months) after tillage resulting in not much difference in P loads annually (Djodjic et al., 2002).

Nutrient management is another major factor influencing P loss in tiles. Poor management practices (i.e. over application of fertilizer) in the past have resulted in an accumulation of P in soils (Daloğlu et al., 2012), which can increase the risk of P export if soil P thresholds are exceeded (Sharpley et al., 2001, 2014). This is defined as a limit within the soil where nutrient application resulting in soil levels above the limit will result in increased P contamination in runoff due to a decrease in the number of sorption sites. Furthermore, organic nutrient sources, such as manure, are associated with increased P loss, which has been attributed to a decreased sorption capacity and strength promoting increased P leaching (McDowell et al.,

2005). In addition, P loss in tiles generally increases with broadcast application, compared to incorporated application of P, depending on the source and degree of incorporation (King et al., 2015). However, irrespective of method or source, application rates have been shown to be the key driver of increased P loss in tiles (Kleinman et al., 2009; Elliott et al., 2001). Finally, the timing of application is increasingly important, as P export increases with precipitation after P application (Sharpley et al., 2001). Based on this, recently in Ontario, the province has embraced 4R Nutrient Stewardship, which stipulates right source, at the right rate, time, and place for proper management of nutrients to meet its environmental goals (Fertilizer Canada, 2016).

#### *1.2.2.2 Nitrogen dynamics in the environment*

Although P contamination is of foremost concern in Ontario, N contamination is also an issue that can have an adverse effect on the environment and even human health. N is a major nutrient applied to fields for proper plant growth. Consequently, within tile-drained settings, N has been shown to be a major factor contributing to an increase in both surface and groundwater contamination (Bengtson et al. 1984; Randall et al., 1997). This has potential to affect 30% of people in Ontario that rely on groundwater for drinking water (Goss et al., 1998) and many others that rely on clean water since it can also increase algae growth, especially in marine environments. In southern Ontario, nitrate ($NO_3^-$; plant available) leaching is the form of N of principal concern, especially for young infants because they are at increased risk of methemoglobinemia with augmented concentrations of $NO_3^-$ and nitrite ($NO_2^-$). These forms can naturally occur through ammonification of organic nitrogen to ammonium ($NH_4^+$) or ammonia ($NH_3$), or nitrogen fixation (i.e. gaseous nitrogen to $NH_3$ or $NH_4^+$), and subsequent nitrification. Furthermore, high concentrations of $NO_3^-$ and $NH_4^+$ in surface water has been linked with fish kills, and development anomalies in amphibians (Steenvoorden et al., 2002).

##### *1.2.2.2.1 Nitrogen transport in the subsurface*

Nitrate originates from manure, the mineralization and nitrification of organic matter, or inorganic fertilizers. Unlike orthophosphate and $NH_4^+$, it is much more mobile in the subsurface because it is an anion

and thus not attracted to negatively charged soil particles. This allows $NO_3^-$ to quickly travel through the soil matrix into tiles, which can contribute a large proportion of the annual runoff and N loads (Li et al., 2010; Rozemeijer et al., 2010). Tiles also decrease water residence times; further decreasing the opportunity for denitrification benefits (Panno et al., 2008). However, like P, most of the N export also occurs with flows that are part of the high stream flow regime (Petry et al., 2002; Macrae et al., 2007b).

In addition to tile flow, the texture of the soil also controls the intensity of leaching through the subsurface into tiles and groundwater. The transport of $NO_3^-$ is related to water volumes; therefore, clay soils will have reduced leaching through the soil matrix since they have a lower saturated hydraulic conductivity, greater water retention, and cation exchange capacity (Gaines & Gaines, 2008; Miner 1995). Conversely, the increase in macropores in fine-grained soils mentioned earlier also has potential to help to offset slower soil matrix leaching rates and can increase particulate associated N losses (Rasouli et al., 2014). The amount of residual soil nitrogen left in soil will be important factor contributing to the magnitude of $NO_3^-$ export. This is influenced by many components, including atmospheric N deposition, N management practices (source, rate, time, and place), crop residue, and cropping system (Rasouli et al., 2014). For example, corn is a large portion of the crop acreage in Ontario and requires high N inputs (up to 316 kg N/ha) for growth (Ministry of Agriculture and Rural Affairs, 2017). Consequently, this crop in continuous rotation is known to cause increased N leaching due to a buildup of residual soil nitrogen each year (Bolton et al., 1970; Fleming et al., 1998). This build up can contribute to a reduction in the observed effectiveness of BMPs due to the effect of legacy N (Van Meter et al., 2018). Additionally, climate variability between years will play a role in controlling the annual N loads in tiles and can cause large fluctuations. In dryer years, more N is stored in the soil profile, which can be flushed during subsequent wetter years (97 cm above the historic 30-year average; Gentry et al., 2009). Finally, once $NO_3^-$ leaches past the tiles it contributes to the groundwater, which has been shown to store a large proportion of the N inputs (Wang et al., 2015a), especially in aquifers with long residence times. Furthermore, $NO_3^-$ concentrations can be lower in groundwater because of denitrification, which occurs when soil conditions

are anaerobic causing microbes to respire forms of nitrogen bound with oxygen to produce dinitrogen (Petry et al., 2002).

##### *1.2.2.2.2 Nitrogen dynamics in surface runoff*

While tile drains export more N than surface runoff, losses in this pathway are still of concern. Runoff N loads and concentrations can quickly increase over a short period given the correct conditions, such as connectivity, manure application on frozen soils, timing of nutrient application, and intense rain (Neilsen et al., 1978; Smith et al., 2001). As previously mentioned $NO_3^-$ is more mobile and soluble in water. Therefore, after the start of a rainfall event most of the $NO_3^-$ will infiltrate in to the soil; consequently, the dominant form of N remaining in the soil surface and in surface runoff is typically ammonium or organic N (Sharpley et al., 1987). Although, there are some cases where $NO_3^-$ can be a greater contributor in surface runoff (Jiao et al., 2012). In addition, $NH_4^+$ in the environment is mainly a result of the decomposition and mineralization of organic matter originating from crop residue or manure applications. $NH_4^+$ readily travels with sediment and is less prone to leaching due to its positive charge binding it with the fine-grained sediments or organic matter, and this results in $NH_4^+$ typically being mobilized during storm events and associated with surface runoff (Pärn et al., 2012).

## 1.3 Climate change and agriculture

Through human activities such as farming, energy generation, and transportation there has been a steady increase in greenhouse gas (GHG) concentrations in the atmosphere, which consist of three main gases: methane, carbon dioxide, and nitrous oxide (Intergovernmental Panel on Climate Change, 2015). As these GHG accumulate in the atmosphere, they increase the amount of incoming long-wave solar radiation retained within the earth's atmosphere, increasing global mean air temperature and changing precipitation patterns (Intergovernmental Panel on Climate Change, 2015). Furthermore, through various terrestrial and aquatic feedback mechanisms that can be either positive (increase in GHG) or negative, the rate of GHG concentration increase will be modified. Climate change has already had wide reaching impacts on human

and natural systems, and is projected to cause irreversible harm unless it is properly mitigated (Intergovernmental Panel on Climate Change, 2015).

General Circulation Models (GCM) are numerical models capable of forecasting the effects that changes in GHG concentrations have on the global climate system. GCMs are a useful tool for understanding climate responses to GHGs and allow us to better mitigate and adapt; however, there are some key sources of uncertainty to consider. First, future changes in global anthropogenic GHG emissions are unpredictable. Second, knowledge and predictability of system feed backs (natural emissions) in GCMs is still not perfect. Third, the downscaling and bias correction approach used to create regional climate models for smaller scale impact studies results in further uncertainty due to the assumptions made and all contribute to a cascade of uncertainty in climate change projections (Giorgi, 2010). Despite these challenges, the array of GCM simulations provide a reasonable way to reduce uncertainty and simulate future changes in climate.

### 1.3.1 Climate change in southern Ontario

Recently, Representative Concentration Pathways (RCP) were developed to describe plausible trajectories for net radiative forcing by the year 2100 relative to preindustrial conditions (Taylor, 2012). Each of the four emission scenarios range from best case (RCP2.6) to high emissions (RCP8.5), with two intermediate scenarios (RCP4.5 and RCP6). Within southern Ontario, all pathways indicate an increase in annual precipitation from 2040 onward, with the average annual precipitation increase varying from 99 to 123 mm by the 2080s in all RCPs. Furthermore, there will be clear increases in the average annual air temperature in all of the RCPs, and changes will range from 2.4 to 9 degrees Celsius by the 2080s (McDermid et al., 2015). In addition, there will be an increase in the magnitude and frequency of extreme precipitation events (Rudra et al., 2015; Wang et al., 2014, 2015b). This is expected to be coupled with an increase in the percent of time there will be extremely wet and then dry conditions (Grillakis et al., 2011).

This will affect seasonal climate characteristics. Based on the study by King et al. (2012) in the Upper Thames River Basin (UTRB), winter and spring will have definitive increases in precipitation volumes, while in summer there will be a bit more variability associated in percent change in precipitation, with ranges of -14.5 to 28.8 percent by the 2041 to 2070 period. High variability in summer for precipitation is mostly likely due to the GCMs limitations associated with capturing convective summer storms (Maraun, 2016). In winter, temperature changes will be the greatest and are projected to increase by 3.5 to 8.6 degrees Celsius on average by the 2080s (McDermid et al., 2015). Due to this increase in temperature in winter, more precipitation is expected as rain (Marianne et al., 2003; Golmohammadi et al., 2017); also reducing the snowpack melt and timing in spring (Demaria et al., 2016). In summer, in addition to increased temperatures, there is expected to be increased frequency and magnitude of heat waves (Li et al., 2017), which will mostly likely result in greater drought risk.

### 1.3.2 Climate change effects on NPS contamination

In southern Ontario, agriculture is a major driver of the economy and many jobs rely on its prosperity. In order to understand the long-term impacts that climate change will have on crop yield, water quality and quantity at a more local scale GCMs outputs are typically bias corrected and downscaled to be used as input with models (Carter et al., 1994). Through a better understanding, mitigation strategies can be developed to help adapt to the changes. Currently, in the Great lakes drainage area, most studies indicate that increased precipitation will lead to increases in the annual flow (Grillakis et al., 2011; Rahman et al., 2012), resulting in increased TP, SS, and $NO_3^-$ loads (Bosch et al., 2014; Verma et al., 2015; Wang et al., 2018) by the late-century (2070-2100). With some mid-century (approximately 2020 to 2050) projections, indicating a decrease in precipitation will result in decreased annual flows (Golmohammadi et al., 2017; Verma et al., 2015). Contrary to this, one study has projected decreased flows and variable sediment load changes in the late century period with increased precipitation depending on the emission scenario and evapotranspiration rates (Cousino et al., 2015).

In southern Ontario, we know that the majority of nutrient loads are exported during peak flows and in the NGS (Macrae et al., 2007b; Royer et al., 2006; Van Esbroeck et al., 2016). Therefore, understanding the impact of climate change during the months in the NGS will be important in reducing NPS contamination. Due to the changes in climate characteristics noted earlier and expected in winter, we will start to see less snowpack in the Great Lake basin. This in turn will affect soil temperatures, which will get colder due to the insulating properties of snow (Isard et al., 1998). With the changes in snowpack, soil temperatures, soil moisture, and precipitation form and intensity there will potentially be a shift or increase in dominant flow path that runoff takes to streams. With increased potential for frozen soils, it is hypothesized that there will be more surface runoff in winter due to the decreased capability of infiltration (Marianne et al., 2003; Isard et al., 1998).

Some studies in the Great lake watershed, predict increased flows, TP, sediment, and $NO_3^-$ export during the NGS months due to climatic shifts (Crossman et al., 2013; Verma et al. 2015; Wang et al., 2018). Rahman et al. (2012) corroborate this hydrologic change for a watershed in southern Ontario and show that winter and spring flows increase along with surface runoff and base flow. Furthermore, in a study by Jyrkama et al., 2007 for southern Ontario they show infiltration and recharge to increase due to warming soil and air temperatures, reducing early spring runoff. This is indicative of the potential for spatial variability of NGS hydrology and the potential for unexpected flow path changes. Therefore, understanding of the soil freezing dynamics and climate behavior in different regions with different methods will be import in quantifying the impact that climate change has on flow path partitioning, flow regimes, and subsequent nutrient transport forms and magnitude, especially in tile-drained landscapes due to the connectivity they provide in the subsurface. Finally, with the climate intensification resulting in more erratic temperatures there will be an increase in the freeze-thaw cycles, which is factor controlling nutrient losses from crops, soil structure (increase in macropores), and microbial communities that should start to be considered in future studies (Henry, 2008).

## 1.4 Controlled tile drainage

In the past few sections there have been indications of the detrimental effects and complexity involved with tile drained systems. Due to the issues associated with hypoxia in the Gulf of Mexico, in the Midwest US controlled tile drainage (CD) has been recommended as a practice to reduce nitrate leaving in tile drains and entering the Mississippi river. CD involves the installation of a control structure at the tile outlets where inside a gate can be raised or lowered to control the water table height by forcing water to rise above the gate before leaving the tile outlet. Typically, CD installation is limited and more suitable to low sloped areas (<1%) that are slow to drain.

Due to the significance of the NGS recent research has focused on CD during this time and found that it will reduce nutrient loads (N and P) in tile drains through flow reductions (Skaggs et al., 2012; Sunohara et al., 2010; Williams et al., 2015). Also, in some cases increases denitrification causing further N reductions (Skaggs et al., 2010; Wesström & Messing, 2007). Although this benefits tile reductions, there is very little understanding of the tradeoffs associated with CD, like increased surface runoff and nutrient (N and P) export in runoff (Drury et al., 2009; Ross et al., 2016; Tan & Zhang 2011; Zhang et al., 2017). Also, increased potential for anoxic condition promoting soluble P forms through increased potential for desorption and organic P mineralization (Ardón et al., 2010; Van Dijk et al., 2011; Yaghi & Hartikainen, 2013). For it to be extensively accepted as a BMP by managers in southern Ontario there needs to be more research related to the tradeoffs and the potential to function outside the typical criteria for certain field conditions.

Although the growing season (GS) is not as significant a season in terms of its contributions to nutrient transport, it contributes to plant growth, which may be impacted under a changing climate. For example, in spring, with less snowpack and snowmelt due to the shift in seasonality, farmers will be able to access fields earlier, resulting in a longer growing season and accelerated maturation due to increased $CO_2$ and temperatures. However, increased soil moisture stress may occur, which can have a detrimental effect on crop yields (Singh et al., 1998). To mitigate the effects that water stress has on crop yields recently

drainage water management has also been studied and shown to provide benefits during the GS (Sunohara et al., 2010).

## 1.5 Hydrological and NPS contamination modeling

### 1.5.1 Quantifying the effect of climate change and agriculture on water quality

As previously mentioned, numerous anthropogenic environment changes have resulted in water quality problems and these now require improved management and planning to help reduce the impact of their sources. Typically, experimental and observational field to watershed scale studies have been used to provide this; however, they require significant time, effort, and resources to obtain results. This makes modeling a useful tool in understanding agricultural systems across a range of scales and realities due to the ability to alter the simulated environment. However, to be successful, modelling efforts require field studies for proper development, making both approaches highly integrated and dependent on each other to develop proper mitigation strategies (Vadas et al., 2013).

Given the usefulness of models, numerous models have been created. These are typically described according to criteria found in the study by Tsakiris and Alexakis (2012). Model selection is determined by the purpose of the study, region characteristics (stressors and processes), data availability, time-step, and scale of analysis. Careful selection is necessary since there are many models that are able to simulate P in drains and NPS contamination, each with their own capabilities (Gao & Li, 2014; Qi & Qi, 2017; Tsakiris & Alexakis, 2012; Vadas et al., 2013). One frequently used model is the Soil Water Assessment Tool (SWAT), which has over 3350 peer-reviewed articles (https://www.card.iastate.edu/swat_articles/index.aspx). In agricultural landscapes, this model is frequently used in BMP and climate change impact assessments in the Great Lakes area (Ahmadi et al., 2014; Bosch et al., 2014; Liu et al., 2016; Robertson et al., 2016; Rahman et al., 2012; Wallace et al., 2017). This is a semi-distributed, process and empirically based watershed scale eco-hydrological model. The smallest spatial unit within SWAT is the HRU, which is not spatially referenced and is a unique combination of soil, slope and land use within a subbasin, each having a set of associated management practices. Precipitation

and temperature inputs drive landscape processes at the HRU scale, these are aggregated to the subbasin, then watershed scale. Outputs from the landscape are used to drive channel process, which determine outputs at the watershed outlet (Neitsch et al., 2011). As a result, in SWAT there is a large number of parameters, which first require calibration to observed conditions (i.e. stream flow), and validation to confirm the calibrated parameter set for a different set of observed conditions (Arnold et al., 2012b; Daggupati et al., 2015).

### 1.5.2 Model development and assessment

There is a constant need to redevelop SWAT to reduce the uncertainty in model predictions and improve performance to make policy decisions more reliable since they are made at the watershed scale (Beven, 2001). Experimental and observational studies are useful for identifying model limitations and improving the model through increased understanding of the small-scale processes. Since process are simulated in the HRU and scaled up, good performance starts here. However, during model building there are some inherent issues that complicate spatial consistency of HRUs, making it harder to analyze HRU outputs, confidently recommend model improvements, or inform decisions in the modeled area, especially if there is a lack of field scale data in the watershed to validate HRU processes.

A key issue affecting HRU consistency is equifinality, where a calibrated model can have multiple acceptable parameter sets, some causing the right results but for the wrong reasons (Beven & Binley 1992; Beven, 2006). Given that SWAT typically operates on a watershed scale, there is increased spatial heterogeneity in watershed properties and complex processes, which exacerbates this issue. Watershed scale models such as SWAT attempt to capture this increased complexity through the number of parameters; thereby enhancing the potential for equifinality (McDonnell et al., 2007). Calibration at the HRU scale using field scale hydrometric data is not frequently done, but permits the evaluation and testing of new model routines, which subsequently leads to model improvement, because testing the model at a small HRU scale removes the complications of large-scale heterogeneities.

This thesis uses SWAT models under present and future climate simulations, and at different scales to predict the impacts of climate change on nutrient transport from agricultural landscapes, and, to determine whether CD can mitigate some of these water quality issues. In addition to exploring changes in annual hydrologic and biogeochemical fluxes, this thesis investigates seasonality in these fluxes due to the importance of the NGS in nutrient export and our limited understanding of process during this time.

# Chapter 2 - Impacts of climate change on seasonal hydrology, nutrient, and sediment loads in the Medway Creek watershed in southern Ontario

## 2.1 Overview

Within southern Ontario, climate change is expected to cause an increase in precipitation patterns and air temperature by the late century period (2080-2100). This is expected to cause changes to hydrological and biogeochemical cycling, further impacting losses from agricultural fields, which are currently a significant driver of non-point source contamination in Lake Erie. In this study a model was created using the Soil Water Assessment Tool (SWAT) for the Medway Creek watershed (200 $Km^2$), a subwatershed within the Upper Thames River Watershed in Ontario, Canada, within the Lake Erie watershed. The objective of this chapter is to determine the effect that future climates will have on the seasonal characteristics of hydrology, suspended sediment, nitrate, and total phosphorus export. A climate ensemble was used to force the SWAT model, which consisted of six different quantile bias corrected general circulation models (GCM) obtained from the Coupled Model Intercomparison Project Phase 5 (CMIP5) using the 4.5, 8.5, or both representative concentration pathways (RCP). The climate ensemble indicates that temperate and precipitation quantity, magnitude and frequency will increase in all seasons, with the largest and least variable climatic changes projected to occur in winter. These shifts will cause a shift in the seasonal distributions of runoff and the relative contributions of flow paths. An increase in annual nutrient (N, P) loads is projected, driven not only by changing precipitation volumes but form, magnitude, and frequency, which will increase peak flows. In contrast, suspended sediment is mostly driven by changing average stream flows and surface runoff, which decrease in winter and spring due to changes in the seasonal water balance due to increased air temperatures. This work highlights the importance of understanding processes driving non-growing season (NGS) nutrient export with climate change in a tile-drained setting, and will assist land managers in the development of more effective watershed management plans.

## 2.2 Introduction

The eutrophication of inland lakes is a significant issue throughout North America that has environmental and societal consequences (Michalak et al., 2013). The occurrence of frequent Harmful Algal Blooms (HABs) and nuisance algae have been attributed primarily to non-point source pollution from agricultural watersheds, with particular emphasis on total phosphorus (TP) loading (EPA, 2015; Jarvie et al., 2013; Michalak et al., 2013). Consequently, considerable effort has been put into the development of Beneficial Management Practices (BMPs) and aggressive targets have been set for reductions in TP loads from agricultural systems. In addition, within the Great Lakes region of North America, climate change is expected to lead to higher temperatures and changes in the form, intensity, quantity, and timing of precipitation (McDermid et al., 2015; Rudra et al., 2015; Wang et al., 2014). This is anticipated to have consequences for hydrology through the modification of runoff pathways, quantity, and timing, and consequently, biogeochemical export from agricultural watersheds. To better understand BMP efficacy and the potential for current nutrient reduction targets to be met, an improved understanding of the impacts of climate change on runoff quantity and quality are needed.

Tile drainage is a BMP that is prevalent throughout much of southwestern Ontario. This flow pathway increases subsurface connection between fields and streams, reducing surface runoff and increasing the proportion of precipitation leaving as subsurface flow (Muma et al., 2016). Consequently, tile drainage reduces the contribution of surface runoff to annual TP, organic nitrogen, ammonium ($NH_4^+$), and suspended sediment (SS) loads (King et al., 2015, and Skaggs et al., 1994). Although surface runoff can be reduced following the installation of tile drains (Muma et al., 2016), this pathway can still provide an efficient transport mechanism for nitrate ($NO_3$) and P depending on soil characteristics such as slope and macroporosity (e.g. Kleinman et al., 2015), soil biogeochemistry (Plach et al., in press), land management practices such as nutrient management, tillage and P application strategies (e.g. Lam et al., 2016; Jarvie et al., 2017; Plach et al., 2018), and precipitation event duration, and intensity (Sharpley et al., 2008; Van Esbroeck et al., 2017; Chapi et al., 2015; Reid, et al., 2012; Vidon & Cuadra, 2010).

In southwestern Ontario, Canada, most nutrient export currently occurs during the NGS where contributions to annual loads from agricultural systems are often dominated by a few peak flow events (Ministry of the Environment and Climate Change, 2012; Macrae et al., 2007b, Van Esbroeck et al., 2016, 2017). Additionally, the timing and form of precipitation events influence antecedent hydrologic conditions (AHC), which play a key role in determining the nutrient form (Beauchemin et al., 1998), event response, and overall loads (Macrae et al., 2010; Vidon et al., 2009), in part due to their control over hydrologic flow paths (Van Esbroeck et al., 2017; Macrae et al., 2007a). Given the current behavior and projections for an intensification of the hydrologic cycle under a warmer climate (Wang et al., 2014), it is likely that the temporal distribution of runoff and the relative contributions of different hydrologic flow paths may change, which may impact nutrient loading from agricultural watersheds. Therefore, studies at the watershed scale that include the seasonal fluctuations in hydrology are needed to produce more accurate estimates of the impacts of agricultural land management on water quantity and quality (Labeau et al., 2015).

Field scale process studies are often costly and labor-intensive, and there is a paucity of long-term data sets, particularly those that include the NGS. To shed insight into longer time periods and the future, scientists employ hydrological and water quality models forced with general circulation models (GCM); however, careful parameterization, calibration and validation of the models using high-quality field data is crucial. The Soil Water Assessment Tool (SWAT) is frequently used around the world in agricultural watersheds to predict the impact of climate change on water quality (Marcinkowski et al., 2017; Mehdi et al., 2016; Woznicki & Nejadhashemi, 2012; Ye & Grimm, 2013; Zabaleta et al., 2014). Although this model was developed in a warm, dry region (Neitsch et al., 2011), it has been calibrated successfully in more northern regions with complex agricultural practices and hydro-climatic conditions to assess water quality issues associated with climate change (Gombault et al., 2015; El-khoury et al., 2015; Mehdi et al., 2015; Shrestha & Wang, 2018). However, to date, there have been few detailed modeling studies focusing on providing a better understanding of how future precipitation characteristics and temperature changes will influence flows, water balance, and water quality responses within the Great lakes region, particularly over

the different seasons (Ahmadi et al., 2014; Bosch et al., 2014; Robertson et al., 2016; Rahman et al., 2012; Wallace et al., 2017). Therefore, in this study, the objectives were to predict how climate change will affect the water balance, flow regimes, sediment, and nutrient loads in the Medway Creek Watershed (MCW) using the SWAT model at the (a) annual scale and (b) seasonal scale (Cousino et al., 2015; Crossman et al., 2013; Verma et al., 2015; Wang et al., 2018). Results from this study will assist other modelling efforts, watershed stewards, and managers in identifying suitable nutrient loss mitigation strategies, and will shed insight into the current potential to achieve nutrient reduction targets that have been set for the MCW through model simulations using future climates.

## 2.3 Methodology

### 2.3.1 Study area

The MCW is a small (205 $Km^2$) watershed located in southwestern Ontario (43°00'52.9"N 81°16'36.6"W; Figure 1) and is one of 28 sub-watersheds that contribute to the Upper Thames River Basin (UTRB), which subsequently drains into Lake St. Claire, and eventually into Lake Erie. Managers and landowners within the Thames River watershed have been tasked with achieving a springtime P load reduction of 40% by 2025 (Environmental Protection Agency, 2015).

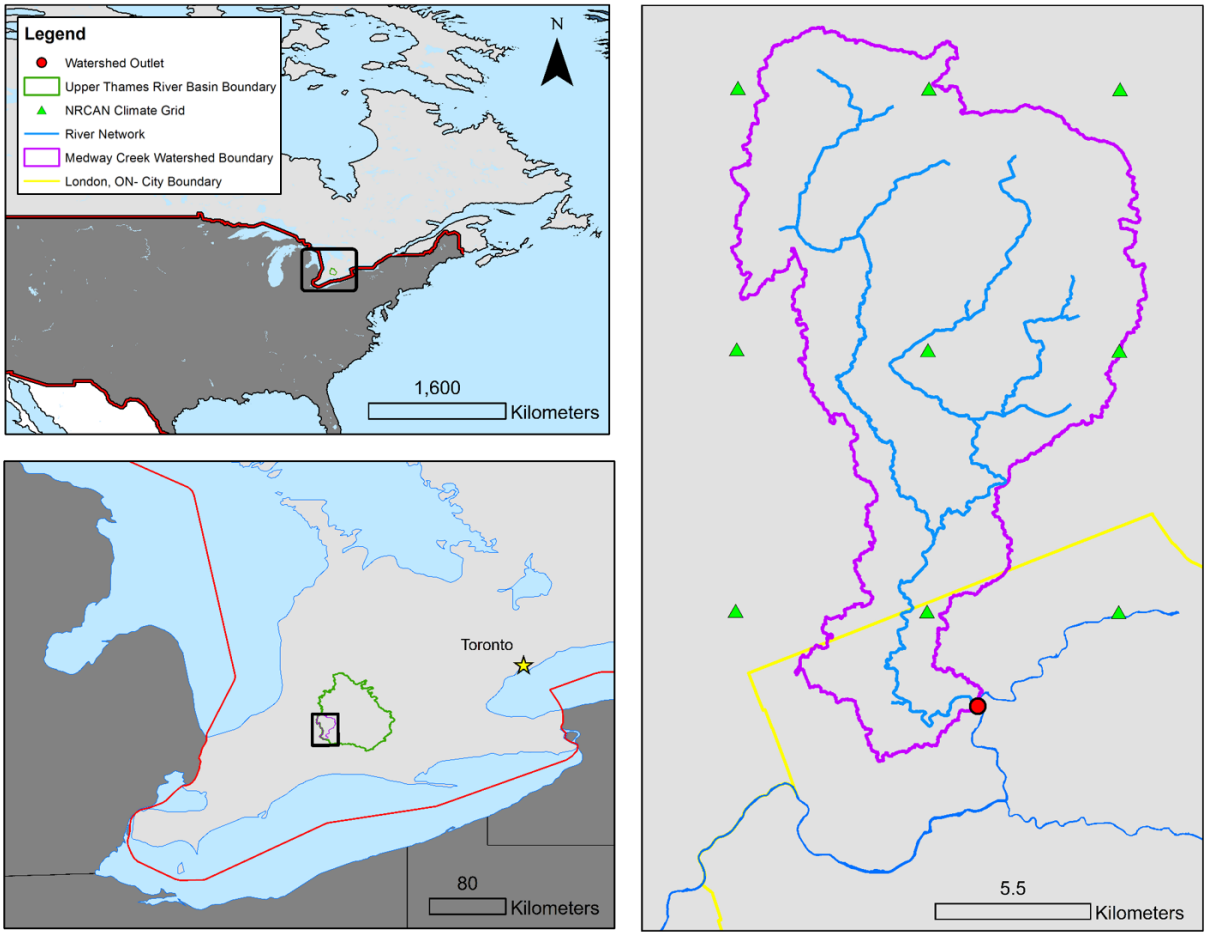


*Figure 2.1.* Location of the MCW in Canada. With the distribution of the climate station grid (green) and area inside London city limits (yellow).

Land use within the watershed is primarily agricultural (83%), with some natural (11%) and urban (6%) areas. Since most of the land use is agricultural, a significant portion of the MCW has tile drainage (~ 65%) to facilitate field access in spring and improve crop yields. Major agricultural land uses within the watershed consist of corn, pasture, soybean, and winter wheat. There are many livestock operations within the watershed with an average density of 24 animals per hectare. Poultry represent the majority of livestock operations (97%) and manure P production in the watershed (31%), and swine operations represent 1% of livestock operations. Populations of dairy and beef cattle are relatively small in the watershed. Approximately 85% of the total soil area within the watershed consists of clay loam (33%), silty loam (32%), or silty clay loams (20%) (Upper Thames River Conservation Authority, 2012). The watershed has a mean slope of 2 degrees, with the northwestern part of the watershed increasingly sloped because the

watercourse is located between two moraines causing rolling topography. The southern portion of the watershed is also steep and mostly consists of urban land use, whereas the central portion is much flatter.

The climate in this region is classified as humid continental with an average 30-year historic normal monthly precipitation of 84 mm (1012 mm annually, 19% as snowfall; Environment and Climate Change Canada, 2018b). As is typical for the region of southern Ontario, there is a distinct seasonal pattern in annual runoff with maxima in spring associated with snowmelt and convective spring storms, and minima in summer due to high evapotranspiration (ET) rates. Although flow occurs throughout the year, the summer high average temperatures (19.6 ˚C) can occasionally result in the occurrence of drought conditions (Prodanovi & Simonovi, 2006).

### 2.3.2 Watershed modelling

#### *2.3.2.1 The Soil Water Assessment Tool*

SWAT is a semi-distributed physically based watershed model capable of continuous simulation over long periods (Neitsch et al., 2011). It uses a combination of empirical relationships and process-based equations. The user divides the watershed up into sub-basins, which can be further subdivided into hydrological response units (HRUs) which are unique combinations of land use, soils, and slope (Neitsch et al., 2011 ). Within the model structure, precipitation plays a key role and is a major driver of all other processes that occur. Hydrologic processes simulated by SWAT include surface runoff, infiltration, canopy storage, percolation, evapotranspiration (Hardgreves method; IPET=2), lateral subsurface flow, and base flow (Arnold et al., 2012a). Soil erosion is determined using the Modified Universal Soil Loss Equation (Williams 1975) which is influenced by rainfall and surface runoff, and estimated using the Soil Conservation Service (SCS) curve number method (Soil Conservation Service, 1972; ICN=1). Within the soil profile, the SWAT model is able to simulate nutrient transformations and movement using the P and nitrogen cycles. Once the nutrients reach the main hydrological channel, an adapted version of QUAL2E is used for nutrient routing (Neitsch et al., 2011).

Given that the SWAT model was developed in Texas, percolation through the soil profile is not as representative of what occurs in Canada, where soil textures, moisture conditions and precipitation patterns differ from those in Texas. Therefore, SWAT-MAC was used (modified version of SWAT 2012), as it is adapted to better simulate flow to tile drains by altering the hydrological algorithms influencing percolation through the subsurface (Michaud et al., 2008; Poon, 2013).

#### *2.3.2.2 Data used in model parameterization*

A DEM (10 m resolution) supplied by the Upper Thames River Conservation Authority (UTRCA) and derived using aerial imagery from the Southwestern Ontario Orthophotography Project (SWOOP) in 2010 was used (Ministry of Natural Resources and Forestry, 2015). Land use data was obtained from Agriculture and Agri-Food Canada's (AAFC) annual crop inventory in 2014 (AAFC, 2016). These data are derived using satellite imagery taken during important plant growth stages and combined with ground truthing to identify crops present each year. Soil physical parameters, at a scale of 1:50000 were obtained from the soil map distributed through Land Information Ontario (LIO; Ministry of Agriculture, Food and Rural Affairs & Canadian Soil Information Service, 2015). This included soil texture, bulk density, soil depths, but did not include data for soil available water capacity or soil albedo. Soil available water capacity was estimated using the pedotransfer function developed by Saxton and Rawls (2006). Soil albedo was estimated using the ranges mentioned by Dobos (2003). Climate data, including gridded (10 km resolution) daily precipitation and daily maximum and minimum temperatures for 63 years (1950-2013) was generated by Natural Resources Canada (NRCAN) using thin-plate smoothing splines (McKenney et al., 2011; McKenney et al., 2013) and was provided by Ouranos, a consortium on regional climatology and adaptation to climate change.

Streamflow quantity (daily interval) and quality (monthly sampling interval) data for the MCW, collected between 1978-2014 at the watershed outlet, were provided by the UTRCA (Figure 1). Monthly load estimates of sediment and nutrients (TP, $NO_3^-$) were determined using Flux32 and a regression applied to individual daily flows (Method 6) based on the procedure developed by Walker (1996). The mean

coefficient of variation was subsequently calculated as a measure of error to asses if SS, TP, and $NO_3^-$ would be suitable for modelling.

### 2.3.3 SWAT set-up and calibration

To delineate subbasins, the automatic watershed delineation option in ArcSWAT with the recommended threshold drainage area and a stream network created by the UTRCA. Land use, soil, and slope were subsequently overlain to create hydrologic response units (HRUs) and a minimum area threshold of 10/15/15 percent respectively was applied to reduce the number of HRUs to 318 with 19 subbasins. For the creation of the HRU management files, crop rotations were assumed to have minimal effect on the overall hydrology. Given that HRUs were not spatially explicit within the subbasin and eventually cycled back to the original crop, it was assumed that there would be minimal effect on nutrients over a longer term. Using the AAFC crop inventory data from 2011-2014, a crop rotation map was created through ArcMap overlay and it was determined that the dominant crop rotation was corn-soybean-winter wheat. Representative tillage systems and fertilizer application rates for each crop were developed based on the dominant rotation (UTRCA and Wanhong Yang, personal comm.). Yearly estimates of manure production in the watershed were calculated based on livestock statistics for the MCW, and all manure was divided up amongst the corn HRUs to fulfill N needs. A tile drainage map obtained from LIO (Ministry of Agriculture, Food and Rural Affairs, 2015) was used to determine the distribution in the watershed. Given that the full extent of tile drainage within Ontario is not known and the abundance of tile drains in the watershed is not known, all cash cropped HRUs within the MCW were assumed to be tile drained. Tile drainage parameters including depth to subsurface tile drain (DDRAIN= 900 mm), time to drain soil to field capacity (TDRAIN= 24 hours), and tile drain lag time (GDRAIN = 12 hours) were set based on what is typically observed in Ontario.

For sensitivity analysis, calibration, and validation of the model, the SWAT- Calibration and Uncertainty Programs (SWAT-CUP) software package was used with the SUFI-2 algorithm for parameter calibration (Abbaspour, 2015). This program is a stochastic auto-calibration software, which is widely used

in studies around the world (Ekstrand et al., 2010; Rouholahnejad et al. 2014). The SWAT model has a large number of parameters that can be calibrated (Arnold et al., 2012a). To reduce the number of parameters used in calibration to only the most sensitive and avoid over-parametrization, global sensitivity analysis (GSA) and one-at-a-time sensitivity analyses (OATSA) were performed on 72 parameters. For GSA, SWAT-CUP uses multiple regression analyses and employs a p-value and t-stat statistic (Student's t-distribution) to indicate the sensitivity (Abbaspour, 2015). For OATSA, each parameter is tested individually; all other parameters remain fixed to the default values and the model is run three times. Parameter sensitivity is calculated with:

$$ParSen_i = \frac{50 \times |Y_i - Y_{i-1}|}{(Y_i + Y_{i-1})} \quad [1]$$

where $Y_i$ is the value of the objective function for simulation run $i$ (Veith & Ghebremichael, 2009). GSA parameters were selected for calibration if the p-value was less than 0.05 and the t-stat was larger than 1.5. Results from OATSA were also considered if the sensitivity was larger than 0.05 and it caused an increase in the objective function. Additional consideration was given to parameters that met at least half the above criteria from each of the sensitivity analysis types.

The data used for calibration were from 2006 to 2010, and the data used for validation were from 2011 to 2013, to capture both wet and dry years, both on a monthly time step with a 3-year warm up period to mitigate the effect of initial conditions. At the watershed outlet, observed flow, SS, $NO_3^-$, and TP variables were calibrated sequentially with multiple iterations (3-5) using SWAT-CUP until there was only a marginal increase in the objective function, which was the Nash-Sutcliffe coefficient of model efficiency (NS). To measure the performance of the fitted parameters set and model during the calibration period, NS and the percent bias (PBIAS) was used and evaluated based on criteria developed by Moriasi et al. (2007b). PBIAS proved a useful statistic in conjunction with the NS because it provides a percentage describing how much the model over or under estimated a variable.

### 2.3.4 Future climate scenarios

To assess the impact that climate change will have on water quality and quantity, a bias corrected GCM ensemble was developed and coupled with the parameterized SWAT model simulated from 1980-2100, while keeping land use and management constant. A climate ensemble consists of multiple GCMs and (sometimes emission scenarios) that are combined and used in analysis to reduce the uncertainty associated with future climate projections (Fowler et al., 2007; Honti et al., 2014). The bias corrected GCM ensemble consisted of a 10km x 10km gridded daily temperature (max and min) and precipitation dataset provided by Ouranos, a consortium experienced in climate sciences, modelling, and developing regional climate projections for researchers (Ouranos, 2018).

To develop the climate change scenarios used in this study all available CMIP5 global climate models with precipitation, minimum temperature, and maximum temperature were obtained (Taylor et al., 2013). For each model, two emission scenarios known as Representative Concentration Pathways (RCP; Meinshausen et al., 2011) were used to drive each of the GCMs. Each RCP is named after the amount of net radiative forcing (W/m2) expected by 2100 due to projected GHG emissions. In this study, the two RCPS selected were RCP4.5 and RCP8.5, where RCP8.5 is the worst-case scenario (i.e. no implementation of policies to mitigate climate change) in terms of GHG emissions and concentration trajectories. The RCP4.5 emission scenario represents a stabilizing radiative forcing by 2100 due to implementation of GHG emission prices and represents a more optimistic representation of future GHG concentrations.

To reduce the number of scenarios and retain maximum uncertainty coverage in changes of temperature and precipitation in the future, k-means cluster analysis was used on all the CMIP5 GCMs with the RCP4.5 and 8.5 emission scenarios (Casajus et al., 2016). The 22 retained simulations were ordered in such a way that each subsequent scenario in the selection sought to maximize uncertainty coverage. To reduce SWAT model input/output processing time and still capture the uncertainty associated with climate model outputs, the first 10 scenarios from the final selection were chosen for the final ensemble and the remaining 12 in the 22 simulations were not used. The selected simulations are listed in Table 2.1. To create

the ensemble of catchment-scale future climate scenarios, data was empirically downscaled using the gridded NRCAN (10 km) interpolated station data and the quantile mapping method (Mpelasoka and Chiew, 2009).

*Table 2.1.* General Circulation models used in this study after using K-means clustering to reduce the final number of future climate scenarios. Models were obtained from the World Climate Research Programme's Coupled Intercomparison Project phase 5 (CMIP5).

| GCM abbreviation | Institute ID | RCP | Description |
|---|---|---|---|
| INM-CM4 | INM | 4.5 and 8.5 | Institute for Numerical Mathematics |
| GFDL-ESM2M | NOAA GFDL | 4.5 | NOAA Geophysical Fluid Dynamics Laboratory |
| MPI-ESM-LR | MPI-M | 4.5 and 8.5 | Max-Planck-Institut für Meteorologie (Max Planck Institute for Meteorology) |
| CanESM2 | CCCMA | 4.5 and 8.5 | Canadian Centre for Climate Modelling and Analysis |
| ACCESS1.3 | CSIRO-BOM | 4.5 and 8.5 | Commonwealth Scientific and Industrial Research Organization (CSIRO) and Bureau of Meteorology (BOM), Australia |
| BNU-ESM | GCESS | 8.5 | College of Global Change and Earth System Science, Beijing Normal University |

## 2.4 Results and discussion

### 2.4.1 Model calibration and validation

After sensitivity analysis, the 73 parameters were reduced to those considered the most sensitive to flow at the watershed outlet (23) and sediment and nutrient loads (18; Table A.1). By adjusting these parameters within their realistic maximum and minimum ranges in SWAT-CUP, an acceptable model was achieved. For the calibration and validation periods, the timing of observed peak flows matched the simulated values. Based on the criteria devolved by Moriasi et al. (2007b) all calibrated and validated variables (Table 2.2) had a satisfactory performance rating or above, with flow having a very good performance rating with respect to the NS and a good rating based on the PBIAS. During calibration and validation, the overall performance rating for SS was good, while TP and $NO_3^-$ were satisfactory with respect to the NS. The model's PBIAS for sediment and nutrient variables had a very good performance rating in both the calibration and validation period.

*Table 2.2.* Performance statistics for each of the calibrated variables in the SWAT model

| **Variable** | Calibration | | Validation | |
|---|---|---|---|---|
| | NS | PBIAS | NS | PBIAS |
| Stream Flow | 0.87 | -10.2 | 0.81 | -10.9 |
| Suspended Sediment | 0.75 | 2.2 | 0.62 | -14.8 |
| Nitrate | 0.61 | -0.2 | 0.57 | 3.9 |
| Total Phosphorus | 0.62 | 17.9 | 0.52 | 14.8 |

### 2.4.2 Future and baseline climate simulations

In the analysis of the forecasted climate ensemble (2080-2100) relative to the baseline (1990-2010), the projected climate data provided by Ouranos was grouped by seasons, as the data displayed similar trends within a season. Although the climate simulations are not an output of the current study, they are briefly summarized here to provide context and explain simulated changes in water balance, flow, nutrient, and sediment export. The future climate scenarios used in the current study project mean annual temperatures to increase by 0.9 to 3 degrees Celsius by 2050, and 1.3 to 7.1 by 2100. Additionally, the downscaled GCM ensemble in the current study (Figure 2.2) shows greater temperature increases in winter than in summer (Table B.4). These estimates are comparable to previous research that projected mean annual air temperatures in the Lake Erie basin to increase by 2.4 to 7.2 ˚C by 2080 (McDermid et al., 2015). Climate change projections from the Canadian Coupled Global Circulation Model's (CGCM2) A2 scenario also predict seasonal differences in air temperature changes, where the average change in temperature by 2080 will be 4-5 ˚C in winter and 2-3 ˚C in the summer seasons (Columbo et al., 2007).

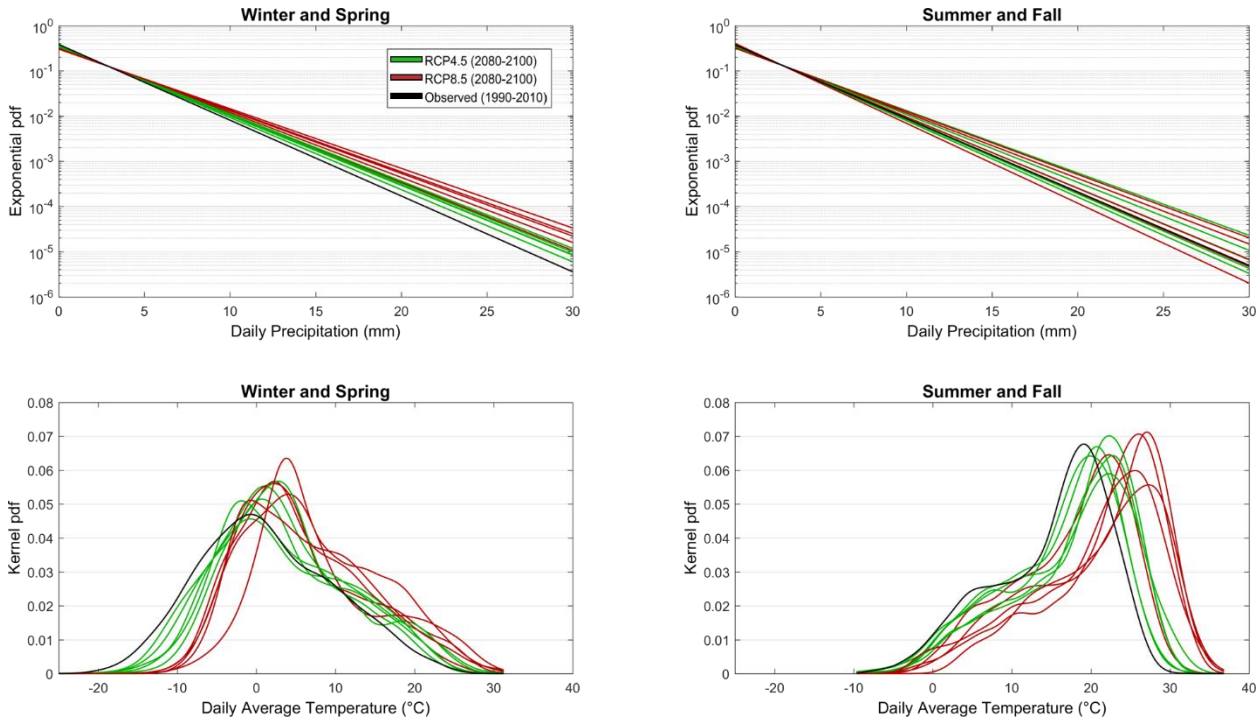


*Figure 2.2.* Probability density function of the exponentially fitted distribution of daily precipitation (top panels) and kernel fitted distribution of daily temperature (bottom panels) for the ensemble of two future climate scenarios (red, green) from 2080-2100 compared to the average baseline observed from 1990-2010 (black).

As a result of temperature changes in southern Ontario, shorter winters, longer growing seasons, and more extreme heat waves in summer are expected (Reid et al., 2007). This is corroborated by the results of the current model projections (Figure 2.2), where there is a shift in the distribution to the right of the baseline for both groups, indicating an increase in the probability of extreme temperatures and a decrease in lower temperatures in all seasons.

Local GCM precipitation outputs have an inherent uncertainty and are difficult to compare because they vary depending on the climate model structure, scaling technique, geographical differences (i.e. landform, elevation, proximity to water, etc.), natural variability, and GHG emission scenario used (Giorgi, 2010). In addition, precipitation predictions (unlike temperature) from downscaled climate models tend to be controversial because they do not account for non-stationarity of climate model bias corrections (Chen et al., 2015). The above factors must be taken into consideration when interpreting the projected impacts of climate change and comparing studies in geographically dissimilar regions. Annual projections for the

Great Lakes Basin indicate an average annual increase of 106 mm for the RCP4.5 and RCP8.5 scenarios by 2080 (McDermid et al., 2015), which is comparable to the average of the ensemble projections in the current study (Figure 2.3a) that indicate a 90 mm annual precipitation increase (Table B.4). Although a mean annual increase of 90 mm is projected, there is considerable variability across the simulations (due to the biases described above).

Currently, climatic conditions in the NGS are an important factor contributing to total annual water yields and nutrient export in southern Ontario (Macrae et al., 2007; Van Esbroeck et al., 2017). The future climate ensemble in winter and spring unanimously predict increases in the frequency and magnitude of extreme precipitation events (Figure 2.2) and a significant increase in precipitation volumes (Figure 2.3b and c). Furthermore, due to temperature changes, there will be a greater proportion of precipitation as rain, with more snowmelt events (Marianne et al., 2003). There is more variability in precipitation projections for the summer period, where the ensemble average indicates an increase in precipitation volumes (Figure 2.3a), contrary to other studies (McDermid et al., 2015; Verma et al, 2015). However, this increase is not unanimous among all scenarios in the ensemble due to the variability associated with the change in frequency and magnitude of precipitation events relative to the baseline period (Figure 2.2), and the uncertainty associated with climate models during these seasons (Giorgi, 2010). This is corroborated by King et al. (2012) who projected that summer precipitation could either increase or decrease in the UTRB. Overall, the projected shifts in precipitation and temperature distributions in Figure 2.2 indicate a shift towards longer dry periods between events, further increasing drought risk, with drought periods interrupted by more extreme rainfall.

### 2.4.3 Water balance and stream flow changes

#### *2.4.3.1 Annual and seasonal changes in flow paths*

As noted above, the future climate ensemble projects that by the 2080-2100 period, the average annual precipitation will increase by 90 mm (range: 4 to 205 mm), and changes will be most pronounced

during winter. The SWAT model predicts ET to increase on average by only 50 mm (range: 6 to 88 mm), resulting in an increase in surplus water. Consequently, the model predicted that water yield would increase by an average of 38 mm (range: -4 to 114 mm) annually by the 2080-2100 period (Figure 2.3a, f, k, and Table C.5). Seasonally, the future climate ensemble predicted that water yield would increase in winter and summer, but decrease in the spring and fall (Figure 2.3) (with the exception of the RCP4.5 group that predicted an increase in spring, Figure 2.3m). In winter, the model predicted a large increase in subsurface flow through tiles and a simultaneous decrease in surface runoff for both RCP groups (Figure 2.4b, g, and l), whereas in spring projected changes are much smaller (Figure 2.4c, h, and m), although water surpluses are large (Precipitation change>ET). In contrast, projected water balance changes in summer and fall months are small relative to winter and spring, have greater variability, and are generally not significant , with the exception of fall ET and water yield, and summer tile flow (RCP8.5 group; Figure 2.3 and 2.4).

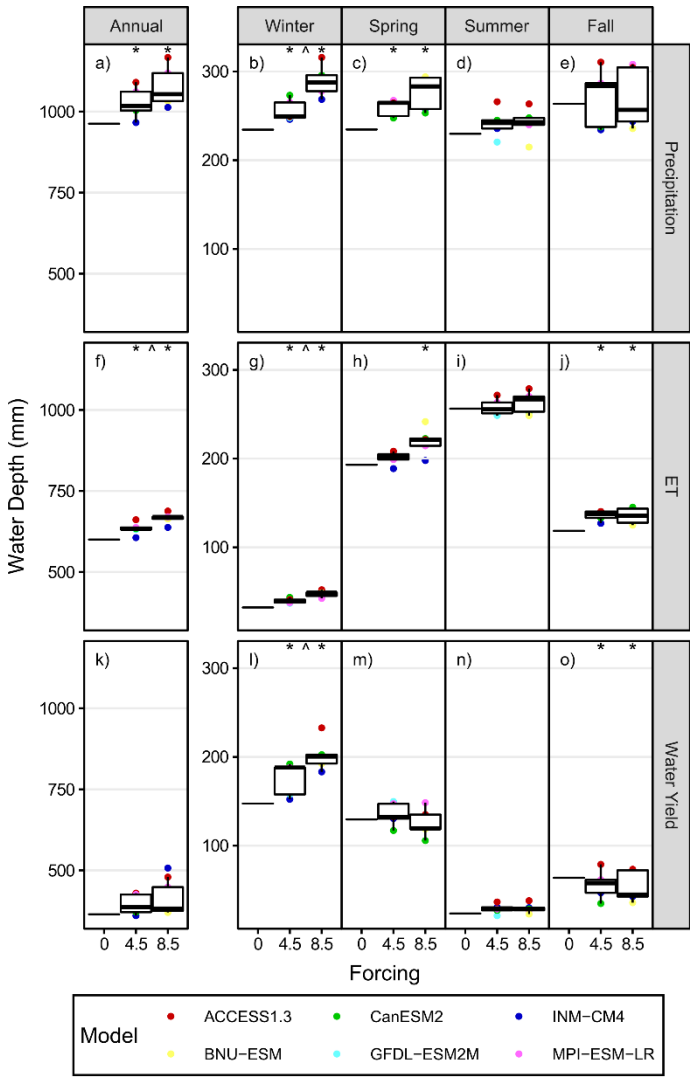


*Figure 2.3.* Annual and seasonal precipitation, ET, and water yield for the historic (0 forcing; 1990-2010) and future climate periods (RCP4.5 and 8.5 forcing; 2080-2100). Color indicates the climate model, when outside of the interquartile range. * indicates significant difference ($p<0.05$) from historic model based on two-tailed Student t-test and ^ indicates significant difference ($p<0.05$) between forcings from unpaired two-sample Student t-tests.

In winter, the model predicts increased tile flow because air temperatures in the future climate are warmer, which leads to modification of the soil frost extent and the dominant flow pathways in winter. As the surface air temperature becomes increasingly higher, there will be an increase in the number of days that soil temperatures are above freezing, which was corroborated for other areas in the region (Sinha & Cherkauer, 2010). Within the model, this will result in increased infiltration and subsurface activity causing surface runoff decreases and soil water storage depletion. This is also supported by Jyrkama & Sykes

(2007), who predicted increased infiltration and groundwater recharge in a southern Ontario watershed due to decreased ground frost, making soil freezing dynamics an important factor controlling projected pathway losses (Xiuqing & Flerchinger, 2001).

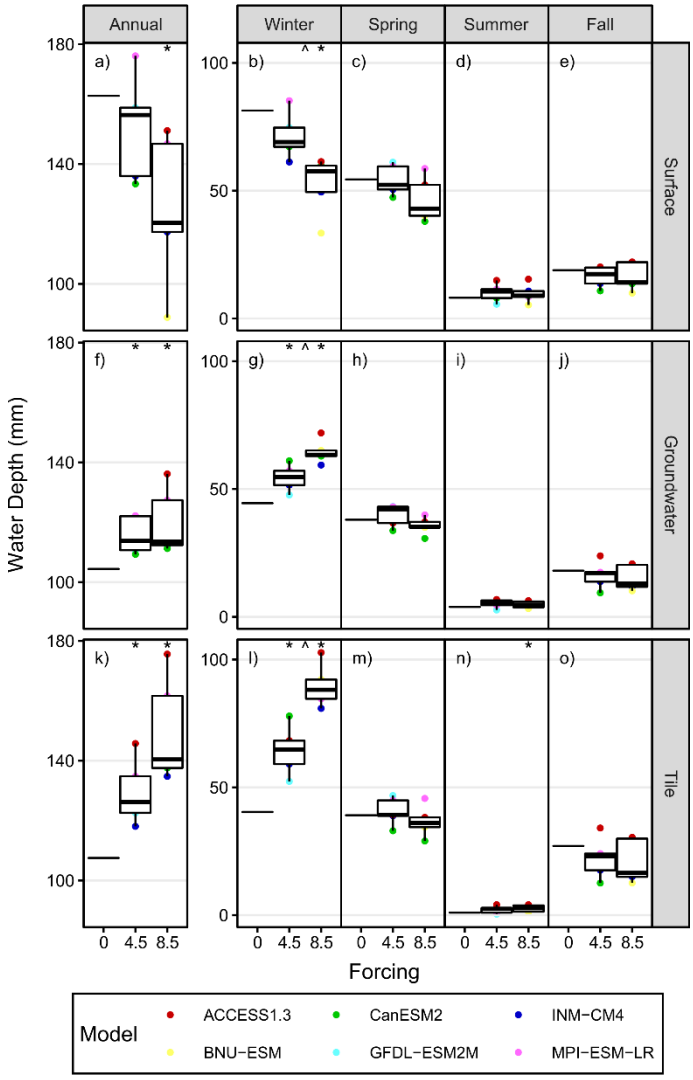


*Figure 2.4.* Annual and seasonal surface runoff, tile flow, and groundwater for the historic (0 forcing; 1990-2010) and future climate periods (RCP4.5 and 8.5 forcing; 2080-2100). Color indicates the climate model, when outside of the interquartile range. * indicates significant difference ($p<0.05$) from historic model based on two-tailed Student t-test and ^ indicates significant difference ($p<0.05$) between forcings from unpaired two-sample Student t-tests.

Although there were large water surpluses in spring (precipitation > ET = 16 mm), a significant change in surface runoff was not observed during this period. This is likely a result of increased hydrologic activity in winter that lessens the potential for saturation overland flow in spring. Indeed, as temperatures

increase in winter, the amount of precipitation as snow and snowpack will decrease, spring melt will occur earlier (Demaria et al., 2016), and the large tile flow increases in winter will decrease the water availability in spring. This is somewhat corroborated by surface runoff increase in spring for the RCP4.5 GFDL-ESM2M scenario (Figure 2.4c), which had the smallest tile flow increase in winter (Figure 2.4l).

#### *2.4.3.2 Annual and seasonal changes in flow*

Overall, results indicate that there will be a definitive but varying flow magnitude increase for the high stream flow regime and decrease for the low flow regime in all seasons (Figure 2.6). This corresponds to an average annual flow decrease (12%), which has been similarly predicted in another study (Cousino et al., 2015). For all scenarios in winter and spring, flows occurring at 50% exceedance probability will decrease relative to the baseline period, indicating a reduction in the median flow (8% and 12% decreases respectively) and average flow (Figure 2.5). In summer, for all scenarios there will be much higher flows occurring up to 15 percent exceedance when compared to the baseline period, with all scenarios less than the baseline not until 40 percent exceedance. The extent of high stream flow regime increases are reflected by variability in the average flow projections (Figure 2.5). Fall behaves similarly to summer except there is a bit more variability for the flow magnitudes occurring from 30 to 80 percent exceedance (Figure 2.6). In this range, most of the flows become higher at around 50 percent exceedance indicating an overall median flow increase, which is contrary to the average flow (Figure 2.5), and therefore also indicative of variability.

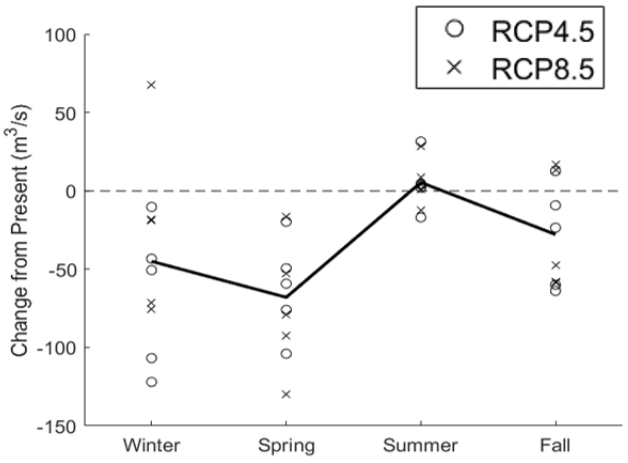


*Figure 2.5.* Average stream flow changes by season for all scenarios (black line) with each individual scenario grouped by RCP. All were during the period 2080-2100 and values are the difference between the projected and the observed from 1990-2010.

In winter, considering the overall decrease in surface runoff and increase in subsurface flow, this will result in attenuation of the stream response time to a precipitation event, reducing stream flows. In spring, stream flow decreases the most due to the previously mentioned causes of the change in the winter and spring water balance combined with the changing precipitation patterns. In winter and spring, increased frequency and magnitude of more extreme daily precipitation events, will increase runoff intensity and the magnitude of the infrequent peak flows, which is opposing for the low flow regime that responds to smaller precipitation events decreasing in magnitude and frequency, but generally have a greater probability of occurring.

In summer, the precipitation magnitude and frequency changes seen in Figure 2.2 are not the only factors influencing the high flow regime given that all scenarios show increases over a large range of exceedance probabilities. Due to changes in the timing of precipitation, there could be potential for a greater segregation of extremely wet (increased precipitation) and dry periods resulting in surface runoff pattern changes. This corroborated by the large discrepancy between the baseline and future scenarios at low flow conditions, which indicates a potential increase in the risk of drought conditions and decrease in soil storage (Figure 2.6). SWAT uses the SCS curve number updated daily based off daily plant evapotranspiration

(PET) to estimate direct surface runoff. Therefore, in fall, the projected increase in ET greater than precipitation will result in water deficiency, reduced surface runoff volumes, and average flow. As a result, in comparison to summer, surface runoff will have less influence on the high stream flow regime, and the precipitation pattern changes will reduce the percent of time during which all of the scenarios have high flows that are greater than the baseline period from 15 to 3.5 percent of the time.

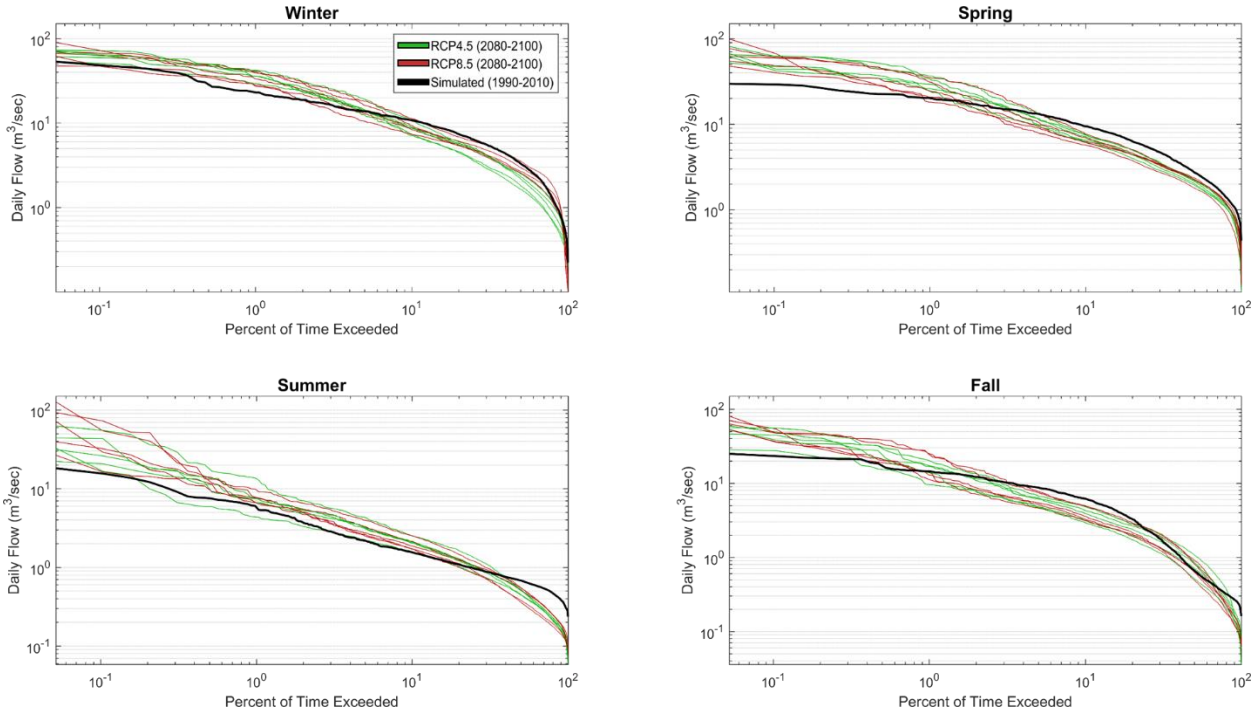


*Figure 2.6.* Flow duration curves for the watershed outlet with daily flow in 1990-2010 and for 2080-2100 in each season and future climate scenario

## 2.4.4 Nutrient and sediment loads in the future climate

### *2.4.4.1 Nitrate Export*

The model predicted a significant increase in annual nitrate loads and flow-weighted mean concentrations (FWMC; Figure 2.7a and f). In winter, median nitrate loads increased from 8 Kg $ha^{-1}$ to 14.1 Kg $ha^{-1}$ (77% increase), and FWMCs from 4.5 mg/L to 8.6 mg/L (91% increase) in the 2080-2100 period. The median spring loads decreased from 9.2 Kg $ha^{-1}$ to 8.8 Kg $ha^{-1}$ (4.2% decrease), and increased FWMCs from 5.3 mg/L to 6.8 mg/L (28.3% increase), with changes in load varying from -3.6 to 2.6 Kg $ha^{-}$

$^{1}$ between scenarios (Figure 2.7c). In summer and fall, we see increases in the $NO_3^-$ loads, (1.1 and 1.5 Kg $ha^{-1}$ increases respectively), but these are much smaller changes than are predicted in winter.

The increase in the annual and seasonal loads and FWMCs can be attributed to the changes occurring in the NGS. Since $NO_3^-$ is highly mobile in the subsurface, tile drains are known to contribute a large proportion of the total $NO_3^-$ loads to streams (Arenas Amado et al., 2017). This results in increased $NO_3^-$ losses (Figure 2.7b) due to the large tile flow increase in winter (Figure 2.4l) and a shift in the timing of residual soil nitrogen (RSN) remobilization towards the winter months. In spring, results suggest that extent of tile flow increases and soil water depletion in winter will cause the variability in spring loads. For example, the RCP 4.5 GFDL-ESM2M scenario had the smallest winter tile flow increase (Figure 2.4l), which corresponds with the largest spring tile flow (Figure 2.4m) and $NO_3^-$ load increase (Figure 2.7c).

In summer, $NO_3^-$ loads increase slightly due to tile flow, small median flow increases at the outlet, and large increases in the FWMC because of potentially longer periods between precipitation events initiating subsurface flow and high flow conditions. This could cause greater accumulation of $NO_3^-$ in the soil before it is flushed during the next storm event and exported via tiles (Van Meter et al, 2016; Vidon et al., 2009). In fall, load and FWMC increases are similar to summer, yet most flow pathways are decreasing, which indicates that the interactive effects of mineralization and decomposition of organic matter, a dominant $NO_3^-$ process in SWAT (Mehdi et al., 2016), and timing of high flow conditions are important. However, more analysis is needed to understand changes in export patterns and the exact contribution each pathway or process is contributing to the majority of these changes throughout the season.

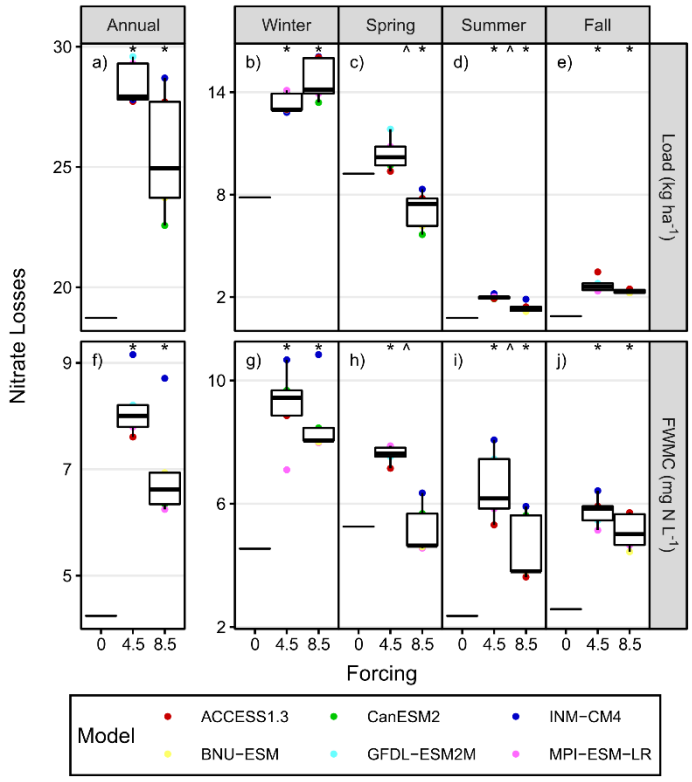


*Figure 2.7.* Boxplots for $NO_3^-$ loads and FWMC at the watershed outlet in 2080-2100 grouped seasonally, annually, and by GCM forcing (RCP4.5 and 8.5). With forcing "0" representing the historic period (1990-2100). Color indicates the climate model, when outside of the interquartile range. * indicates significant difference ($p<0.05$) from historic model based on two-tailed Student t-test and ^ indicates significant difference ($p<0.05$) between forcings from unpaired two-sample Student t-tests.

#### *2.4.4.2 Suspended Sediment Export*

In contrast to $NO_3^-$ loads, which the model predicted would increase in winter and decrease in spring by the 2080-2100 period, SS loads were predicted to decrease in both winter (8.1 Kg $ha^{-1}$; 10%) and spring (16.1 Kg $ha^{-1}$; 24%; Figure 2.8) along with FWMC (Figure 2.8). This reduction is mostly driven by reduced surface runoff and stream flow, which decreases hillslope sediment supply and sediment transport capacity in the stream. Within the model, surface runoff increases SS export from the HRUs. It is interesting to note that the model predicted that spring would have a substantial decrease in SS loads compared to winter, despite the smaller decrease in surface runoff. This may be partially driven by earlier crop growth in spring, which would lessen SS losses from fields. However, winter SS loads vary from -32 to 18 Kg $ha^{-}$

[1] despite the fact that a substantial decrease in surface runoff is projected, which suggests that streamflow may be a more important controlling factor.

In contrast to the projected reductions in SS loads in winter and spring, the model predicted that summer and fall SS loads will increase, offsetting the winter/spring increases and resulting in no significant annual change (Figure 2.8a). In summer, there will be significant increase in the median SS loads (20 Kg $ha^{-1}$; 340%) and FWMC by the 2080-2100 period (Figure 2.8d and i). This should be expected given the combination of increased surface runoff and average stream flow. In fall, loads have a significant median increase of 17.5 Kg $ha^{-1}$ (195%) and this corresponds to a 25 mg/L (95%) FWMC median increase for all scenarios by the 2080-2100, despite the fact that flow and water balance changes are small and variable, which makes the reason for the fall changes less clear. These changes may be driven by higher intensity rainfall and shifts between wet and dry periods, which would not lead to an increase in overall flow but could lead to elevated losses of SS during peak flow events.

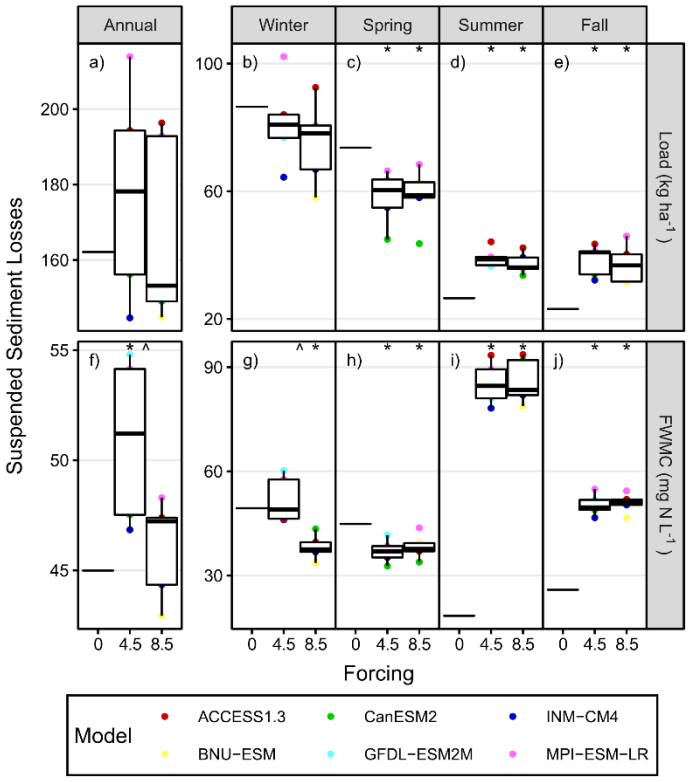


*Figure 2.8* Boxplots for SS loads and FWMC at the watershed outlet in 2080-2100 grouped seasonally, annually, and by GCM forcing (RCP4.5 and 8.5). With forcing "0" representing the historic period (1990-2100). Color indicates the climate model, when outside of the interquartile range. * indicates significant difference ($p<0.05$) from historic model based on two-tailed Student t-test and ^ indicates significant difference ($p<0.05$) between forcings from unpaired two-sample Student t-tests.

#### *2.4.4.3 Total phosphorus*

In winter and spring, the model predicted a median increase in TP loads for all scenarios by 0.07 (31%) and 0.025 (19%) Kg $ha^{-1}$ respectively (Figure 2.9b and c). Changes in TP would be expected to behave similarly to SS and surface runoff given that the SWAT model lacks a subsurface P transport component (Neitsch et al., 2011). Although TP loads and FWMC did not decrease, some similarities are found between SS and TP export. For example, the model scenario with the smallest decrease (or an increase) in SS and surface runoff were associated with increased TP export. Overall, results suggest an increased potential for changing climate to alter TP:SS export ratios in winter and spring, causing median FWMC in winter to increase by 0.05 (39%) and 0.033 (37%) mg/L in spring (Figure 2.9g and h). A plausible reason for these changes would be the increase in high flows, which are known to increase P transport

(Royer et al., 2006). Large surface runoff and precipitation events associated with these increased peak flows could flush P accumulated in the soil between smaller events. It is possible that more fine-grained material, which is enriched in P, or, dissolved P species are being mobilized, which would not lead to an observed increase in SS. This is supported by the fact that there is a sensitivity of solution P export in SWAT to increased precipitation intensity (Michalak et al., 2013), and, there may be an increase in solution P resulting from increased decomposition and mineralization of organic residue due to temperatures and soil moisture increases.

In summer and fall, load changes are significantly greater relative what is typically observed in these seasons with increases of 0.023 (200%) and 0.02 (121%) Kg $ha^{-1}$, respectively (Figure 2.9d and e). Although these increases are large, they are considerably smaller than what is observed in the winter (200% greater). Results suggest that TP will primarily be exported with SS due to their coordinated increase. Within the MCW, water quality conditions are ranked using a standardized grading system developed by Conservation Ontario. The current overall surface water quality condition has a score of D with not much change occurring since 2005; however, P levels have improved but are still at levels 4 times the provincial aquatic life guidelines (0.03 mg/L). In the final period (2080-2100) concentrations are expected to increase by 0.042 mg/L in winter and spring, which is almost 1.4 times water quality guidelines.

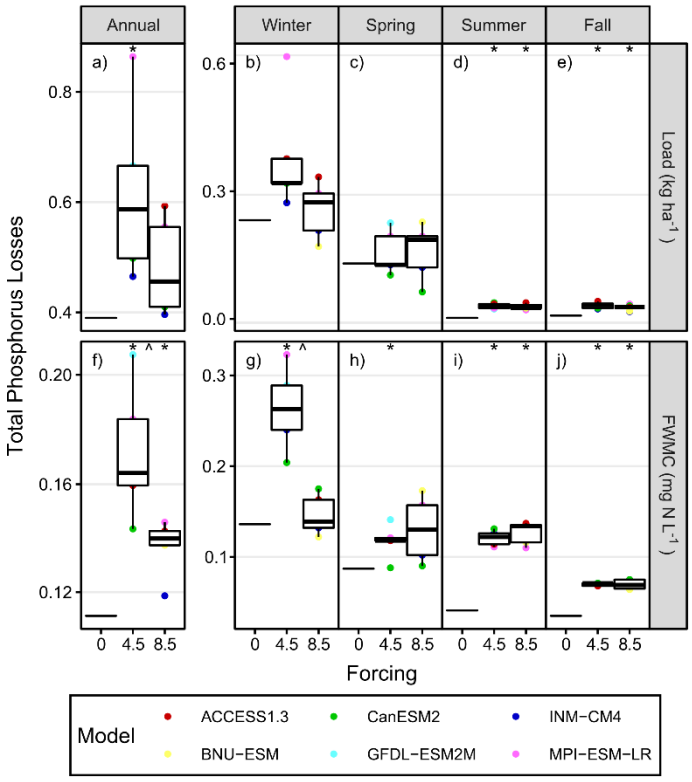


*Figure* 2.9. Boxplots for TP loads and FWMC at the watershed outlet in 2080-2100 grouped seasonally, annually, and by GCM forcing (RCP4.5 and 8.5). With forcing "0" representing the historic period (1990-2100). Color indicates the climate model, when outside of the interquartile range. * indicates significant difference ($p<0.05$) from historic model based on two-tailed Student t-test and ^ indicates significant difference ($p<0.05$) between forcings from unpaired two-sample Student t-tests.

## 2.5 Conclusions

In this study, the SWAT model forced with an ensemble of future climate change scenarios were used to evaluate the implications of seasonal changes in climate on water quality in the MCW, in southwestern Ontario. Land use and management practice inputs were static through time, which is a limitation since population increases are, expected (Ministry of Finance, 2017), followed by increased urbanization, which would increase the impervious surface area, further exacerbating surface runoff and the projected P loading problems we see (Labeau et al., 2014). Furthermore, as global needs change, prevailing crop types will shift and as a result changes in management practices and fertilizer application rates will change.

Given increased temperatures and precipitation, seasonal shifts in temperature, and increased frequency of extreme rainfall, SWAT predicted annual increase in water yield, $NO_3^-$ (9; Range: 4 to 11 Kg $ha^{-1}$), TP (0.14; Range: 0.01 to 0.47 Kg $ha^{-1}$), SS (5; Range: -17 to 52 Kg $ha^{-1}$), and decrease in average flow (12; Range: 5 to -23%) by the 2080-2100 period. Generally, these changes were controlled by changing precipitation characteristics and flow paths in the NGS that also affected stream flow regimes, increasing peak flows. In winter, there was a large increase in subsurface flow (mostly tile flow), potentially due a decrease in the soil frost extent and more precipitation as rain due to warmer temperatures, decreasing surface runoff and the average streamflow. While in spring, the shift in seasonality decreased surface runoff and streamflow, potentially due to less snowpack and water availability. These changes result in a shift in nutrient export timing towards winter, which had the greatest increase in nutrient export.

Due to the variability between some of the GCM outputs, this study highlights the importance of including multiple climate change scenarios to capture uncertainties in climate model projections. In addition, the resulting increase in loads during the NGS cannot be ignored. It is clear that we need to prioritize an increased understanding of the shift in seasonality and its effect on the NGS nutrient export behavior to reduce non-point source loads. Agricultural management practice development and reduction targets cannot be static, decision makers need to consider the effect a changing climate will have, especially in the NGS.

# Chapter 3 - Controlled tile drainage impacts on field scale runoff pathways and phosphorus losses in southern Ontario

## 3.1 Overview

Agricultural fields are major contributors to non-point source nutrient contamination and eutrophication, resulting in more frequent occurrences of harmful algal blooms and degraded water quality. To address this issue, numerous best management practices (BMPs) have been implemented to mitigate nutrient export while maintaining agricultural productivity; however, the efficacy of individual BMPs is uncertain. Controlled tile drainage (CD) is one BMP that has the potential to reduce nitrate and phosphorus export via tile drains. However, with CD, little is known about water quality trade-offs, such as the increased potential for surface runoff and the associated nutrient export, and if different types of CD management may influence the potential for these trade-offs to occur. In this study, the Soil Water Assessment Tool (SWAT) was used to create a model for a clay loam field site in southern Ontario to examine the impact of CD on runoff pathways and edge-of-field total phosphorus (TP) export. CD management depths of 500 mm were compared to freely drained (840 mm) conditions, and the use of CD both continuously and seasonally was assessed. Results indicate that CD practices of keeping drain invert raised longer throughout the year will have a tendency to increase TP export in runoff (4 to 13% increase) due to increased overland flow. However, most of these losses occur during the non-growing season due to wetter soil conditions, increasing the potential for saturation excess overland flow. Due to drier soils, the use of CD only during the growing season can reduce this risk, but will do little to reduce edge-of-field losses given that tiles are not the primary TP pathway at the site. This work highlights the need for improved understanding of all water quality tradeoffs associated with BMPs, particularly during the non-growing season.

## 3.1 Introduction

The eutrophication of fresh water sources has become a major issue affecting ecosystem health and economic prosperity in southern Ontario (Bingham et al., 2015; Diaz, 2001; Ludsin et al., 2013). In freshwater systems, this issue is largely caused by non-point source (NPS) phosphorus (P) contamination, originating from agricultural landscapes (Scavia et al., 2014). In a large majority of agricultural fields

where soils are poorly drained, tile drains have become a necessary best management practice (BMP) used to drain the excess soil water to increase crop productivity and trafficability (Irwin, 1977; Skaggs et al., 1994). The introduction of this pathway modifies hydrology by increasing the proportion of annual precipitation transported through the subsurface to streams (King et al., 2015), reducing the amount of surface runoff (Muma et al., 2016), and therefore, often decreasing total edge of field TP losses (Ball Coelho et al., 2012; Haygarth et al., 1998). Indeed, higher concentrations of TP are typically found in surface runoff (McDowell et al, 2001; Van Esbroeck et al., 2017). However, subsurface flow can be enhanced by macropores that increase the connectivity between surface soils and tile drains (Simard et al., 2000), increasing concentrations of particulate phosphorus (PP) (Uusitalo et al., 2001) and soluble reactive phosphorus (SRP; Pease et al., 2018), and thus P loads through tiles (Kung et al, 2000). Tile drains can also have greater nitrate (NO3) loads (Royer et al., 2006) relative to surface runoff, which is problematic in the Mississippi River watershed as the hypoxia in the Gulf of Mexico is driven by nitrate (Rabotyagov et al., 2014). Thus, it has been argued that tile drains may exacerbate water quality issues, rather than improve them. Consequently, some managers and land stewards have recommended the use of controlled tile drainage (CD) to mitigate P losses.

Controlled drainage permits control of water table position and soil water storage using a series of gates installed near the tile network outlet that can be raised or lowered. This results in decreased tile flow, which leads to a reduction in P and NO3 loads from tiles (Ale et al., 2012; Lalonde et al., 1996; Lavaire et al., 2017; Skaggs et al., 2012; Sunohara et al., 2016; Tan & Zhang 2011; Wesström et al., 2014; Williams et al., 2015; Youssef et al., 2018) and fecal pollution (Wilkes et al., 2014). Additionally, when using CD during the growing season, this can decrease plant water stress, which increases crop yields (Poole et al., 2013; Sunohara et al., 2016), thereby providing economic benefits (Crabbé et al., 2012). Finally, CDs can provide N reduction benefits through increased denitrification due to the creation of anaerobic conditions (Skaggs et al., 2010; Wesström & Messing, 2007). Although CD has the potential to improve water quality in subsurface drainage, few studies have considered potential water quality tradeoffs such as increased

surface runoff, which may increase total phosphorus (TP) loads and impact SRP:TP ratios (Riley et al., 2009; Ross et al., 2016; Tan & Zhang 2011; Zhang et al., 2017). Moreover, in cool temperate climates such as the Great Lakes region, many landowners do not employ controlled drainage during the non-growing season (NGS) due to the potential for ground frost to damage tile drains. Given that the majority of annual runoff and P loss in the Great Lakes region of North America occur during the NGS (Macrae et al., 2007b; Van Esbroeck et al., 2017; Williams et al., 2016), it is unclear if and how CD may affect year-round runoff and nutrient losses from fields.

The potential for CD to mitigate year-round nutrient losses can be investigated using modelling techniques such as the Soil Water Assessment Tool (SWAT; Arnold et al., 2012a), DRAINMOD (Skaggs, 1978), or the Agricultural Drainage and Pesticide Transport model (ADAPT; Alexander, 1988), as they permit simulation of the natural environment under variable conditions. Indeed, models are frequently used in conjunction with field observations to inform decision makers on the practicality of different BMPs. However, most models lack the combination of tile flow, macropore flow, controlled tile drainage, and subsurface TP and soluble reactive phosphorus (SRP) export routines (Qi & Qi, 2017), confounding our ability to determine how drainage management may impact water quality. A new tile drainage modeling routine (H-K-DC), recently added to SWAT (in Revision 495) was added improve our consistency in simulating tile drainage (and controlled drainage) in the SWAT model. The H-K-DC routine is based on equations developed by Kirkham (1957) and Hooghoudt (1940), which are used in DRAINMOD (Moriasi et al., 2007a). The new H-K-DC routine has not yet been employed extensively across different regions and scales (Bauwe et al., 2016; Boles et al., 2015; Guo et al., 2018; Ikenberry et al., 2017; Malagó et al., 2017; Moriasi et al., 2012, 2013). However, given that tile drains dominate the agricultural landscape in southern Ontario, confidence through testing of these routines will be important to future studies.

Therefore, the objectives for this study are to: (1) Calibrate a single HRU SWAT model of a field site in southern Ontario, Canada to demonstrate the capability of the SWAT and the H-K-DC routines to accurately simulate tile flow and surface runoff; and (2) Simulate the impact of CD on flow path partitioning

using the SWAT HRU model and estimate the impacts of these changes on edge-of-field TP and SRP losses using field data.

## 3.2 Methods

### 3.2.1 Field site description

The Londesborough site (LON) is a small ~8.1 ha field located in southwestern Ontario, Canada (43°38'33.0"N 81°24'42.6"W; Figure 3.1), within the Maitland Valley watershed that drains in to Lake Huron. Londesborough has a humid continental climate with an elevation above sea level of ~350 m. Long-term (1981-2010) climate normal for the region are mean temperatures of -5.3 ˚C in winter (December to February), and 19.2 ˚C in summer (June-August), with mean annual precipitation amounts of 1245 mm (374 mm as snowfall from October to April) (Environment and Climate Change Canada, 2018a). The current study uses a dataset collected over the 2012-2015 water years (Oct 1 – Sept 30). Weather over this period was variable, with 3 of the 4 years receiving an average of 187 mm less than the 30-year average and one year receiving 241 mm more. Temperatures occurring throughout the study period were also variable, but consistent with long-term normals for the region.

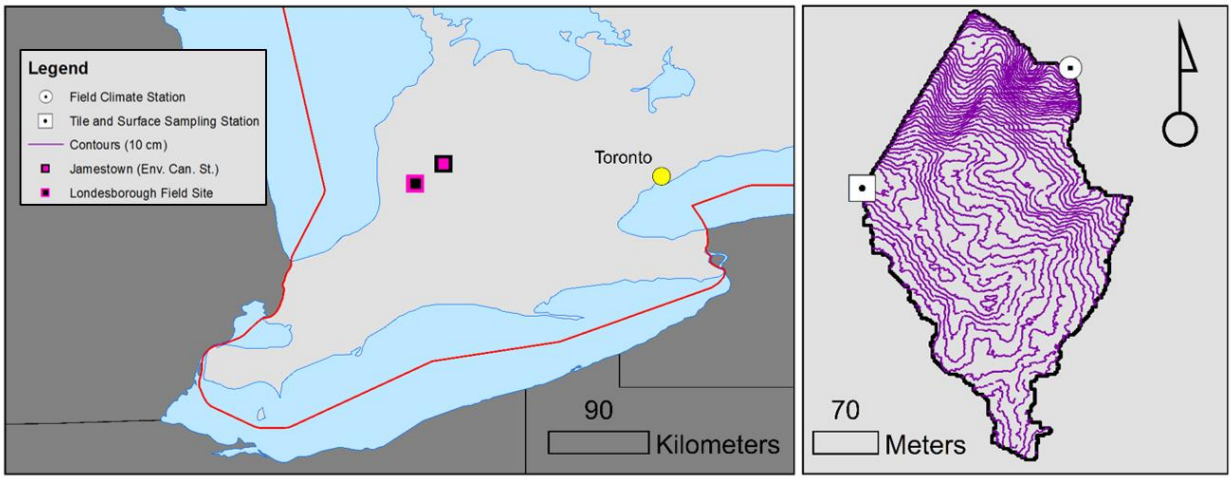


*Figure 3.1.* Location of LON in Ontario (grey), Canada (left) and other field site details (right; topography, observation station locations, and boundary). Also shows the location of the climate station used to supplement missing data at the field site (Jamestown).

Soil in the field is classified as a Perth clay loam (Plach et al., 2018), which is imperfectly drained. The average slope of the field site ranges from is 0.2 to 3.5%. Tile drains are installed within the field at ~ 75-90 cm depth with a spacing of 14 m. The tile drainage system is restricted to the field site and does not receive inputs from adjacent fields. Within the field, 10 cm lateral tiles drain into a larger header tile at the field edge. The crop rotation is a corn (*Zea mays* L.), soybean (*Glycine max* L.), and winter wheat (*Triticum aestivum* L.), a rotation that is common in southern Ontario. The field is managed with a rotational shallow conservation till (vertical tillage to 5 cm depth). Soil test P concentrations are 16 ppm (Olsen P) in the top 15 cm of soil. P is applied as monoammonium phosphate (MAP) via subsurface placement prior to corn (15 Kg P $ha^{-1}$), and via surface broadcast following winter wheat harvest (92 Kg P $ha^{-1}$), concurrent with the rotational till. Cover crops (red clover; *Trifolium pretense* L.) are planted in the spring (air seeded in April) in years during which winter wheat is cropped, and killed in October using an herbicide.

### 1.2.2. Field Data Collection

Hydrometric data are collected continuously (15-min intervals) at the field edge, year-round. Meteorological data (rainfall, air temperature, windspeed and direction, relative humidity, soil temperature and moisture) are recorded on-site using a standard meteorological tower (Onset Ltd.). Because the on-site weather station does not measure snowfall, precipitation data was obtained from a nearby weather station (Environment and Climate Change Canada, 2018b). Water table position is monitored continuously at the field edge using a pressure transducer in a 2 m deep well (ID 5 cm) (U20, Onset Ltd.). Surface runoff drains from the field via a single culvert (ID 45 cm) and tiles drain via a single header tile. Flow in both surface drainage and tile drainage are measured using depth-velocity sensors (Flo-tote, Hach Ltd.) and recorded on FL900 data loggers (Hach Ltd.). Water samples of surface and subsurface runoff are collected at high frequencies (2-8 hr intervals) during storm and thaw events, and periodically during baseflow (when tiles are flowing) using automated field samplers (ISCO) that are triggered by a flow response. Unfiltered samples are acidified to 0.2% $H_2SO_4$ (final concentration) and digested using acid persulphate digestions

and colorimetric analyses in the Biogeochemistry Lab at the University of Waterloo. For more detailed information on the field site and data collection, refer to Van Esbroeck et al. (2017).

### 3.2.2 SWAT model description

For the study, the SWAT2012, rev. 664 was used. SWAT is a semi-distributed, process/empirical, continuous time-step-based model capable of simulating hydrology, water quality, and plant growth (Arnold et al., 2012a). It requires detailed information related to climate, land use, soil, topology, and, depending on the watershed and project goals, detailed information about management practices. Management practices are added to the smallest spatial unit within the model, which is the HRU, a unique combination of soil, land use, and slope within each sub-basin.

Within the most recent versions of SWAT, a new tile drainage routine (H-K-DC routine) was added by the developers that uses a combination of either the Hooghoudt or Kirkham equations depending on the water table depth (Moriasi et al., 2013). Tile flow only occurs once the perched water table rises above the drains (Neitsch et al., 2011). When the water table is below the soil surface and above the drains, the Hooghoudt equation (Hooghoudt, 1940) is used to calculate tile drainage flux:

$$q = \frac{8Km+4Km^2}{L^2} \quad [1]$$

Where $q$ is the drainage flux (mm $h^{-1}$), $K$ is the lateral saturated hydraulic conductivity (mm $h^{-1}$), $d$ is the depth from the drains to the impermeable layer (mm), $m$ is the midpoint water table height above the tile drains (mm), and $L$ is the distance between drains (mm). When the water table eventually rises above the soil surface SWAT will use the Kirkham equation (Kirkham, 1957):

$$q = \frac{4\pi K(t+b-r_e)}{gL} \quad [2]$$

Where $t$ is the perched water height above the soil surface (mm), $b$ is the depth from soil surface to the tile drains (mm), $r_e$ is the effective radius of the tile drain (mm), and $g$ is dimensionless factor, see Kirkham

(1957). Finally, when the drainage flux is greater that the drainage coefficient, tile flux is set equal to the drainage coefficient (DRAIN_CO; mm $d^{-1}$).

### 3.2.3 SWAT HRU model setup

#### *3.2.3.1 Input data*

To create the SWAT model for LON consisting of only one HRU and subbasin all input files needed for a single HRU model were created and altered to ensure the model was representative of the field site. Some initial modifications were made to parameters usually initialized in the ArcSWAT model builder based on the available field data. For example, in the .sub input file the subbasin area (SUB_KM) was set to be equivalent to the field site surface runoff area (8.1 ha) and the input files linked with the subbasin file (.sub) were set to one of each input type. In the HRU input file (.hru), the fraction of subbasin area contained in HRU (HRU_FR) was set to one and the slope (HRU_SLP) was changed to 1.6%. This value is the mean slope of the field site calculated using the SWOOP digital elevation model (2 m resolution; Ministry of Natural Resources and Forestry, 2015).

The soil input file (.sol) parameters were set and representative of the fields soil type (Perth clay loam), which was determined using the Ontario Soil Survey Complex data (1:50000 scale) obtained from the Land Information Ontario (LIO) database (Ministry of Agriculture, Food and Rural Affairs, & Canadian Soil Information Service, 2015). Soil layer data was available to a depth of 1100 mm, and had a bulk soil texture consisting of 27% clay and 25% sand. The pedotransfer function developed by Saxton and Rawls (2006) was used to estimate available water capacity, saturated hydraulic conductivity, and bulk density for each soil layer using the available texture data.

Climate input data sets were made using the field site (Figure 3.1) rain and temperature data. During the months with snow and the part of the year in 2015 when there was no precipitation data, more was obtained from a nearby climate station to supplement the field site data and make a continuous precipitation data set (Jamestown, ON, 25 Km away; Figure 3.1; 43°48'09.1"N 81°11'01.0"W, Environment and Climate

Change Canada, 2018b). Agricultural management practices were input using reported field activities at the site (noted above), with the remainder of the parameters used in SWAT set to default before calibration.

#### *3.2.3.2 Calibration software description*

In this study, the Optimization Software Toolkit for Research Involving Computational Heuristics (OSTRICH) was used to auto-calibrate the SWAT model. This toolkit is able to function with any model that operates using text files and has many options to choose from with respect to the calibration and optimization algorithms available (Matott, 2017). During calibration, the Dynamically Dimensioned Search (DDS) algorithm was selected due to its computational efficiency and ability to determine a globally optimum solution within a selected number of iterations (Tolson and Shoemaker, 2007).

To auto-calibrate the model both the percent bias (PBIAS) and the Nash–Sutcliffe model efficiency coefficient (NS) within OSTRICH, the general-purpose Constrained Optimization Platform (GCOP) were used. Within the GCOP module, the multiplicative penalty method (MPM) was selected to calculate the overall objective function, which is a combination of the system cost and the penalty function (Chan-Hilton and Culver, 2000). To determine the system and penalty cost associated with the applied constraints a MATLAB script was developed to extract model outputs and calculate response variables to use within OSTRICH after each iteration.

#### *3.2.3.3 Calibration and validation approach*

Monthly tile (2012-2015) and surface runoff (2013 and 2015) depths were determined from the 15-minute field site data. Surface runoff (2013 and 2015) and tile flow (2012-2014) were calibrated together at a monthly time step using the field site data with a three-year warm up period. During calibration, the average NS for tile flow and surface runoff was used as the system cost, and the penalty cost was calculated by constraining the surface runoff and tile flow PBIAS to ± 25 and 20 percent respectively. The perturbation factor and maximum number of iterations were set to 0.2 and 1500 respectively, and after calibration, tile flow was validated using the data in 2015.

Some parameters that control calculation methods within the model were changed from default. These were the daily potential evapotranspiration calculation (PET), which now uses the Hargreeves method (IPET=2) and the Soil Conservation Service (SCS) curve number (CN), which now varies with accumulated plant ET (ICN=1; Arnold et al., 2012a). To use the new tile flow routine mentioned above, ITDRN was set to one. Additionally, the default value for the Manning's overland flow roughness (OV_N) was too low so it was increased to 0.15 to be representative of the site, which used either no-till or vertical tillage, and leaves crop residue.

Parameters known to affect HRU runoff were included in the calibration (Abbaspour et al., 2007, 2015; Arnold et al., 2012b, Guo et al., 2018; Wang & Melesse, 2005; Table A.2 and A.3), as well as additional parameters required by the new H-K-DC routine. Site-specific information and collected agricultural management data were used to fix some of the parameters to improve the model. For example, the distance between drains (SDRAIN) was set to 14 m, pump capacity (PC; mm $h^{-1}$) was set to 0, and based on the results of Golmohammadi et al. (2016a) in Ontario, the effective radius (RE) was set to be 15 mm. The depth to drains (DDRAIN) was known to be between 750 to 900 mm and allowed to vary during calibration. Other tile specific parameters used in calibration include the drainage coefficient (DRAIN_CO; mm $d^{-1}$) and multiplication factor to determine lateral saturated hydraulic conductivity (LATKSATF; mm $h^{-1}$).

Due to the lack of soil data past 1100 mm, an unknown depth to the impervious layer, high sensitivity of the impervious layer depth, and its control over shallow aquifer seepage (Bauwe et al., 2016; Neitsch et al., 2011), an iterative approach was used to define reduced ranges for calibration. To ensure a realistic impervious layer depth after calibration, tiles were removed (DDRAIN = 0) and the layer depth was increased until the shallow aquifer recharge was between 15 to 20 percent of the average annual precipitation, which is typical in Ontario clay and silt soils (David Rudolph, personal comm.). This value was used as the maximum limit during calibration of the impervious layer depth (DEPIMP; range of 1500-3000 mm) and was similar to the ranges used by Guo et al. (2018). Additionally, some soil parameters were

added due to the uncertainty in actual conditions with depth and their importance in percolation and water table depth calculations (Neitsch et al., 2011). Using the available data, saturated hydraulic conductivity (SOL_K), bulk density (SOL_BD), and the available water capacity (SOL_AWC) were allowed to vary ± 25 percent of the initial value for the layers.

### 3.2.4 Tile drainage scenarios and TP load estimation

To determine the effect that tile drains have on the flow paths contribution to runoff two tile drain scenarios were created. The calibrated HRU model was used as the free tile drainage (FTD) scenario (DDRAIN= 840 mm). Tile height was subsequently raised (DDRAIN = 500 mm) to be representative of depths typically used for CD in southern Ontario (Upper Thames River Conservation Authority, personal comm.) for the continuously raised tile drainage ($RTD_{cont}$) scenario over the study period. Each height was run during the calibration period (2012-2015) with no other modification of the parameters. Since SWAT is unable to change tile heights during a simulation, pseudo CD data sets were created for two typical management scenarios found in southern Ontario (Figure 3.2). Where HRU model outputs from the $RTD_{cont}$ and FTD scenarios were joined together based on the planting and harvest dates for the crops reported at the field. Monthly TP and SRP FWMCs were calculated for each flow path during the study period using field site data obtained using the methods mentioned in Van Esbrock et al. (2017). To calculate the monthly TP and SRP FWMC for surface runoff and tile flow the following equation was used:

$$FWMC = \frac{\sum_{n}^{1}(C_i t_i q_i)}{\sum_{n}^{1}(t_i q_i)} \quad [3]$$

Where $C_i$ is the concentration, $t_i$ is the time window, and $q_i$ is the flow, all for the $i^{th}$ sample, which is the total load divided by the total flow over the period (i.e. month). TP and SRP loads were then determined by multiplying the monthly FWMC by the corresponding surface runoff and tile flow volumes output in each scenario because nutrient reductions have been shown to be primarily driven by flow (Sunohara et al., 2010) and SWAT lacks the capability to model P subsurface loses through tile drains (Qi & Qi, 2017).

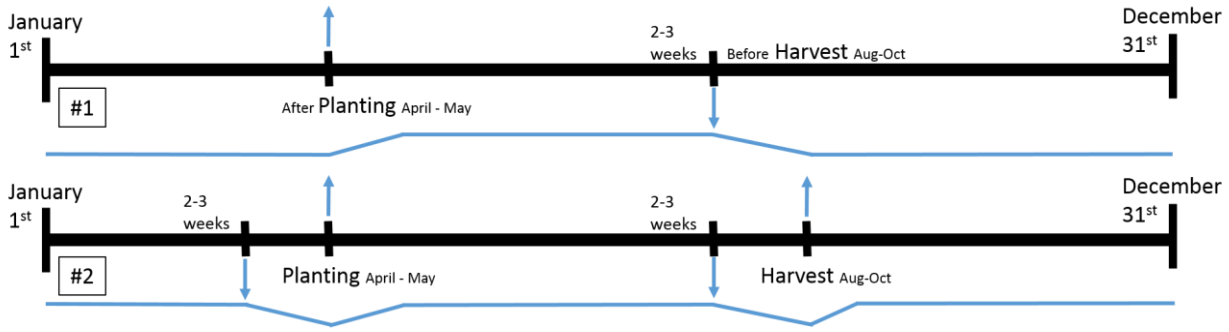


*Figure 3.2.* Shows two typical CD management approaches used in southern Ontario (#1 = $RTD_{GS}$; #2 = $RTD_{NC}$). Blue arrows represent the raising or lowering of the drain gate 3 weeks before planting and harvest, while blue lines represents a simplified representation of the water table depth changes. Major difference is the management during the NGS, which typically occurs from late fall to early spring for most crops.

### 3.2.5 HRU performance evaluation

To evaluate the performance of the HRU flow pathways, the NS (Nash & Sutcliffe, 1970), PBIAS (Gupta et al., 1999), and coefficient of determination ($R^2$) statistics were used in conjunction with graphical methods. The model evaluation criteria developed by Moriasi et al. (2007b) and based on the streamflow outputs, were used to provide performance ratings for NS and PBIAS statistic. For the $R^2$, performance was considered good if it was higher than 0.6 (Santhi et al., 2001).

## 3.3 Results

### 3.3.1 SWAT HRU performance: Surface runoff and tile drainage

Following calibration, the model performance was good (Table 3.1). The model simulated surface runoff more precisely than tile flow, despite the fact that there were fewer surface runoff events. The model evaluation criteria developed by Moriasi et al. (2007b) that uses NS and PBIAS to rate model performance, the ratings for surface runoff were very good and good respectively, while tile flow was satisfactory for both, with $R^2$ performance also well within the acceptable range (>0.6; Santhi et al., 2001; Table 3.1). Tile flow during the validation period slightly underperformed with respect to the NS and $R^2$, but had a satisfactory PBIAS.

*Table 3.1.* Performance statistic values (NS, PBIAS, and R2) after calibration for surface runoff and tile flow

| Performance Measure | Monthly Surface Runoff | Monthly Tile Flow | |
|---|---|---|---|
| | 2012 and 2015 | Calibration (2012-2014) | Validation (2015) |
| NS | 0.79 | 0.60 | 0.23 |
| PBIAS | -12.7 | 17.3 | 15.6 |
| R2 | 0.81 | 0.64 | 0.46 |

Through visual assessment, the model reasonably captured the timing and magnitude of monthly surface runoff peaks, with slightly decreased performance for tile flow (*Figure 3.3*). Although the model generally simulated NGS surface runoff well, there were some irregularities in October of 2013 and 2015. The model simulation of tile drainage was erratic in summer and winter but was generally good in the spring and fall. There were several tile drain responses that the model had difficulty simulating (February 2013, January 2014, March 2014, and June 2012 and 2013). The winter events were associated with cold conditions/snowmelt. Despite these events that were missed by the model, runoff coefficients in 2013 and 2015 simulated by the model were 0.29, which is close to the observed runoff coefficients of 0.33.

Other water balance components were representative of southern Ontario conditions, where evapotranspiration (ET) was ~54% (42 to 66% ) of the average annual precipitation over the 2012-2015 period (Table 3.2), which was within the range reported by Parkin et al., 1999. With tiles shallow aquifer recharge is 7% and when removed ~11.3% (range: 10 to 15%) of the annual precipitation over the 4 years, which is close to the ~15% expected for silt and clay soils in Ontario (Table 2; David Rudolph, personal comm.).

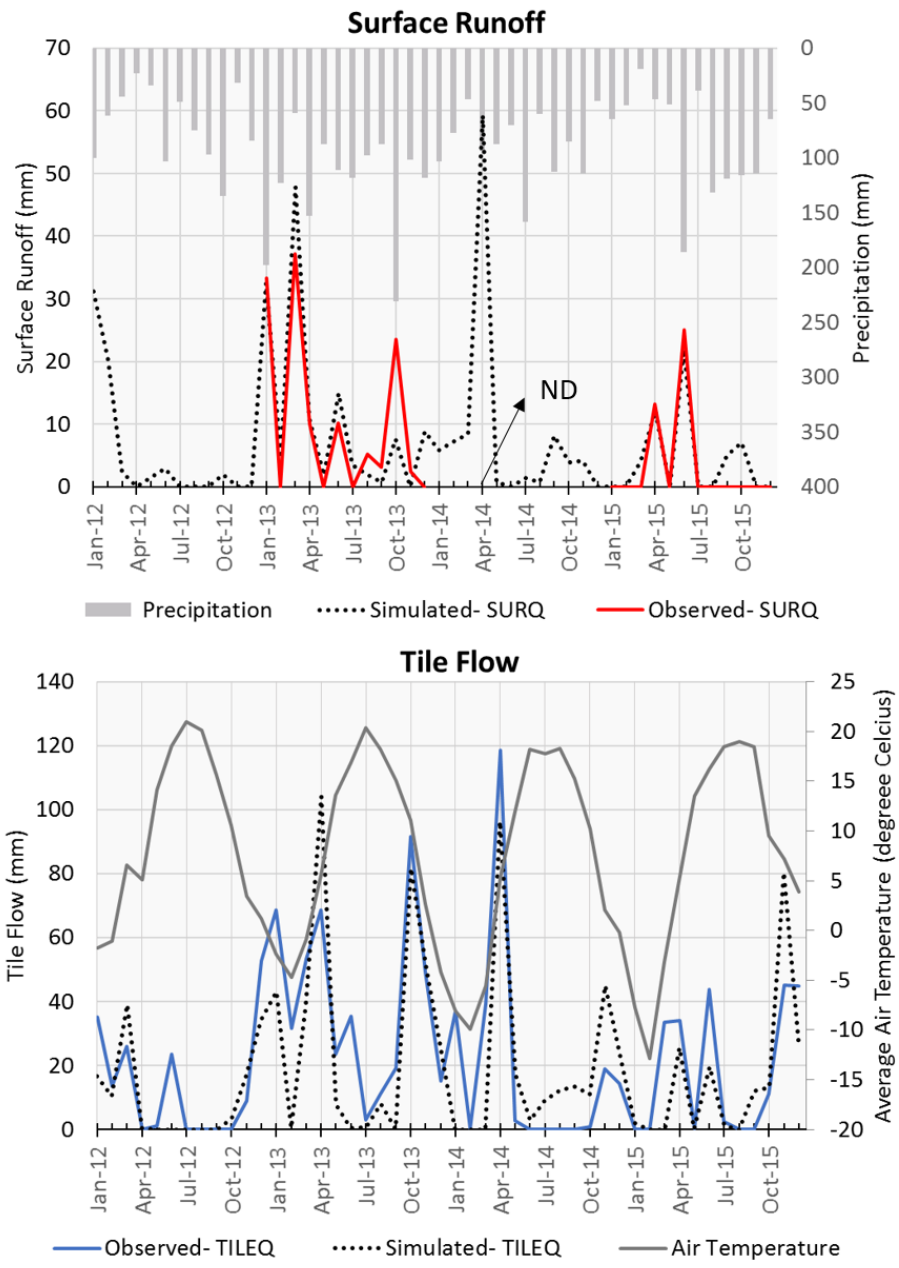


*Figure 3.3.* Graphical performance of surface runoff (top; SURQ) and tile flow (bottom; TILEQ) after calibration of the LON HRU model. In addition to performance, it shows monthly precipitation (top) and average air temperatures (bottom) over the 2012 to 2015 period. Arrow with ND indicates no data due to sensor failure.

### 3.3.2 Effects of modified tile depths on runoff and flow paths

The depth of tile drains was modified in the model to simulate the effects of (a) no tile drainage and (b) continuously controlled drainage ($RTD_{cont}$) on both runoff magnitude and the reallocation of precipitation

among the pathways (e.g. surface runoff, tile drainage, groundwater recharge). Altering the tile drain depths modified both the total water yield ($RTD_{cont}$, 4% decrease) as well as the flow paths through which the runoff moved. Raising the tile drain depths from 84 cm to 50 cm resulted in reduced tile drainage by 41 mm (22%), of which 55% was redistributed to surface runoff and 24% to aquifer recharge, with minor changes in ET and lateral flow. A similar reallocation was observed when tile drains were removed from the model altogether, with the 224 mm change in tile flow largely redistributed to surface runoff (57%) and lateral flow (5%). However, there was a 4% decrease in the shallow aquifer redistribution, and 3% increase in tile flow redistributed as ET compared with the raised tile scenario.

*Table 3.2.* Average annual water balance with permanent changes in the tile height for the 2012 to 2015 period

| Water Balance | Free Tile Drainage (FTD; 840 mm) | | Raised Tile Drainage ($RTD_{cont.}$; 500 mm) | | No Tiles (0 mm) | |
|---|---|---|---|---|---|---|
| | mm | % | mm | % | mm | % |
| Precipitation | 1097 | 100 | 1097 | 100 | 1097 | 100 |
| Surface runoff | 86 | 8 | 109 | 10 | 214 | 20 |
| Lateral soil Q | 14 | 1 | 16 | 1 | 25 | 2 |
| Tile Q | 224 | 20 | 183 | 17 | 0 | 0 |
| Total aquifer recharge | 77 | 7 | 87 | 8 | 124 | 11 |
| Total water yield | 342 | 31 | 328 | 30 | 268 | 24 |
| ET | 594 | 54 | 594 | 54 | 604 | 55 |

There were seasonal trends in how the reduced tile drainage was reallocated. For example, in general, most tile flow was redistributed to surface runoff during the winter, early spring, and late fall months (i.e. the NGS), whereas during the GS, the reduced tile flow was typically redistributed to aquifer recharge (Figure 3.4) and rarely resulted in increased surface runoff. Although this general pattern existed, there was variability among years within the NGS, demonstrating the complexity associated with simulating winter runoff generation. For example, more surface runoff was observed in the winter (JFM) months of 2012 (a dry year with 871 mm annual precipitation) than during a wetter year (2015, 1003 mm annual precipitation) due to the fact that temperatures were warm in 2012 (9 $^{o}$C) and 71 mm more precipitation was received

during the winter months of 2012 than 2015, despite the fact that both years received less winter precipitation than normal (Figure 3; Environment and Climate Change Canada, 2018a).

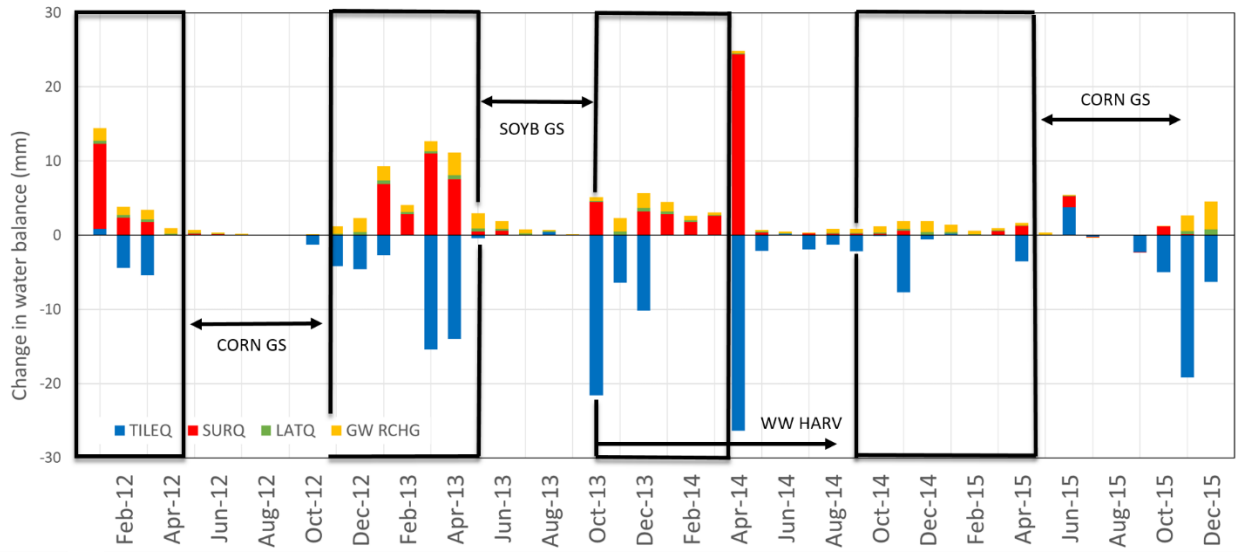


*Figure 3.4.* Monthly changes in the water balance over the 2012 to 2015 period with continuously raised tiles ($RTD_{cont}$). Bars show the difference between $RTD_{cont}$ and the free tile drainage (FTD) scenario (840 mm. A positive value denotes an increase in flow and a negative denotes a reduction in flow. Black bars indicate the growing season over the study period and boxes showing the NGS.

Examples of seasonal differences in flow path responses to raised tile drains are illustrated in Figure 3.5, which contrasts a rain on snowmelt event, where temperatures were below freezing but rose in combination with a large precipitation event (Figure 3.5a), with a summer thunderstorm that was preceded by multiple smaller events (Figure 3.5b). With RTD, this increased surface runoff by 6.2 mm, and soil moisture by 5.9 mm. For the large precipitation event in summer (Figure 3.5b), tile drainage and soil moisture with RTD have opposing responses. However, contrary to Figure 3.5a, there was no difference in the surface runoff between FTD and RTD. Key dissimilarities between the two events include the temperature, which affects the PET. Average PET in the 2012 and 2014 event was 1 and 3.4 mm respectively. Additionally, the average soil moisture, which was on average 10 mm greater during the dates shown in March 2013.

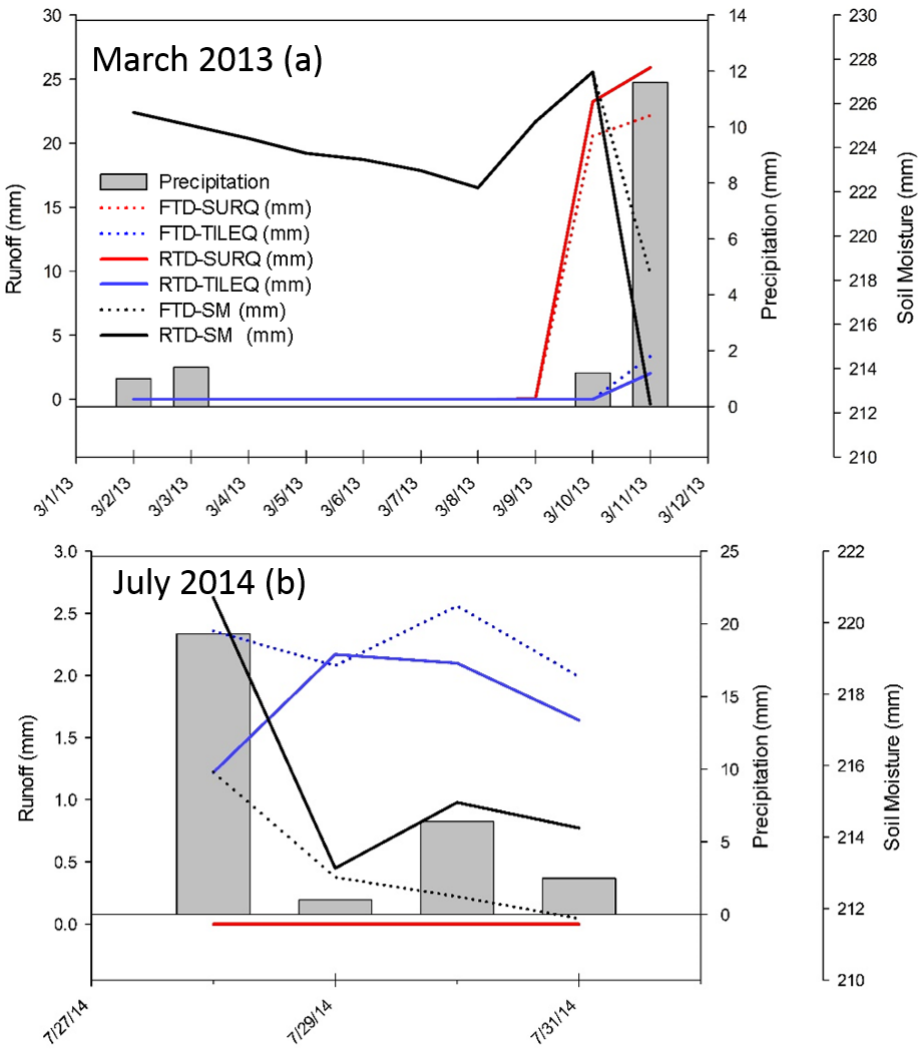


*Figure 3.5.* Shows two different months, one event during the NGS (spring) and the other during the summer on a daily time step. (a) March 2013 was the month with the highest observed surface runoff (SURQ; red) in the NGS, while (b) July 2014 was an example of a typical event in summer. The free tile drainage (FTD; DDRAIN = 840 mm; dotted line) and raised tile drainage (RTD; DDRAIN =500 mm; solid line) scenarios were compared. Soil moisture content (SM; black) and tile flow (TILEQ; blue) responses are also plotted.

### 3.3.3 Effects of controlled tile drain management on runoff and phosphorus export

The patterns discussed previously in this study had the same treatment year-round (i.e. free-drainage, raised tiles or no tile). However, as noted earlier, controlled drainage can be managed differently across seasons. In the model, the $RTD_{GS}$ scenario (free drainage within the NGS but raised to 500mm in the GS) and $RTD_{NC}$ scenario (drainage controlled year-round near continuously, with tile depths raised to

500mm; Figure 3.2) both resulted in very small decreases in annual runoff ($RTD_{GS}$ = 2%, $RTD_{NC}$ = 5%) relative to the FTD scenario. The subtle difference in flow reduction between the $RTD_{NC}$ and $RTD_{GS}$ scenarios was because the increase in surface runoff (44 mm cumulative total over study period, largely during the NGS) offset the decrease in tile flow (cumulative decrease 84 mm over study period).

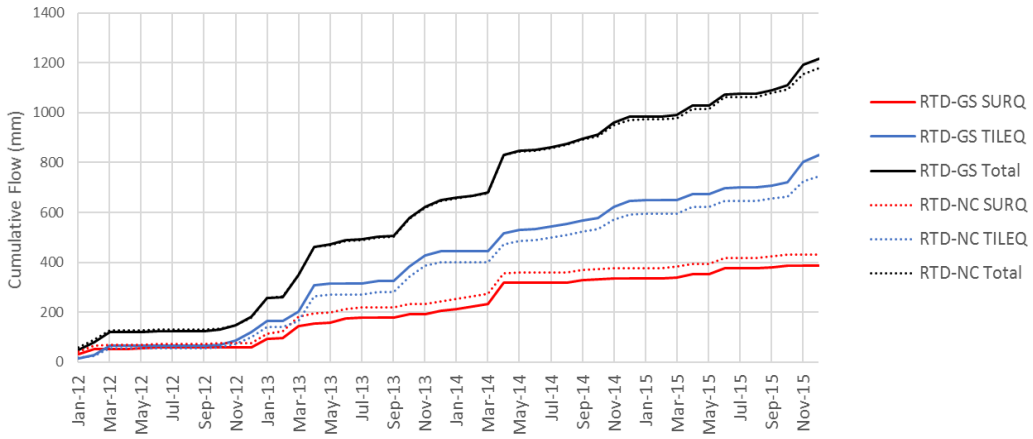


*Figure 3.6.* Cumulative tile flow (TILEQ; blue), surface runoff (SURQ; red), and total runoff (black) for $RTD_{GS}$ (solid line) and $RTD_{NC}$ (dotted line) over the 2012 to 2015 period

Because the SWAT model cannot yet simulate P in tile drainage, hypothetical changes in edge-of-field TP loss under different controlled drainage scenarios were estimated using observed field data (seasonal average flow-weighted mean concentrations, FWMC, Table 3.3) applied to the different flow paths (Figure 3.7). At the study site, FWMC of TP in surface runoff were typically ~10x greater than in tile flow (e.g. Van Esbroeck et al., 2017; Plach et al., 2018). Consequently, given that $RTD_{GS}$ and $RTD_{NC}$ have surface increases they have a 0.2 Kg TP $ha^{-1}$ (8%) and 0.32 Kg TP $ha^{-1}$ (13%) load increase respectively in runoff relative to the FTD scenario. Given that tile drainage P export was a smaller component of the edge of field loss to begin with and FWMC were smaller, tile flow reductions did little to reduce TP losses, whereas small increases in surface runoff increased TP losses considerably. Of the two CD scenarios, $RTD_{NC}$ increased surface runoff and TP export by more compared to $RTD_{GS}$ because this mostly occurred in the NGS. The increase in surface runoff under the $RTD_{NC}$ scenario (Figure 3.6) compared to the $RTD_{GS}$ scenario resulted in a cumulative increase in TP in surface runoff of 0.18 Kg TP $ha^{-1}$ than was simulated

under scenario $RTD_{GS}$, Figure 3.7). In contrast, the tile flow reduction associated with scenario $RTD_{NC}$ (Figure 3.6) only led to a cumulative reduction in tile flow TP export of 0.06 Kg TP $ha^{-1}$ relative to $RTD_{GS}$. While cumulative SRP losses were on average 29 and 45 percent of TP in tile flow and surface runoff for all scenarios, with runoff losses increasing almost correspondingly to TP ($RTD_{GS}$ 12% and $RTD_{NC}$ 15% increase relative to FTD).

*Table 3.3.* Summarized TP and SRP FWMCs from the field site used to create estimates of TP export from the surface runoff and tile flow paths

Surface Runoff FWMC

| Season | TP (mg/L) | SRP (mg/L) | SRP:TP Ratio |
|---|---|---|---|
| Winter | 0.54 | 0.10 | 0.18 |
| Spring | 0.68 | 0.41 | 0.60 |
| Summer | 0.80 | 0.24 | 0.30 |
| Fall | 0.25 | 0.12 | 0.47 |

Tile Flow FWMC

| Month | TP (mg/L) | SRP (mg/L) | SRP:TP Ratio |
|---|---|---|---|
| Jan | 0.037 | 0.004 | 0.11 |
| Feb | 0.004 | 0.003 | 0.72 |
| Mar | 0.074 | 0.020 | 0.27 |
| Apr | 0.102 | 0.045 | 0.44 |
| May | 0.025 | 0.001 | 0.05 |
| Jun | 0.024 | 0.003 | 0.13 |
| Jul | 0.016 | 0.0001 | 0.01 |
| Aug | 0.023 | 0.007 | 0.32 |
| Sep | 0.050 | 0.003 | 0.06 |
| Oct | 0.054 | 0.018 | 0.33 |
| Nov | 0.105 | 0.066 | 0.63 |
| Dec | 0.170 | 0.034 | 0.20 |
| Average | 0.057 | 0.017 | 0.274 |

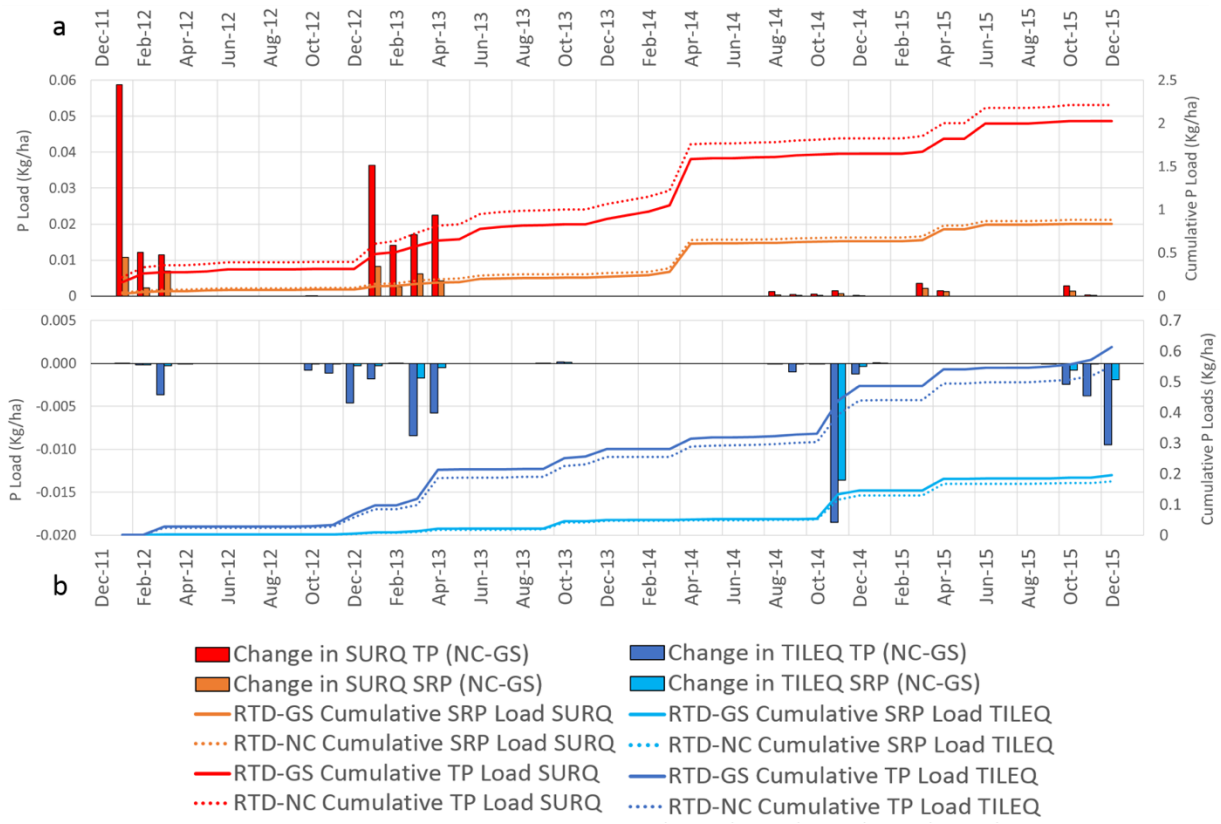


*Figure 3.7.* Shows the monthly cumulative loads (lines) and change in loads between $RTD_{GS}$ and $RTD_{NC}$ from 2012 to 2015 for TP and SRP in surface runoff (SURQ; a) and tile flow (TILEQ; b)

## 3.4 Discussion

### 3.4.1 SWAT HRU performance

The model performed adequately with respect to tile flow and surface runoff to perform the subsequent analysis. These results are comparable to a study by Guo et al. (2018) where tile flow performance with respect to the NS ranged from 0.53 to 0.61 and 0.50 to 0.81 for surface runoff. Some of the performance issues may be explained by model inputs. The uncertainty associated with soil conditions at depth and the location of the impervious layer impacted the calculations of percolation, water table depth, and tile flow (Neitsch et al., 2011). In winter, precipitation data was supplemented by the nearby Jamestown station data (43 km away from site, Figure 3.1) because snowfall was not measured continuously at the field site, and consequently, may have varied slightly from what occurred at the site.

Tile performance issues could also be explained through model structure. For example, in February 2013 there is no surface runoff probably because of precipitation being added to the snowpack. This should increase the soil temperatures and allow for the tile flow response that was observed because winter soils are typically at field capacity or saturated (Lam et al., 2016). However, within the model, when soil layer is frozen, water movement does not occur (Neitsch et al., 2011). This indicates that there might be issues with the soil temperature calculations in SWAT. The model is unable to capture this response due to the known simplicity of the empirically based soil temperature algorithm, and its inability to simulate soil temperatures in cold regions with regular of freeze-thaw conditions (Qi et al., 2016). As well, SWAT had performance issues in summer due to underperforming soil water estimation (Rajib & Merwade, 2016) and erratic water table estimation related to dryer soils (Moriasi et al., 2009).

In summer, it is uncertain if macropore flow is a large contributor to tile flow at the field site, which is a clay loam. Furthermore, there was no surface runoff data from the summer of 2014 to confirm if infiltration was overestimated. In October 2015, it is uncertain what caused the overestimation of surface runoff since precipitation data was from the nearby Jamestown station (Figure 3.1), which cannot be validated using field site data. However, similar precipitation events in October 2013 were validated with field data, and the small 4% difference indicates another reason. The poor validation performance is most likely due to the limited time span of the dataset that did not capture a range of wet, dry, and average years for validation.

### 3.4.2 Impact of CD on flow paths and TP export

The results of this study suggest that the use of CD throughout the NGS may increase annual TP losses in runoff (8 to 13%) and could exacerbate eutrophication; however, the use of CD during the GS has relatively little effect on TP losses. These results are in contrast to Tan and Zhang (2011) who predicted a 12% decrease in annual TP losses over their study period. The primary difference between the current study and the work of Tan and Zhang (2011) is that the current study was conducted in coarser textured soils on sloping ground, whereas the study by Tan and Zhang (2011) was conducted in lacustrine clays. Indeed, the

current study reported a very different water balance distribution than Tan and Zhang (2011) who reported that 97% of runoff (tile flow and surface runoff) occurred as tile flow with FTD. Other differences between the two studies include narrower tile spacing (3X narrower) and the use of sub-irrigation at the clay site.

The current study has shown that any decrease in tile depth (either no tiles, $RTD_{NC}$, or $RTD_{GS}$) will reduce the drainable soil water volume and lead to decreased tile flow, which increases the amount of soil water and precipitation redistributed as surface runoff. This finding is consistent with what has been shown in other studies (Ross et al., 2016; Skaggs et al. 2012; Tan & Zhang, 2011). Although, the extent of which this occurs will differ due to a number of field and climate related factors. With CD, the amount of precipitation redistributed as surface runoff will increase with slower aquifer recharge rates since less soil water will be lost through this pathway and soil moisture levels can remain higher. Furthermore, drain spacing, drain depth, and NGS management can significantly influence tile flow reductions; consequently, the surface runoff response (Ross et al., 2016). This is reflected by Golmohammadi et al. (2016b) where tile flow reductions were similar to $RTD_{NC}$ (2% difference); conversely, their surface runoff increase was much greater, which indicates other influencing factors like climate and soil storage capacity. Youseff et al. (2018) have also predicted larger increases in surface runoff (average 120%); however, FTD yearly average surface runoff was also only 39 mm $yr^{-1}$, and the initial tile distribution was almost double the spacing and depth. Additionally, even though the surface runoff increase was not as large as other studies or greater than the tile flow reduction, the larger FWMC in surface runoff offset the TP reductions from tile flow. With CD, typically it is installed and recommended on low sloping fields; nevertheless, there are many other factors to consider and these will also be key in making comparisons or deciding whether CD is feasible considering the large surface runoff increases reported in other studies

In our study, $RTD_{GS}$ exported less TP in runoff than $RTD_{NC}$ relative to FTD because of reduced surface runoff in the NGS. Surface runoff increases in the $RTD_{NC}$ scenario during the NGS resulted from the higher soil water levels, decreasing the water table depth from the surface and making saturation excess surface runoff a greater risk. This response was typically spread out over the entire winter or did not occur

in every year, because the southern Ontario climate facilitates multiple snowmelt events with a wide range of pre-event soil conditions and precipitation form variability in the NGS (Van Esbroeck et al., 2017). In the summer, surface runoff does not increase much, because the model calculates the surface runoff using the SCS-CN method (Soil Conservation Service, 1972) where the curve number (CN) and retention parameter is updated using PET and the previous day's parameter (Neitsch et al, 2011). Therefore, high PET values result in a reduction of the CN compared to winter, increasing the infiltration for the day. As a consequence of increased PET, soil water levels are initially very low and even though precipitation intensity might be greater, it requires substantially more rain and reduced PET to trigger surface runoff. The positive increase of water in soil storage because of decreased tile flow with RTD (Figure 3.5a) confirms this, since surface runoff increases almost proportionally.

How tiles are managed during the winter NGS will be increasingly important since they can increase surface runoff and TP loads, contrary to the GS where there are benefits of using CDs (Sunohara et al., 2015, 2016). Furthermore, in humid climates, most N leaching occurs during the winter (Bohne, Storchenegger, & Widmoser, 2012) and P losses as well (Macrae et al., 2007b; Van Esbroeck et al., 2017; Williams et al., 2016). This will provide some management challenges due to the variability in responses to CD, and the clear benefits in NO3 export (Drury et al., 2009; Ross et al., 2016). In our study, CD results indicate that cumulative TP runoff losses could be reduced by 4% (or more) if tiles were free draining during a portion (Oct. to late May) of the time winter wheat is planted, which suggests that CD with winter wheat might not be beneficial for TP losses in LON. Furthermore, due to a large increase in FWMC because of the primary P application occurring at the end of wheat harvest CD during November 2014, $RTD_{GS}$ loads could have been reduced further. Finally, due to the winter weather there will be variability in the 2012 (warm and dry) NGS versus 2015 (cold and dry) affecting surface runoff responses to CD and TP export, which suggests that prediction of precipitation form and quantity during the NGS will be useful in determining the management of controlled tile drains and impact on surface runoff.

Phosphorus load estimation was based on observed FWMCs that generally had low SRP:TP FWMC ratios (<0.5). Overall, this caused SRP export to be a smaller fraction of TP loads in both tile and surface runoff (Table 3.3; Figure 3.7). Both SRP and TP are projected to increase; however, there was very little effect on SRP:TP export ratios in runoff (0.5 to 1.5 % increase), which is important as more significant increases in SRP:TP ratios could further increase the risk of algae growth. Although P is mostly driven by flows (Sunohara et al., 2010), in the RTD scenarios, there is potential for increased SRP:TP ratios as prolonged waterlogged conditions create anoxic conditions, which could increase the desorption of Fe and Ca bound P and mineralization of organic P (Ardón et al., 2010; Van Dijk et al., 2011; Yaghi & Hartikainen, 2013).

### 3.4.3 Conclusion

In this study, SWATs new tile flow routines were assessed at the HRU scale. Then the impact of CDs on flow pathways, SRP, and TP export was analyzed for a clay loam soil in southern Ontario. The H-K-DC routine performed well, but the SWAT model still needs improvement simulating soil temperatures in the NGS. Overall, year round tile management ($RTD_{NC}$) causes an increase in average annual surface runoff (26%) and edge of field TP losses (13%) over the study period, specifically due to the increase in NGS (January to April) surface runoff. Tile management practices that keep the water table lower most of the year ($RTD_{GS}$) may not have as great an impact on TP losses in runoff (4 to 8% increase) or surface runoff volumes (8 to 13% increase). However, any TP increase still corresponds to increased potential for SRP losses, which is the P form with the greatest risks. Furthermore, controlled drainage management should not be planned strictly based on the rotation's planting and harvest dates, but nutrient contaminant risks. Tile drain management during the NGS does have potential to reduce both N and P loads depending on the resulting water balance redistribution and FWMC in runoff pathways, which have been shown to be variable depending on many factors. In future CD and P assessments for this region, spatial variations in large-scale adoption over a varied landscape with predominantly low slopes (<1 %) and a longer period should be assessed. Controlled drainage may provide many benefits with respect to tile drainage water

quality; however, care should be taken when deciding on how to best manage the tile drains in the NGS considering the effects it can have on surface runoff P export.

## Chapter 4 - Major conclusions of thesis

Within the Great Lakes drainage area non-point source (NPS) nutrient contamination from agricultural activities has been attributed to increased eutrophication sometimes causing harmful algae blooms impairing water quality (EPA, 2015; Jarvie et al., 2013; Michalak et al., 2013). Currently, most of the annual nutrient export occurs during the non-growing season (NGS), specifically early spring (Macrae et al., 2007b; Van Esbroeck et al., 2017; Williams et al., 2016). Furthermore, due to climate change the hydrological and biogeochemical cycles are expected to be impacted, further affecting water quantity and quality. Therefore, the objectives in *Chapter 2* were to use the Soil Water Assessment Tool (SWAT) to quantify the seasonal export of nutrients and sediment with climate change and to understand the processes driving the projected changes to make watershed management more effective over the long-term.

Results from *Chapter 2* suggest that there will be a decrease in average annual streamflow. However, despite this decrease, changing precipitation characteristics and temperature will still cause increases in annual nutrient export and runoff. This is in contrast to other studies that report increases in nutrient export due to climate change causing increased streamflow and precipitation volumes (Bosch et al., 2014; Crossman et al., 2013; Verma et al., 2015). The apparent increase in nutrient fluxes under decreased annual flows can partially be attributed to the increase in the magnitude and frequency of extreme precipitation events that can also increase the size of the peak flows. *Chapter 2* also showed that air temperatures will increase in all seasons, particularly in winter. This will decrease the number of soil frost days (Sinha & Cherkauer, 2010) and increase the amount of snow expected as rain (Marianne et al., 2003). In the Medway Creek watershed (MCW) this will modify the flow paths and streamflow, where less soil frost will allow more water to pass through the vadose and saturated soil zones, reducing surface runoff volumes, stream flow response times for most events, and the average stream flow in winter. Furthermore, the potential for less snow and more drainage in winter will reduce water availability and surface runoff in spring. Due to this shift in seasonality, the timing of residual nutrient export will also shift towards the winter months causing the largest nutrient export increases (nitrate and TP). Suspended sediment (SS) export at the

watershed outlet will be limited by surface runoff, the transport capacity of the stream, and average streamflow, resulting in decreased SS export in winter and spring.

Within agricultural settings, best management practices (BMP) are implemented to help reduce contamination while still maintaining productive crops (i.e. tile drainage). Recently, controlled tile drainage (CD) has been used in some areas to help reduce tile flow phosphorus and nitrogen export (Lavaire et al., 2017; Skaggs et al., 2012; Sunohara et al., 2016). However, little is known about the export response when all runoff pathways are considered. Recent work, including this thesis, suggests that understanding the water balance and nutrient export responses during the NGS will be important. Therefore, the objective of *Chapter 3* was to simulate the effects of CD management on runoff quantity and flow paths using SWAT, and to quantify potential water quality tradeoffs such as increased surface runoff P export associated with CD management.

Results from *Chapter 3* shows that total phosphorus (TP) and soluble reactive phosphorus export will increase if tiles are managed, in contrast to other studies that have explored TP export in tile drainage and surface runoff (Tan & Zhang, 2011; Zhang et al., 2017). The difference between the current study and the work of Tan and Zhang, 2011 and Zhang et al., 2017, is that their work was conducted in flat, lacustrine clays whereas the current study was conducted in a sloping clay loam. This suggests that the effects of CD as a BMP may vary regionally. This thesis showed that although the decreases in tile flow exceeded the increases in surface runoff volume when CD management was employed, the significantly greater FWMC in surface runoff resulted in an overall increase in runoff TP. Thus, the use of CD exacerbated water quality issues in the model simulations. In the model, most of the TP export occurred over the NGS, as this was when most of the surface runoff increases occurred in response to CD, wetter soils, and decreased water demand. Consequently, the use of CD during the GS only offset the water quality issues associated with elevated surface runoff during the NGS, but did little to improve water quality as so little flow occurs during the GS.

Overall, both chapters indicated that weather characteristics in the NGS will have a major impact on the behavior of the flow paths and nutrient export. However, the assimilation of both CD and climate change on nutrient export is yet to be determined. Therefore, the field scale SWAT model was forced with the MCW historical and future climate to speculate on what may occur to nutrients and sediment at the edge of field if CD were used in a future climate.

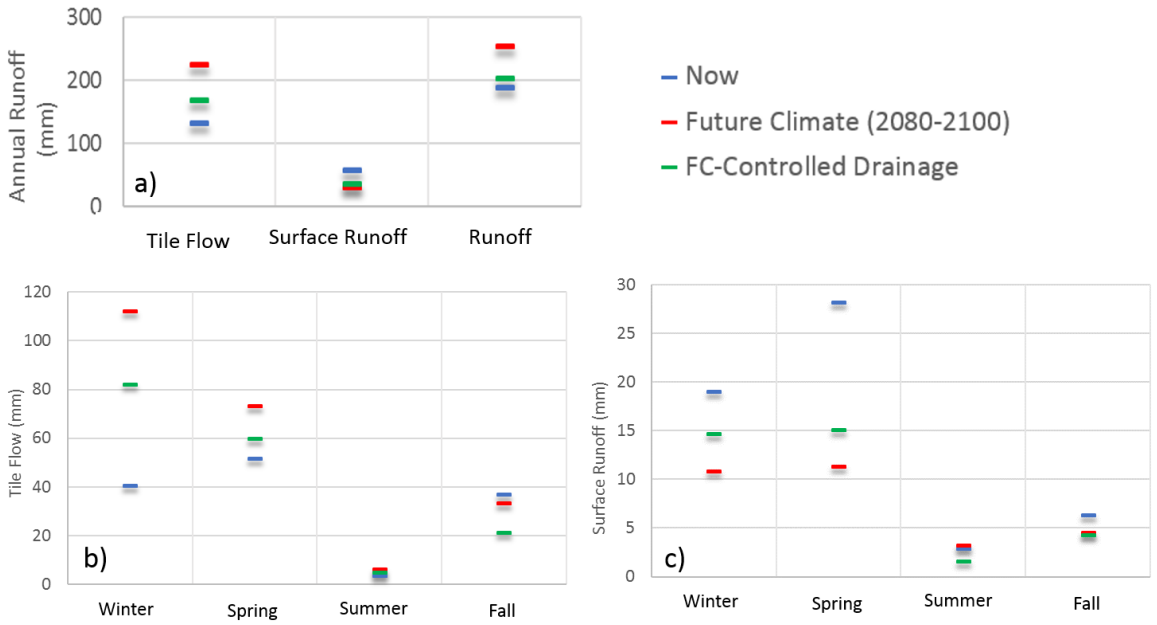


*Figure 4.1.* (a) Shows the changes in the tile flow, surface runoff, and runoff (tile flow + surface runoff) annually in the LON field site transplanted into the MCW during the 1990-2010 period (blue), 2080-2100 period (red), and 2080-2100 period with continuous CD (green). Also, shows tile flow seasonally (b) and surface runoff seasonally (c).

On an annual basis, water balance changes due to CD and climate change are very similar to what was observed in *Chapters 2 and 3*. Since runoff remains greater with CD in the future climate due to water surpluses, this suggests that CD will most likely exacerbate annual TP export trends. Indeed, the increase in surface runoff caused by CD (Figure 4.1a) and will only increase the potential for greater and more occurrences of saturation excess overland flow events, which is a major factor in TP export from fields. In the case of $NO_3^-$, average $NO_3^-$concentrations were almost equivalent between tile flow and surface runoff pathways at Londesborough. Therefore, because the decrease in tile flow is greater than the increase in surface runoff, there could be a net reduction in $NO_3^-$ export under a future climate. Although, CD promotes

anaerobic conditions that increase the potential for denitrification (Skaggs et al., 2010; Wesström & Messing, 2007) the exact effect of climate change on denitrification is unknown (Barnard et al., 2005). When combined, we could expect further decreased nitrate losses due to increased denitrification rate from increased soil moisture and temperature; however, there are many other complex feedbacks to consider (Karmakar et al., 2016; Singh et al., 2010; Veraart et al., 2011). Consequently, either CD management scenario will provide nitrate reductions and near continuous management ($RTD_{NC}$) will have the greatest reduction due to larger tile flow reductions throughout the year.

Similar to *Chapter 2 and 3* we will see the majority of the hydrologic changes occurring in the winter, with surface runoff increases due to CD in a future climate (Figure 4.1c). Considering the large-scale adoption of CD in the MCW, based on the above and the watershed characteristics, $RTD_{NC}$ might not be feasible for the reduction of P in the MCW. Furthermore, considering CD installed selectively on agricultural land that was low sloped (<1%) and nutrient losses at the watershed scale. If surface runoff losses were minimal during the NGS and the tile flow reductions managed to reduce TP losses, it might not make a significant difference relative to the projected future increases in TP when also considering that only 23% of the tiled-drained land has low slopes. Finally, during the summer hydrological changes are much smaller in comparison to winter and spring. Therefore, if losses can be reduced when it matters most (i.e. winter) the risk of using $RTD_{GS}$ might be increasingly necessary to prevent economic and excessive crop yield losses due to drought. With increased potential for heat waves (Li et al., 2017), CD can provide crop yield benefits through water storage (Poole et al., 2013; Sunohara et al., 2016).

More work is needed on this topic as the precise responses of fields and watersheds to CD and climate change will be spatially variable given that runoff and nutrient loss are dependent on many field specific characteristics such as tile spacing and depth, NGS management depth, FWMC runoff ratios, slope, soil characteristics and specific land management practices. Therefore, future work should confirm the effect of large-scale adoption of CD and climate change on TP export in watersheds that have fields with different characteristics (i.e. tile layouts and NGS management) and in combination with other BMPs.

However, in order to do this, SWAT needs some improvement, mainly to the soil temperature and TP tile routing algorithm given the winter season responses found in this study.

Overall, this study has demonstrated the importance of understanding the effects of future climates and BMPs on NPS contamination so that management strategies can be implemented more effectively now and in future. Moreover, this thesis has further enforced the importance of understanding the processes and factors controlling the NGS nutrient export responses. Finally, it is clear that BMPs limiting NGS nutrient export will be increasingly important in reducing eutrophication. Specifically reducing their availability for transport (i.e. cover crops) and balancing crop nutrient needs (4Rs) within the soil due to the decreased mitigation efficacy caused by future climatic drivers. Controlled drainage as a mitigation strategy should be used with caution given its potential to exacerbate water quality issues under larger flow events due to greater surface runoff.

## References


Abbaspour, K. C. (2015). *SWAT - CUP: SWAT Calibration and Uncertainty Programs-A User Manual*. Eawag: Swiss Federal Institute of Aquatic Science and Technology.

Abbaspour, K. C., Rouholahnejad, E., Vaghefi, S., Srinivasan, R., Yang, H., & Kløve, B. (2015). A continental-scale hydrology and water quality model for Europe: Calibration and uncertainty of a high-resolution large-scale SWAT model. *Journal of Hydrology*, *524*, 733–752. http://doi.org/10.1016/j.jhydrol.2015.03.027

Abbaspour, K. C., Yang, J., Maximov, I., Siber, R., Bogner, K., Mieleitner, J., … Srinivasan, R. (2007). Modelling hydrology and water quality in the pre-alpine/alpine Thur watershed using SWAT. *Journal of Hydrology*, *333*(2–4), 413–430. http://doi.org/10.1016/j.jhydrol.2006.09.014

Agriculture and Agri-Food Canada. (2016). *Annual Crop Inventory 2014*. [Data file]. Retrieved from https://open.canada.ca/data/en/dataset/ae61f47e-8bcb-47c1-b438-8081601fa8fe

Ahmadi, M., Records, R., & Arabi, M. (2014). Impact of climate change on diffuse pollutant fluxes at the watershed scale. *Hydrological Processes*, *28*(4), 1962–1972. http://doi.org/10.1002/hyp.9723

Ale, S., Bowling, L. C., Youssef, M. A., & Brouder, S. M. (2012). Evaluation of Simulated Strategies for Reducing Nitrate–Nitrogen Losses through Subsurface Drainage Systems. *Journal of Environmental Quality*, *41*(1), 217. http://doi.org/10.2134/jeq2010.0466

Alexander, C. (1988). *ADAPT—A model to simulate pesticide movement into drain tiles* (Master's thesis). Retrieved from https://etd.ohiolink.edu/!etd.send_file?accession=osu1145373108&disposition=inline

Andreini, M. S., & Steenhuis, T.S. (1990). Preferential paths of flow under conventional and conservation tillage. *Geoderma*, *46*, 85-102. http://doi.org/10.1016/0016-7061(90)90009-X

Arbuckle, K. E., & Downing, J. A. (2001). The influence land use on lake N : P in a predominantly of watershed agricultural landscape. *Limnology and Oceanography*, *46*(4), 970–975.

Ardón, M., Montanari, S., Morse, J. L., Doyle, M. W., & Bernhardt, E. S. (2010). Phosphorus export from a restored wetland ecosystem in response to natural and experimental hydrologic fluctuations. *Journal of Geophysical Research: Biogeosciences*, *115*, 1–12. http://doi.org/10.1029/2009JG001169

Arenas Amado, A., Schilling, K. E., Jones, C. S., Thomas, N., & Weber, L. J. (2017). Estimation of tile drainage contribution to streamflow and nutrient loads at the watershed scale based on continuously monitored data. *Environmental Monitoring and Assessment*, *189*(9). http://doi.org/10.1007/s10661-017-6139-4

Arnold, J. G., Kiniry, J. R., Srinivasan, R., Williams, J. R., Haney, E. B., & Neitsch, S. L. (2012a). *Soil and Water Assessment Tool: Input/Output Documentation, version 2012*.

Arnold, J. G., Moriasi, D. N., Gassman, P. W., Abbaspour, K. C., White, M. J., Srinivasan, R., … Jha, M. K. (2012b). SWAT: Model Use, Calibration, and Validation. *American Society of Agricultural and Biological Engineers*, *55*(4), 1491–1508.

Arnold, J. G., Youssef, M. A., Yen, H., Sheshukov, A. Y., Sadeghi, A. M., Moriasi, D. N., … Gowda, P. H. (2015). Hydrological Processes and Model Representation: Impact of Soft Data on Calibration. *American Society of Agricultural and Biological Engineers*, *58*(6), 1637–1660. http://doi.org/10.13031/trans.58.10726

Ball Coelho, B., Murray, R., Lapen, D., Topp, E., & Bruin, A. (2012). Phosphorus and sediment loading to surface waters from liquid swine manure application under different drainage and tillage practices. *Agricultural Water Management*, *104*, 51–61. http://doi.org/10.1016/j.agwat.2011.10.020

Barnard, R., Leadley, P. W., & Hungate, B. A. (2005). Global change, nitrification, and denitrification: A review. *Global Biogeochemical Cycles*, *19*(GB1007), 1–13. http://doi.org/10.1029/2004GB002282

Bauwe, A., Kahle, P., & Lennartz, B. (2016). Hydrologic evaluation of the curve number and Green and Ampt infiltration methods by applying Hooghoudt and Kirkham tile drain equations using SWAT. *Journal of Hydrology*, *537*, 311–321. http://doi.org/10.1016/j.jhydrol.2016.03.054

Beauchemin, S., Simard, R. R., & Cluis, D. (1998). Forms and Concentration of Phosphorus in Drainage Water of Twenty-Seven Tile-Drained Soils. *Journal of Environment Quality*, *27*(3), 721. http://doi.org/10.2134/jeq1998.00472425002700030033x

Bengtson, R. L., Carter, C. E., Fouss, J.L., Southwick, L.M., & Willis, G.H. (1995). Agricultural drainage and water quality in the Mississippi delta. *Journal of Irrigation and Drainage Engineering*, *121*(4), 292–295. http://doi.org/10.1061/(ASCE)0733-9437(1995)121:4(292)

Beven, K. (2001). *Rainfall-runoff modelling: The primer*. *Benchmark papers in hydrology*. Chichester, U.K.: John Wiley and Sons.

Beven, K. (2006). A manifesto for the equifinality thesis. *Journal of Hydrology*, *320*(1–2), 18–36. http://doi.org/10.1016/j.jhydrol.2005.07.007

Beven, K., & Binley, A. M. (1992). The future of distributed models: model calibration and uncertainty estimation. *Hydrological Processes*, *6*, 279–298.

Bingham, M., Sinha, S. K., & Lupi, F. (2015). *Economic benefits of reducing harmful algal blooms in Lake Erie*. Retrieved from http://ijc.org/files/tinymce/uploaded/Publications/Economic-Benefits-Due-to-Reduction-in-HABs-October-2015.pdf

Bohne, B., Storchenegger, I. J., & Widmoser, P. (2012). An easy to use calculation method for weir operations in controlled drainage systems. *Agricultural Water Management*, *109*, 46–53. http://doi.org/10.1016/j.agwat.2012.02.005

Bolster, C. H., & Sistani, K. R. (2009). Sorption of phosphorus from swine, dairy, and poultry manures. *Communications in Soil Science and Plant Analysis*, *40*(7–8), 1106–1123. http://doi.org/10.1080/00103620902753822

Bolton, E. F., Aylesworth, J. W., & Hore, F. R. (1970). Nutrient loses through tiled rains under three cropping systems and two fertility levels on a Brookston clay soil. *Canadian Journal of Soil Science*, *50*, 275–279. http://doi.org/10.4141/cjss70-038

Bosch, N. S., Evans, M. A., Scavia, D., & Allan, J. D. (2014). Interacting effects of climate change and agricultural BMPs on nutrient runoff entering Lake Erie. Journal of Great Lakes Research, *40*(3), 581–589. http://doi.org/10.1016/j.jglr.2014.04.011

Boström, B. (1984). Potential Mobility of Phosphorus in Different Types of Lake Sediment. *Internationale Revue Der Gesamten Hydrobiologie Und Hydrographie*, *69*(4), 457–474. http://doi.org/10.1002/iroh.19840690402

Carpenter, S. R., Caraco, N. F., Correll, D. L., Howarth, R. W., Sharpley, A. N., & Smith, V. H. (1998). Nonpoint pollution of surface waters with phosphorus and nitrogen. *Ecological Applications*, *8*(3), 559–568.

Carter, T. R., Parry, M. L., Harasawa, H., & Nishioka, S. (1994). *IPCC technical guidelines for assessing climate change impacts and adaptation*s. London, United Kingdom: University College and Center for Global Environmental Research.

Casajus, N., Périé, C., Logan, T., Lambert, M.-C., De Bois, S., & Berteaux, D. (2016). An Objective Approach to Select Climate Scenarios when Projecting Species Distribution under Climate Change. *PLOS ONE*, *11*(3), 1–17. http://doi.org/10.1371/journal.pone.0152495

Chan-Hilton, A. B., & Culver, T. B. (2000). Constraint Handling for Genetic Algorithms in Optimal Remediation Design. *Journal of Water Resources Planning and Management*, *126*(3), 128–137. http://doi.org/http://dx.doi.org/10.1061

Chapi, K., Rudra, R. P., Ahmed, S. I., Khan, A. A., Gharabaghi, B., Dickinson, W. T., & Goel, P. K. (2015). Spatial-Temporal Dynamics of Runoff Generation Areas in a Small Agricultural Watershed in Southern Ontario. *Water Resource and Protection*, *7*(January), 14–40. http://doi.org/10.4236/jwarp.2015.71002

Chen, J., Brissette, F. P., & Lucas-Picher, P. (2015). Assessing the limits of bias-correcting climate model outputs for climate change impact studies. *Journal of Geophysical Research: Atmospheres*, *120*(3), 1123–1136. http://doi.org/10.1002/2014JD022635

Coelho, B., Murray, R., Lapen, D., Topp, E., & Bruin, A. (2012). Phosphorus and sediment loading to surface waters from liquid swine manure application under different drainage and tillage practices. *Agricultural Water Management*, *104*, 51–61. http://doi.org/10.1016/j.agwat.2011.10.020

Columbo, S. J., McKenney, D. W., Lawrence, K. M., & Gray, P. a. (2007). *Climate Change Projections for Ontario : Policymakers and Planners*.

Correll, D. L. (1998). The Role of Phosphorus in the Eutrophication of Receiving Waters: A Review. *Journal of Environmental Quality*, *27*, 261-266. doi:10.2134/jeq1998.00472425002700020004x

Cousino, L. K., Becker, R. H., & Zmijewski, K. A. (2015). Modeling the Effects of Climate Change on Water, Sediment, and Nutrient Yields from the Maumee River Watershed. *Journal of Hydrology: Regional Studies*, *4*, 762–775. http://doi.org/10.1016/j.ejrh.2015.12.039

Crabbé, P., Lapen, D. R., Clark, H., Sunohara, M., & Liu, Y. (2012). Economic benefits of controlled tile drainage: Watershed Evaluation of Beneficial Management Practices, South Nation River basin, Ontario. *Water Quality Research Journal of Canada*, *47*(1), 30–41. http://doi.org/10.2166/wqrjc.2012.007

Crossman, J., Futter, M. N., Oni, S. K., Whitehead, P. G., Jin, L., Butterfield, D., … Dillon, P. J. (2013). Impacts of climate change on hydrology and water quality: Future proofing management strategies in the Lake Simcoe watershed, Canada. *Journal of Great Lakes Research*, *39*, 19–32. http://doi.org/10.1016/j.jglr.2012.11.003

Daggupati, P., Pai, N., Ale, S., Zeckoski, R. W., Jeong, J., Parajuli, P. B., … Youssef, M. A. (2015). A Recommended Calibration and Validation Strategy for Hydrologic and Water Quality Models. *Transactions of the ASABE*, *58*(6), 1705–1719. http://doi.org/10.13031/trans.58.10712

Daloğlu, I., Cho, K. H., & Scavia, D. (2012). Evaluating causes of trends in long-term dissolved reactive phosphorus loads to Lake Erie. *Environmental Science and Technology*, *46*(19), 10660–10666. http://doi.org/10.1021/es302315d

Daly, K., Jeffrey, D., & Tunney, H. (2001). The effect of soil type on phosphorus sorption capacity and desorption dynamics in Irish grassland soils. *Soil Use and Management*, 17, 12-20. http://doi.org/10.1111/j.1475-2743.2001.tb00003.x

Demaria, E. M. C., Roundy, J. K., Wi, S., & Palmer, R. N. (2016). The effects of climate change on seasonal snowpack and the hydrology of the Northeastern and Upper Midwest United States. *American Meteorological Society*, *29*, 6527–6541. http://doi.org/10.1175/JCLI-D-15-0632.1

Diaz, R. J. (2001). Overview of Hypoxia around the World. *Journal of Environment Quality*, *30*(2), 275. http://doi.org/10.2134/jeq2001.302275x

Dils, R. M., & Heathwaite, A. L. (1999). The controversial role of tile drainage in phosphorus export from agricultural land. *Water Science and Technology*, *39*(12), 55–61. http://doi.org/10.1016/S0273-1223(99)00318-2

Djodjic, F., Bergström, L., & Ulén, B. (2002). Phosphorus losses from a structured clay soil in relation to tillage practices. *Soil Use and Management*, *18*, 79-83. http://doi.org/10.1111/j.1475-2743.2002.tb00223.x

Dobos, E. (2003). Albedo. In *Encyclopedia of Soil Science* (pp. 1–3). http://doi.org/10.1081/E-ESS

Drury, C. F., Tan, C. S., Reynolds, W. D., Welacky, T. W., Oloya, T. O., & Gaynor, J. D. (2009). Managing Tile Drainage, Subirrigation, and Nitrogen Fertilization to Enhance Crop Yields and Reduce Nitrate Loss. *Journal of Environment Quality*, *38*(3), 1193. http://doi.org/10.2134/jeq2008.0036

Eastman, M., Gollamudi, A., Stämpfli, N., Madramootoo, C. A., & Sarangi, A. (2010). Comparative evaluation of phosphorus losses from subsurface and naturally drained agricultural fields in the Pike River watershed of Quebec, Canada. *Agricultural Water Management*, *97*(5), 596–604. http://doi.org/10.1016/j.agwat.2009.11.010

Ekstrand, S., Wallenberg, P., & Djodjic, F. (2010). *Process Based Modelling of Phosphorus Losses from Arable Land*. *Ambio* (Vol. 39).

El-khoury, A., Seidou, O., Lapen, D. R., Que, Z., Mohammadian, M., & Sunohara, M. (2015). Combined impacts of future climate and land use changes on discharge, nitrogen and phosphorus loads for a Canadian river basin. *Journal of Environmental Management*, *151*, 76–86. http://doi.org/10.1016/j.jenvman.2014.12.012

Elliott, H. A., O'Connor, G. A., & Brinton, S. (2002). Phosphorus Leaching from Biosolids-Amended Sandy Soils. *Journal of Environmental Quality*, *31*, 681-689. http://10.2134/jeq2002.6810

Environment and Climate Change Canada. (2018a). *Canadian Climate Normals: 1981-2010 Station Data.* Retrieved from http://climate.weather.gc.ca/climate_normals/results_1981_2010_e.html?searchType=stnProv&lstProvince=&txtCentralLatMin=0&txtCentralLatSec=0&txtCentralLongMin=0&txtCentralLongSec=0&stnID=4545&dispBack=0

Environment and Climate Change Canada. (2018b). *Historical Data.* [Data file]. Retrieved from http://climate.weather.gc.ca/historical_data/search_historic_data_e.html

Environmental Protection Agency (2015). *Recommended Phosphorus Loading Targets for Lake Erie*: *Annex 4 Objectives and Targets Task Team Final Report to the Nutrients Annex Subcommittee*. Retrieved from https://www.epa.gov/sites/production/files/2015-06/documents/report-recommended-phosphorus-loading-targets-lake-erie-201505.pdf

Fertilizer Canada (2016). *4R Nutrient Stewardship in Ontario*. Retrieved from https://fertilizercanada.ca/wp-content/uploads/2017/01/Ontario-2016-Report.pdf

Fleming, R., Macalpine, M., & Tiffin, C. (1998). Nitrate levels in soil, tile drainage water and shallow groundwater under a variety of farm management systems. *Canadian Society for Engineering in Agricultural Food, and Biological Systems*, *98–101*, 1–10.

Fowler, H. J., Blenkinsop, S., & Tebaldi, C. (2007). Linking climate change modelling to impacts studies: recent advances in downscaling techniques for hydrological modelling. *International Journal of Climatology*, *27*, 1547–1578. http://doi.org/10.1002/joc.1556

Fox, R. L., & Kamprath, E. J. (1970). Phosphate Sorption Isotherms for Evaluating the Phosphate Requirements of Soils. *Soil Science Society of America Journal*, 34, 902-907. http://doi.org/10.2136/sssaj1970.03615995003400060025x

Fraser, H., & Fleming, R. (2001). *Environmental Benefits of Tile Drainage - Literature Review*. Ridgetown, Ontario.

Gaines, T. P., & Gaines, S. T. (2008) Soil texture effect on nitrate leaching in soil percolates. *Communications in Soil Science and Plant Analysis, 25*(13-14), 2561-2570, http://doi.org/10.1080/00103629409369207

Gao, L., & Li, D. (2014). A review of hydrological/water-quality models. *Frontiers of Agricultural Science and Engineering*, *1*(4), 267–276. http://doi.org/10.15302/J-FASE-2014041

Gaynor, J. D., & Findlay, W. I. (1995). Soil and Phosphorus Loss from Conservation and Conventional Tillage in Corn Production. *Journal of Environmental Quality, 24*, 734-741. http://doi.org/10.2134/jeq1995.00472425002400040026x

Gentry, L. E., David, M. B., Below, F. E., Royer, T. V., &, McIsaac, G. F. (2009). Nitrogen Mass Balance of a Tile-drained Agricultural Watershed in East-Central Illinois. *Journal of Environmental Quality, 38*, 1841-1847. http://doi.org/10.2134/jeq2008.0406

Gentry, L. E., David, M. B., Royer, T. V., Mitchell, C. A, & Starks, K. M. (2007). Phosphorus Transport Pathways to Streams in Tile-Drained Agricultural Watersheds. *Journal of Environment Quality*, *36*(2), 408. http://doi.org/10.2134/jeq2006.0098

Geohring, L. D., McHugh, O. V., Walter, M. T., Steenhuis, T. S., Akhtar, M. S., & Walter, M. F. (2001). Phosphorus transport into subsurface drains by macropores after manure applications: Implications for best manure management practices. *Soil Science*, *166*(12), 896–909. http://doi.org/10.1097/00010694-200112000-00004

George, T. S., Giles, C. D., Menezes-Blackburn, D., Condron, L. M., Gama-Rodrigues, A. C., Jaisi, D., … Haygarth, P. M. (2017). Organic phosphorus in the terrestrial environment: a perspective on the state of the art and future priorities. *Plant Soil*, 1–18. http://doi.org/10.1007/s11104-017-3391-x

Giorgi, F. (2010). Uncertainties in climate change projections, from the global to the regional scale. *EPJ Web of Conferences*, *9*, 115–129.

Golmohammadi, G., Prasher, S., Madani, A., Rudra, R., & Youssef, M. A. (2016a). SWATDRAIN, a new model to simulate the hydrology of agricultural Lands, model development and evaluation. *Biosystems Engineering*, *141*, 31–47. http://doi.org/10.1016/j.biosystemseng.2015.11.003

Golmohammadi, G., Rudra, R., Prasher, S., Madani, A., Goel, P., & Mohammadi, K. (2016b). Modeling the effects of controlled drainage at a watershed scale using SWATDRAIN. *Arabian Journal of Geosciences*, *9*(11). http://doi.org/10.1007/s12517-016-2608-2

Golmohammadi, G., Rudra, R., Prasher, S., Madani, A., Mohammadi, K., Goel, P., & Daggupatti, P. (2017). Water Budget in a Tile Drained Watershed under Future Climate Change Using SWATDRAIN Model. *Climate*, *5*(39), 1–12. http://doi.org/10.3390/cli5020039

Gombault, C., Madramootoo, C. A., Michaud, A., Beaudin, I., Sottile, M. F., Chikhaoui, M., & Ngwa, F. (2015). Impacts of climate change on nutrient losses from the Pike River watershed of southern Québec. *Canadian Journal of Soil Science*, *95*, 337–358. http://doi.org/10.4141/CJSS-2014-012

Goss, M. J., Barry, D. A. J., & Rudolph, D. L. (1998). Contamination in Ontario farmstead domestic wells and its association with agriculture: 1. Results from drinking water wells. *Journal of Contaminant Hydrology*, *32*(3–4), 267–293. http://doi.org/10.1016/S0169-7722(98)00054-0

Grillakis, M. G., Koutroulis, A. G., & Tsanis, I. K. (2011). Climate change impact on the hydrology of Spencer Creek watershed in Southern Ontario, Canada. *Journal of Hydrology*, *409*(1–2), 1–19. http://doi.org/10.1016/j.jhydrol.2011.06.018

Guo, T., Gitau, M., Merwade, V., Arnold, J., Srinivasan, R., Hirschi, M., & Engel, B. (2018). Comparison of performance of tile drainage routines in SWAT 2009 and 2012 in an extensively tile-drained watershed in the Midwest. *Hydrology and Earth System Sciences*, *22*(1), 89–110. http://doi.org/10.5194/hess-22-89-2018

Gupta, V. H., Sorooshian, S., & Yapo, P. O. (1999). Status of automatic calibration for hydrologic models: Comparison with multilevel expert calibration. *Journal of Hydrologic Engineering*, *4*(2), 135–143.

Hart, M. R., Quin, B. F., & Nguyen, M. L. (2004). Phosphorus Runoff from Agricultural Land and Direct Fertilizer Effects. *Journal of Environment Quality*, *33*(6), 1954–1951. http://doi.org/10.2134/jeq2004.1954

Haygarth, P. M., Hepworth, L., & Jarvis, S. C. (1998). Forms of phosphorus transfer in hydrological pathways from soil under grazed grassland. *European Journal of Soil Science*, *49*(1), 65–72. http://doi.org/10.1046/j.1365-2389.1998.00131.x

Heisler, J., Glibert, P., Burkholder, J., Anderson, D., Cochlan, W., Dennison, W., … Suddleson, M. (2008). Eutrophication and harmful algal blooms: A scientific consensus. *Harmful Algae*, *8*(1), 3–13. http://doi.org/10.1016/j.hal.2008.08.006

Henry, H. a L. (2008). Climate change and soil freezing dynamics: Historical trends and projected changes. *Climatic Change*, *87*(3–4), 421–434. http://doi.org/10.1007/s10584-007-9322-8

Honti, M., Scheidegger, A., & Stamm, C. (2014). The importance of hydrological uncertainty assessment methods in climate change impact studies. *Hydrology and Earth System Sciences*, *18*, 3301–3317. http://doi.org/10.5194/hess-18-3301-2014

Hooghoudt, S.B. (1940). Contributions to the knowledge of some physical constants of the soil. *Report Agric. Res*, 46, 515–707.

Ikenberry, C. D., Soupir, M. L., Helmers, M. J., Crumpton, W. G., Arnold, J. G., & Gassman, P. W. (2017). Simulation of Daily Flow Pathways, Tile-Drain Nitrate Concentrations, and Soil-Nitrogen Dynamics Using SWAT. *Journal of the American Water Resources Association*, *53*(6), 1251–1266. http://doi.org/10.1111/1752-1688.12569

Intergovernmental Panel on Climate Change. (2015). *Climate Change 2014: Synthesis Report*. Geneva, Switzerland.

International Joint Commission (IJC) (2012). *Great Lakes Water Quality Agreement*. Retrieved from http://ijc.org/files/tinymce/uploaded/GLWQA%202012.pdf

Irwin, R. W. (1977). Economics of Farm Drainage in Ontario. *Canadian Water Resources Journal*, *2*(2), 62–73. http://doi.org/10.4296/cwrj0202062

Isard, S. A., & Schaetzl, R. J. (1998). Effects of Winter Weather Conditions on Soil Freezing in Southern Michigan. *Physical Geography*, *19*(1), 71–94.

Jarvie, H. P., Sharpley, A. N., Withers, P. J. A., Scott, J. T., Haggard, B. E., & Neal, C. (2013). Phosphorus Mitigation to Control River Eutrophication: Murky Waters, Inconvenient Truths, and "Postnormal" Science. *Journal of Environment Quality*, *42*(2), 295. http://doi.org/10.2134/jeq2012.0085

Jiao, P., Xu, D., Wang, S., Wang, Y., Liu, K., & Tang, G. (2012). Nitrogen loss by surface runoff from different cropping systems. *Soil Research*, *50*(1), 58–66. http://doi.org/10.1071/SR11152

Jyrkama, M. I., & Sykes, J. F. (2007). The impact of climate change on spatially varying groundwater recharge in the Grand River watershed (Ontario). *Journal of Hydrology*, *338*(3–4), 237–250. http://doi.org/10.1016/j.jhydrol.2007.02.036

Karmakar, R., Das, I., Dutta, D., & Raksh, A. (2016). Potential effects of climate change on soil properties: A review. *Science International*, *4*, 51-73.

King, K. W., Williams, M. R., Macrae, M. L., Fausey, N. R., Frankenberger, J., Smith, D. R., … Brown, L. C. (2015). Phosphorus Transport in Agricultural Subsurface Drainage: A Review. *Journal of Environment Quality*, *44*(2), 467–485. http://doi.org/10.2134/jeq2014.04.0163

King, L. M., Irwin, S., Sarwar, R., McLoed, I. A., & Simonovic, P. (2012). The effects of climate change on extreme precipitation events in the Upper Thames River Basin: A comparison of downscaling appraoches. *Canadian Water Resources Journal*, *37*(3), 253–274.

Kirkham, D. (1957). Theory of land drainage. In *Drainage of Agricultural Lands, Agronomy Monograph 7* (pp. 79-285). Madison, WI: American Society of Agronomy.

Kleinman, P. J. A., Sharpley, A. N., Saporito, L. S., Buda, A. R., & Bryant, R. B. (2009). Application of manure to no-till soils: phosphorus losses by sub-surface and surface pathways. Nutrient Cycling in Agroecosystems, 84(3), 215–227. http://doi.org/10.1007/s10705-008-9238-3

Kung, K.-J. S., Steenhuis, T. S., Kladivko, E. J., Gish, T. J., Bubenzer, G., & Helling, C. S. (2000). Impact of Preferential Flow on the Transport of Adsorbing and Non-Adsorbing Tracers. *Soil Science Society of America Journal*, *64*(4), 1290. http://doi.org/10.2136/sssaj2000.6441290x

Labeau, M. B., Mayer, A., Griffis, V., Watkins, D., Robertson, D., & Gyawali, R. (2015). The importance of considering shifts in seasonal changes in discharges when predicting future phosphorus loads in streams. *Biogeochemistry*, *126*(1–2), 153–172. http://doi.org/10.1007/s10533-015-0149-5

Labeau, M. B., Robertson, D. M., Mayer, A. S., Pijanowski, B. C., & Saad, D. A. (2014). Effects of future urban and biofuel crop expansions on the riverine export of phosphorus to the Laurentian Great Lakes. *Ecological Modelling*, *277*, 27–37. http://doi.org/10.1016/j.ecolmodel.2014.01.016

Lalonde, V., Madramootoo, C. A., Trenholm, L., & Broughton, R. S. (1996). Effects of controlled drainage on nitrate concentrations in subsurface drain discharge. *Agricultural Water Management*, *29*(2), 187–199. http://doi.org/10.1016/0378-3774(95)01193-5

Lam, W. V., Macrae, M. L., English, M. C., O'Halloran, I. P., Plach, J. M., & Wang, Y. (2016). Seasonal and event-based drivers of runoff and phosphorus export through agricultural tile drains under sandy loam soil in a cool temperate region. *Hydrological Processes*, *30*(15), 2644–2656. http://doi.org/10.1002/hyp.10871

Lavaire, T., Gentry, L. E., David, M. B., & Cooke, R. A. (2017). Fate of water and nitrate using drainage water management on tile systems in east-central Illinois. Agricultural Water Management, 191, 218–228. http://doi.org/10.1016/j.agwat.2017.06.004

Leytem, A. B., Mikkelsen, R. L., & Gilliam, J. W. (2002). Sorption of Organic Phosphorus Compounds in Atlantic Coastal Plain Soils. *Soil Science*, *167*(10), 652–658.

Li, H., Sivapalan, M., Tian, F., & Liu, D. (2010). Water and nutrient balances in a large tile-drained agricultural catchment: A distributed modeling study. *Hydrology and Earth System Sciences*, *14*(11), 2259–2275. http://doi.org/10.5194/hess-14-2259-2010

Li, X., Wang, B., Yang, T., Zhu, D., Nie, Z., & Xu, J. (2017). Identification of soil P fractions that are associated with P loss from surface runoff under various cropping systems and fertilizer rates on sloped farmland. *PLoS ONE*, *12*(6), 1–16. http://doi.org/10.1371/journal.pone.0179275

Li, Z., Huang, G., Huang, W., Lin, Q., & Liao, R. (2017). Future changes of temperature and heat waves in Ontario, Canada. *Theoretical and Applied Climatology*, 1–10. http://doi.org/10.1007/s00704-017-2123-8

Lilienfein, J., Qualls, R. G., Uselman, S. M., & Bridgham, S. D. (2004). Adsorption of Dissolved Organic and Inorganic Phosphorus in Soils of a Weathering Chronosequence. *Soil Science Society of America Journal*, *68*(2), 620–628. http://doi.org/10.2136/sssaj2004.6200

Liu, Y., Yang, W., Leon, L., Wong, I., Mccrimmon, C., Dove, A., & Fong, P. (2016). Hydrologic modeling and evaluation of Best Management Practice scenarios for the Grand River watershed in Southern Ontario. *Journal of Great Lakes Research*, *42*(6), 1289–1301. http://doi.org/10.1016/j.jglr.2016.02.008

Ludsin, S. A., Kershner, M. W., Blocksom, K. A., Knight, R. L., & Stein, A. (2013). Life After Death in Lake Erie : Nutrient Controls Drive Fish Species Richness, Rehabilitation. *Ecological Applications*, *11*(3), 731–746. http://doi.org/10.1890/1051-0761(2001)011

Luo, L., Lin, H., & Li, S. (2010). Quantification of 3-D soil macropore networks in different soil types and land uses using computed tomography. *Journal of Hydrology*, *393*(1–2), 53–64. http://doi.org/10.1016/j.jhydrol.2010.03.031

Macrae, M. L., English, M. C., Schiff, S. L., & Stone, M. (2007a). Intra-annual variability in the contribution of tile drains to basin discharge and phosphorus export in a first-order agricultural catchment. *Agricultural Water Management*, *92*(3), 171–182. http://doi.org/10.1016/j.agwat.2007.05.015

Macrae, M. L., English, M. C., Schiff, S. L., & Stone, M. (2007b). Capturing temporal variability for estimates of annual hydrochemical export from a first-order agricultural catchment in southern Ontario, Canada. *Hydrological Processes*, *1663*(December 2006), 1651–1663. http://doi.org/10.1002/hyp

Malagó, A., Bouraoui, F., Vigiak, O., Grizzetti, B., & Pastori, M. (2017). Modelling water and nutrient fluxes in the Danube River Basin with SWAT. *Science of the Total Environment*, *603–604*, 196–218. http://doi.org/10.1016/j.scitotenv.2017.05.242

Marcinkowski, P., Piniewski, M., Kardel, I., Szcześniak, M., Benestad, R., Srinivasan, R., … Okruszko, T. (2017). Effect of climate change on hydrology, sediment and nutrient losses in two lowland catchments in Poland. *Water*, *9*(156), 1–23. http://doi.org/10.3390/w9030156

Marianne, A., Mortsch, L., & Scheraga, J. (2003). *Climate Change and Water Quality in the Great Lakes Region*.

Maraun, D. (2016). Bias Correcting Climate Change Simulations - a Critical Review. *Current Climate Change Reports*, *2*(4), 211–220. http://doi.org/10.1007/s40641-016-0050-x

Matott, L. S. (2017). *OSTRICH: an Optimization Software Tool, Documentation and User's Guide, Version 17.12.19*. Buffalo, NY: University at Buffalo Center for Computational Research. Retrieved from www.eng.buffalo.edu/~lsmatott/Ostrich/OstrichMain.html.

McDermid, J., Fera, S., & Hogg, A. (2015). *Climate Change projections for Ontario: An updated synthesis for policymakers and planners*.

McDonnell, J., Sivapalan, M., Vaché, K., Dunn, S., Grant, G., Haggerty, R., … Weiler, M. (2007). Moving beyond heterogeneity and process complexity: A new vision for watershed hydrology. *Water Resources Research*, *43*(7), 1–6. http://doi.org/10.1029/2006WR005467

McDowell, R. W., Monaghan, L. C., Smith, L. C., Koopmans, G. F., & Stewart, I. (2005). Enhanced losses of phosphorus in mole-tile drainage water following short-term applications of dairy effluent to pasture. *Water Pollution: New Research*, 55–76.

McDowell, R. W., Sharpley, A. N., Condron, L. M., Haygarth, P. M., & Brookes, P. C. (2001). Processes controlling soil phosphorus release to runoff and implications for agricultural management. *Nutrient Cycling in Agroecosystems*, *59*(3), 269–284. http://doi.org/10.1023/A:1014419206761

McKenney, D., Hutchinson, M., Papadopol, P., Lawrence, K., Pedlar, J., Campbell, K., & Owen, T. (2011). Customized Spatial Climate Models for North America. *Bulletin of the American Meteorological Society*, 1611–1622. http://doi.org/10.1175/2011BAMS3132.1

Mckenney, D., Pedlar, J., Hutchinson, M., Papadopol, P., Lawrence, K., Campbell, K., & Price, D. (2013). Spatial climate models for Canada's forestry community. *The Forestry Chronicle*, *89*(5), 659–663.

Me, W., Abell, J. M., & Hamilton, D. P. (2015). Effects of hydrologic conditions on SWAT model performance and parameter sensitivity for a small, mixed land use catchment in New Zealand. Hydrology and Earth System Sciences, 19(10), 4127–4147. http://doi.org/10.5194/hess-19-4127-2015

Mehdi, B., Lehner, B., Gombault, C., Michaud, A., Beaudin, I., Sottile, M. F., & Blondlot, A. (2015). Simulated impacts of climate change and agricultural land use change on surface water quality with and without adaptation management strategies. *Agriculture, Ecosystems and Environment*, *213*, 47–60. http://doi.org/10.1016/j.agee.2015.07.019

Mehdi, B., Ludwig, R., & Lehner, B. (2016). Simulated future changes of extreme nutrient loads in a mesoscale agricultural watershed in Bavaria. *Journal of Land Management Food and Environment*, *67*(2), 77–90. http://doi.org/10.1515/boku-2016-0008

Meinshausen, M., Smith, S. J., Calvin, K., Daniel, J. S., Kainuma, M. L. T., Lamarque, J., … van Vuuren, D. P. P. (2011). The RCP greenhouse gas concentrations and their extensions from 1765 to 2300. *Climatic Change*, *109*(1), 213–241. http://doi.org/10.1007/s10584-011-0156-z

Merriman, K., Russell, A., Rachol, C., Daggupati, P., Srinivasan, R., Hayhurst, B., & Stuntebeck, T. (2018). Calibration of a Field-Scale Soil and Water Assessment Tool (SWAT) Model with Field Placement of Best Management Practices in Alger Creek, Michigan. Sustainability, 10, 851. http://doi.org/10.3390/su10030851

Michalak, A. M., Anderson, E. J., Beletsky, D., Boland, S., Bosch, N. S., Bridgeman, T. B., & Zagorski, M. A. (2013). Record-setting algal bloom in Lake Erie caused by agricultural and meteorological trends consistent with expected future conditions. *Proceedings of the National Academy of Sciences*, *110*(16), 6448–6452. http://doi.org/10.1073/pnas.1216006110

Michaud, A., Seydoux, A. S., Beaudin, I., & Gombault, C. (2008). *Beneficial Management Practices and Water Quality: Hydrological Modelling of Two Basins in the Montérégie Region, Quebec (*Report No. 4-65). Gatineau, QC: Environment Canada.

Ministry of Agriculture, Food and Rural Affairs. (2015). *Tile drainage area.* [Data file]. Retrieved from https://www.javacoeapp.lrc.gov.on.ca/geonetwork/srv/en/main.home

Ministry of Agriculture and Rural Affairs. (2017). *Agronomy Guide for Field Crops - Publication 811*. Toronto, Canada. Retrieved from http://www.omafra.gov.on.ca/english/crops/pub811/pub811.pdf

Ministry of Agriculture, Food and Rural Affairs, & Canadian Soil Information Service. (2015). *Ontario Soil Survey Complex.* [Data file]. Retrieved from https://www.javacoeapp.lrc.gov.on.ca/geonetwork/srv/en/main.home

Ministry of the Environment and Climate Change. (2012). *Water quality of 15 streams in agricultural watersheds of Southwestern Ontario 2004-2009*.

Ministry of Finance. (2017). *Ontario Population Projections Update, 2016-2041*. Ontario: Author. Retrieved from https://www.fin.gov.on.ca/en/economy/demographics/projections/projections2016-2041.pdf

Ministry of Natural Resources and Forestry. (2015). *The Southwestern Ontario Orthophotography Project, 2010 digital elevation model*. [Data file]. Retrieved from https://www.ontario.ca/data/2010-digital-elevation-model

Moazed, H., Hoseini, Y., Naseri, A. A., & Abbasi, F. (2010). Determining phosphorus adsorption isotherm in soil and its relation to soil characteristics. *Journal of Food, Agriculture & Environment*, *8*(2), 1153–1157. http://doi.org/10.3923/ijss.2010.131.139

Molder, B., Cockburn, J., Berg, A., Lindsay, J., & Woodrow, K. (2015). Sediment-assisted nutrient transfer from a small, no-till, tile drained watershed in Southwestern Ontario, Canada. *Agricultural Water Management*, *152*, 31–40. http://doi.org/10.1016/j.agwat.2014.12.010

Moriasi, D., Arnold, J., & Green, C. (2007a). Incorporation of Hooghoudt and Kirkham tile drain equations into SWAT2005. *Proc. 4th Intl. SWAT Conf*, 139–147. Retrieved from http://scholar.google.com/scholar?hl=en&btnG=Search&q=intitle:INCORPORATION+of+Hooghoudt+and+Kirkham+Tile+Drain+Equations+into+SWAT2005#0

Moriasi, D., Arnold, J., Van Liew, M. W., Binger, R. L., Harmel, R. D., & Veith, T. L. (2007b). Model evaluation guidelines for systematic quantification of accuracy in watershed simulations. *American Society of Agricultural and Biological Engineers*, *50*(3), 885–900. http://doi.org/10.13031/2013.23153

Moriasi, D., Arnold, J., Vasquesz-Amabile, G. G., Angel, B. A., & Rossi, C. G. (2009). Incorporation of a New Shallow Water Table Depth Algorithm into SWAT2005. *American Society of Agricultural and Biological Engineers*, *52*(3), 771–784. http://doi.org/10.13031/2013.27398

Moriasi, D., Gowda, P. H., Arnold, J., Mulla, D. J., Ale, S., Steiner, J. L., & Tomer, M. D. (2013). Evaluation of the Hooghoudt and Kirkham Tile Drain Equations in the Soil and Water Assessment Tool to Simulate Tile Flow and Nitrate-Nitrogen. *Journal of Environmental Quality* (Vol. 42).

Moriasi, D., Rossi, C., Arnold, J., & Tomer, M. (2012). Evaluating hydrology of the Soil and Water Assessment Tool (SWAT) with new tile drain equations. *Journal of Soil and Water Conservation*, 67, 513–524. https://doi.org/10.2489/jswc.67.6.513

Mpelasoka, F. S., & Chiew, F. H. S. (2009). Influence of Rainfall Scenario Construction Methods on Runoff Projections. *Journal of Hydrometeorology*, *10*, 1168–1183. http://doi.org/10.1175/2009JHM1045.1

Muma, M., Rousseau, A. N., & Gumiere, S. J. (2016). Assessment of the impact of subsurface agricultural drainage on soilwater storage and flows of a small watershed. *Water*, *8*(326). http://doi.org/10.3390/w8080326

Nash, J. E., & Sutcliffe, J. V. (1970). River flow forecasting through conceptual models part 1- A discussion of principles. *Journal of Hydrology*, *10*, 282–290.

Neilsen, G. H., Culley, J. L., & Cameron, D. R. (1978). *Nitrogen Loadings From Agricultural Activities in the Great Lakes Basin Integration Report on Nitrogen, Agricultural Watershed Studies, Task C, Canadian Section, Activity 1*. Ottawa, Ontario.

Neitsch, S. L., Arnold, J. G., Kiniry, J. R., & Williams, J. R. (2011). *Soil & Water Assessment Tool Theoretical Documentation, version 2009*. College Station, Texas.

Ouranos. (2018). *Climate simulation and analysis*. Retrieved from http://www.ouranos.ca/en/scientific-program/climate-sci ence/climate-simulations/default.php

Panno, S. V., Kelly, W. R., Hackley, K. C., Hwang, H. H., & Martinsek, A. T. (2008). Sources and fate of nitrate in the Illinois River Basin, Illinois. *Journal of Hydrology*, *359*(1–2), 174–188. http://doi.org/10.1016/j.jhydrol.2008.06.027

Parkin, G. W., Fallow, D. J., & Brown, D. M. (1999). Estimated Seasonal and Annual Water Surplus in Ontario. *Canadian Water Resources Journal*, *24*(4), 277–292. http://doi.org/10.4296/cwrj2404277

Pärn, J., Pinay, G., & Mander, Ü. (2012). Indicators of nutrients transport from agricultural catchments under temperate climate: A review. *Ecological Indicators*, *22*, 4–15. http://doi.org/10.1016/j.ecolind.2011.10.002

Pease, L. A., King, K. W., Williams, M. R., LaBarge, G. A., Duncan, E. W., & Fausey, N. R. (2018). Phosphorus export from artificially drained fields across the Eastern Corn Belt. *Journal of Great Lakes Research*, *44*(1), 43–53. http://doi.org/10.1016/j.jglr.2017.11.009

Peron, H., Hueckel, T., Laloui, L., & Hu, L. B. (2009). Fundamentals of desiccation cracking of fine-grained soils: experimental characterization and mechanisms identification. *Canadian Geotechnical Journal*, *46*(10), 1177–1201. http://doi.org/10.1139/T09-054

Petry, J., Soulsby, C., Malcolm, I. A., & Youngson, A. F. (2002). Hydrological controls on nutrient concentrations and fluxes in agricultural catchments. *Science of the Total Environment*, *294*(1–3), 95–110. http://doi.org/10.1016/S0048-9697(02)00058-X

Plach, J. M., Macrae, M. L., Ali, G. A., Brunke, R. R., English, M. C., Ferguson, G., … Van Esbroeck, C. J. (2018). Supply and Transport Limitations on Phosphorus Losses from Agricultural Fields in the Lower Great Lakes Region, Canada. *Journal of Environment Quality*, *47*(1), 96–105. http://doi.org/10.2134/jeq2017.06.0234

Plach, J. M., Macrae, M. L., Williams, M.,Lee, B., & King, K. (in press). Dominant glacial landforms in the Lake Erie watershed exhibit differences in soil phosphorus chemistry and potential risk for phosphorus loss. *Journal of Great Lakes Research*.

Poon, D. (2013). *Re-Conceptualizing the SWAT to Better Predict Subsurface Water Flow through Macroporous Soils* (Master's thesis). Retrieved from http://digitool.library.mcgill.ca/webclient/StreamGate?folder_id=0&dvs=1523834861472~686

Prodanovi, P., & Simonovi, S. P. (2006). *Inverse Drought Risk Modelling of the Upper Thames River Basin. CFCAS Project: Assessment of Risk and Vulnerability to Changing Climatic Conditions* (Report No. 052). London, Ontario.

Puustinen, M., Tattari, S., Koskiaho, J., & Linjama, J. (2007). Influence of seasonal and annual hydrological variations on erosion and phosphorus transport from arable areas in Finland. *Soil and Tillage Research*, *93*(1), 44–55. http://doi.org/10.1016/j.still.2006.03.011

Qi, H., & Qi, Z. (2017). Simulating phosphorus loss to subsurface tile drainage flow : a review. *Environmental Reviews*, *25*, 150–162. http://doi.org/10.1139/er-2016-0024

Qi, J., Li, S., Li, Q., Xing, Z., Bourque, C. P. A., & Meng, F. R. (2016). A new soil-temperature module for SWAT application in regions with seasonal snow cover. *Journal of Hydrology*, *538*, 863–877. http://doi.org/10.1016/j.jhydrol.2016.05.003

Rabotyagov, S. S., Kling, C. L., Gassman, P. W., Rabalais, N. N., & Turner, R. E. (2014). The Economics of Dead Zones: Causes, Impacts, Policy Challenges, and a Model of the Gulf of Mexico Hypoxic Zone. *Review of Environmental Economics and Policy*, *8(*1), 58–79.

Rahman, M., Bolisetti, T., & Balachandar, R. (2012). Hydrologic modelling to assess the climate change impacts in a Southern Ontario watershed. *Canadian Journal of Civil Engineering*, *39*(1), 91–103. http://doi.org/10.1139/l11-112

Rajib, M. A., & Merwade, V. (2016). Improving soil moisture accounting and streamflow prediction in SWAT by incorporating a modified time-dependent Curve Number method. *Hydrological Processes*, *30*(4), 603–624. http://doi.org/10.1002/hyp.10639

Randall, G. W., Huggins, D. R., Russelle, M. P., Fuchs, D. J., Nelson, W. W., & Anderson, J. L. (1997). Nitrate Losses through Subsurface Tile Drainage in Conservation Reserve Program, Alfalfa, and Row Crop Systems. *Journal of Environment Quality*, *26*(5), 1240–1247. http://doi.org/10.2134/jeq1997.00472425002600050007x

Rasouli, S., Whalen, J. K., & Madramootoo, C. A. (2014). Review : Reducing residual soil nitrogen losses from agroecosystems for surface water protection in Quebec and Ontario, Canada: Best management practices, policies and perspectives. *Canadian Journal of Soil Science*, *94*, 109–127. http://doi.org/10.4141/CJSS2013-015

Reid, D. K., Ball, B., & Zhang, T. Q. (2012). Accounting for the Risks of Phosphorus Losses through Tile Drains in a Phosphorus Index. *Journal of Environmental Quality*, *41*, 1720-1729. http://doi.org/10.2134/jeq2012.0238

Reid, S., Smit, B., Caldwell, W., & Belliveau, S. (2007). Vulnerability and adaptation to climate risks in Ontario agriculture. *Mitigation and Adaptation Strategies for Global Change*, *12*(4), 609–637. http://doi.org/10.1007/s11027-006-9051-8

Riley, K.D., Helmers, M.J., Lawlor, P.A., & Singh, R. (2009). Water balance investigation of drainage water management in non-weighing lysimeters. *American Society of Agricultural and Biological Engineers*, *25*, 507–513. http://doi.org/10.13031/2013.27470

Robertson, D. M., Saad, D. A., Christiansen, D. E., & Lorenz, D. J. (2016). Simulated impacts of climate change on phosphorus loading to Lake Michigan. *Journal of Great Lakes Research*, *42*(3), 536–548. http://doi.org/10.1016/j.jglr.2016.03.009

Robinson, M. (1990). *Impact of improved land drainage on river flows*. *Institute of Hydrology* (Vol. 113). Wallingford, UK.

Robinson, M., & Rycroft, D. W. (1999). The impact of drainage on streamflow. *Agronomy Monographs*, *38*, 767–800.

Ross, J. A., Herbert, M. E., Sowa, S. P., Frankenberger, J. R., King, K. W., Christopher, S. F., … Yen, H. (2016). A synthesis and comparative evaluation of factors influencing the effectiveness of drainage water management. *Agricultural Water Management*, *178*, 366–376. http://doi.org/10.1016/j.agwat.2016.10.011

Rouholahnejad, E., Abbaspour, K. C., Srinivasan, R., Bacu, V., & Lehmann, A. (2014). Water resources of the Black Sea Basin at high spatial and temporal resolution. *Water Resources Research*, *50*(7), 586–5885. http://doi.org/10.1002/2013WR014132.Received

Royer, T. V., David, M. B., & Gentry, L. E. (2006). Timing of Riverine Export of Nitrate and Phosphorus from Agricultural Watersheds in Illinois: Implications for Reducing Nutrient Loading to the Mississippi River. *Environmental Science & Technology*, *40*(13), 4126-4131. doi:10.1021/es052573n

Rozemeijer, J. C., Van Der Velde, Y., Van Geer, F. C., Bierkens, M. F. P., & Broers, H. P. (2010). Direct measurements of the tile drain and groundwater flow route contributions to surface water contamination: From field-scale concentration patterns in groundwater to catchment-scale surface water quality. *Environmental Pollution*, *158*(12), 3571–3579. http://doi.org/10.1016/j.envpol.2010.08.014

Rudra, R. P., Dickinson, W. T., Ahmed, S. I., Patel, P., Zhou, J., Gharabaghi, B., & Khan, A. A. (2015). Changes in rainfall extremes in Ontario. *International Journal of Environmental Research*, *9*(4), 1117–1126.

Santhi, C., Arnold, J. G., Williams, J. R., Dugas, W. A., Srinivasan, R., & Hauk, L. M. (2001). Validation of the SWAT model on a large river basin with point and nonpoint sources. *Journal of the Amercian Water Resources Association*, *37*(5), 1169–1188.

Saxton, K. E., & Rawls, W. J. (2006). Soil Water Characteristic Estimates by Texture and Organic Matter for Hydrologic Solutions. *Soil Science Society of America Journal*, *70*, 1569–1578. http://doi.org/10.2136/sssaj2005.0117

Scavia, D., David Allan, J., Arend, K. K., Bartell, S., Beletsky, D., Bosch, N. S., … Zhou, Y. (2014). Assessing and addressing the re-eutrophication of Lake Erie: Central basin hypoxia. *Journal of Great Lakes Research*, *40*(2), 226–246. http://doi.org/10.1016/j.jglr.2014.02.004

Schwab, G., Fausey, N. R., Desmond, E. D., & Holman, J. R. (1985). *Tile and Surface Drainage of Clay Soils* (Vol. Research B). Wooster, Ohio, US.

Sharpley, A. N., Gburek, W. J., Folmar, G., & Pionke, H. B. (1999). Sources of phosphorus exported from an agricultural watershed in Pennsylvania. *Agricultural Water Management*, *41*(2), 77–89. http://doi.org/10.1016/S0378-3774(99)00018-9

Sharpley, A. N., Jarvie, H. P., Buda, A., May, L., Spears, B., & Kleinman, P. (2014). Phosphorus Legacy: Overcoming the Effects of Past Management Practices to Mitigate Future Water Quality Impairment. Journal of Environmental Quality, 42(5), 1308–1308. http://doi.org/10.1017/CBO9781107415324.004

Sharpley, A. N., Kleinman, P. J. A., Flaten, D. N., & Buda, A. R. (2011). Critical source area management of agricultural phosphorus: experiences, challenges and opportunities. *Water Science & Technology*, *64*(4), 945. http://doi.org/10.2166/wst.2011.712

Sharpley, A. N., McDowell, R. W., & Kleinman, P. J. A. (2001). Phosphorus loss from land to water: integrating agricultural and environmental management. *Plant and Soil*, *237*(2), 287–307. http://doi.org/Doi 10.1023/A:1013335814593

Sharpley, A. N., Smith, S. J., & Naney, J. W. (1987). Environmental impact of agricultural nitrogen and phosphorus use. *Journal of Agricultural and Food Chemistry*, *35*(5), 812–817.

Shrestha, N. K., & Wang, J. (2018). Predicting sediment yield and transport dynamics of a cold climate region watershed in changing climate. *Science of the Total Environment*, *625*, 1030–1045. http://doi.org/10.1016/j.scitotenv.2017.12.347

Sinha, T., & Cherkauer, K. A. (2010). Impacts of future climate change on soil frost in the midwestern United States. *Journal of Geophysical Research*, *115*(D08105). http://doi.org/10.1029/2009JD012188

Skaggs, R. W. (1978). *A water management model for shallow water table soils*. Raleigh, NC, USA.

Skaggs, R. W., Brevé, M. A., & Gilliam, J.W. (1994). Hydrologic and water quality impacts of agricultural drainage. *Critical Reviews in Environmental Science and Technology*, *24*, 1–32. https://doi.org/10.1080/10643389409388459

Skaggs, R. W., Fausey, N. R., & Evans, R. O. (2012). Drainage water management. *Journal of Soil and Water Conservation*, *67*(6), 167A–172A. http://doi.org/10.2489/jswc.67.6.167A

Skaggs, R.W., Youssef, M., Gilliam, J. W., & Evans, R. (2010). Effect of Controlled Drainage on Water and Nitrogen Balances in Drained Lands. *Transactions of the ASABE*, *53*, 1843-1850. https://doi.org/10.13031/2013.35810

Soil Conservation Service. (1972). *National Engineering Handbook*. Washington, DC: USDA Soil Conservation Service.

Simard, R. R., Beauchemin, S., & Haygarth, P. M. (2000). Potential for Preferential Pathways of Phosphorus Transport. *Journal of Environment Quality*, *29*(1), 97-105. http://doi.org/10.2134/jeq2000.00472425002900010012x

Singh, B., Bardgett, R. D., Smith, P., & Reay, D. S. (2010). Microorganisms and climate change: terrestrial feedbacks and mitigation options. *Nature Reviews Microbiology*, *8*(11), 779–790. http://doi.org/10.1038/nrmicro2439

Singh, B., El Maayar, M., André, P., Bryant, C. R., & Thouez, J. P. (1998). Impacts of a GHG-induced climate change on crop yields: Effects of acceleration in maturation, moisture stress and optimal temperature. *Climatic Change*, *38*(1), 51–86. http://doi.org/10.1023/A:1005392517715

Sloan, B. P., Mantilla, R., Fonley, M., & Basu, N. B. (2017). Hydrologic impacts of subsurface drainage from the field to watershed scale. *Hydrological Processes*, *31*(17), 3017–3028. http://doi.org/10.1002/hyp.11218

Smith, K. A., Jackson, D. R., & Pepper, T. J. (2001). Nutrient losses by surface run-off following the application of organic manures to arable land. 2. Nitrogen. *Environmental Pollution*, *112*, 53–60. http://doi.org/10.1016/S0269-7491(00)00098-1

Spivakov, B. Y., Maryutina, T. A., & Muntau, H. (1999). Phosphorus Speciation in Water and Sediments. *Pure and Applied Chemistry*, *71*(11), 2161–2176. http://doi.org/10.1351/pac199971112161

Starks, P. J., & Moriasi, D. N. (2009). Spatial resolution effect of precipitation data on SWAT calibration and performance: implications for CEAP. Transactions of the ASABE, 52(4), 1171–1180. http://doi.org/ISSN 0001-2351 1171

Steenvoorden, J., Claessen, F., Willems J. (2002). *Agricultural Effects on Ground and Surface Waters: Research at the Edge of Science and Society.* Wallingford, UK: Intl. Assn. of Hydrological Sciences.

Sunohara, M. D., Gottschall, N., Craiovan, E., Wilkes, G., Topp, E., Frey, S. K., & Lapen, D. R. (2016). Controlling tile drainage during the growing season in Eastern Canada to reduce nitrogen, phosphorus, and bacteria loading to surface water. *Agricultural Water Management*, *178*(3), 159–170. http://doi.org/10.1016/j.agwat.2016.08.030

Sunohara, M.D., Gottschall, N., Wilkes, G., Craiovan E., Topp E., Que Z., Seidou O., Frey S. K., & Lapen, D. R. (2015). Long-Term Observations of Nitrogen and Phosphorus Export in Paired-Agricultural Watersheds under Controlled and Conventional Tile Drainage. *Journal of Environmental Quality*, 44(5), 1589-1604. http://doi.org/10.2134/jeq2015.01.0008

Sunohara, M., Youssef, M. A., Topp, E., & Lapen, D. R. (2010). Measured Effect of Agricultural Drainage Water Management on Hydrology, Water Quality, and Crop Yield. In *ASABE - 9th International Drainage Symposium 2010, Held Jointly with CIGR and CSBE/SCGAB*. http://doi.org/10.13031/2013.32147

Tan, C. S., & Zhang, T. Q. (2011). Surface runoff and sub-surface drainage phosphorus losses under regular free drainage and controlled drainage with sub-irrigation systems in southern Ontario. *Canadian Journal of Soil Science*, *91*, 349–359. http://doi.org/10.4141/CJSS09086

Taylor, K.E., Stouffer, R.J., Meehl, G.A. (2012). An Overview of CMIP5 and the experiment design. *Bulletin of the American Meteorological Society*, 93, 485-498. http://dx.doi.org/10.1175/BAMS-D-11-00094.1

Tolson, B. A., & Shoemaker, C. A. (2007). Dynamically dimensioned search algorithm for computationally efficient watershed model calibration. *Water Resources Research*, *43*(1), 1–16. http://doi.org/10.1029/2005WR004723

Tsakiris, G., & Alexakis, D. (2012). Water quality models : An overview. *European Water*, *37*, 33–46.

Ulén, B., Aronsson, H., Bechmann, M., Krogstad, T., Øygarden, L., & Stenberg, M. (2010). Soil tillage methods to control phosphorus loss and potential side-effects: A Scandinavian review. *Soil Use and Management*, *26*(2), 94–107. http://doi.org/10.1111/j.1475-2743.2010.00266.x

Upper Thames River Conservation Authority. (2012). *Medway Creek: Watershed Report Card*. London, Ontario.

Uusi-Kämppä, J., Braskerud, B., Jansson, H., Syversen, N., & Uusitalo, R. (2000). Buffer Zones and Constructed Wetlands as Filters for Agricultural Phosphorus. *Journal of Environmental Quality*, *29*, 151-158. http://doi.org/10.2134/jeq2000.00472425002900010019x

Uusitalo, R., Turtola, E., Kauppila, T., & Lilja, T. (2001). Particulate Phosphorus and Sediment in Surface Runoff and Drainflow from Clayey Soils. *Journal of Environment Quality*, *30*(2), 589–595. http://doi.org/10.2134/jeq2001.302589x

Vadas, P. A., Bolster, C. H., & Good, L. W. (2013). Critical evaluation of models used to study agricultural phosphorus and water quality. *Soil Use and Management*, *29*(Suppl. 1), 36–44. http://doi.org/10.1111/j.1475-2743.2012.00431.x

Van Dijk, J., Stroetenga, M., Bos, L., Van Bodegom, P. M., Verhoeff, H. A., & Arerts, R. (2011). Reduction of Organic Matter Decomposition and Soil Nutrient Dynamics on former Restoring natural seepage conditions agricultural grasslands does not lead to reduction of organic matter decomposition and soil. *Biogeochemistry*, *71*, 317–337.

Van Esbroeck, C. J., Macrae, M. L., Brunke, R., & McKague, K. (2016). Annual and seasonal phosphorus export in surface runoff and tile drainage from agricultural fields with cold temperate climates. *Journal of Great Lakes Research*, *42*(6), 1271–1280. http://doi.org/10.1016/j.jglr.2015.12.014

Van Esbroeck, C. J., Macrae, M. L., Brunke, R., & Mckague, K. (2017). Surface and subsurface phosphorus export from agricultural fields during peak flow events over the nongrowing season in regions with cool, temperate climates. *Journal of Soil and Water Conservation*, *72*(1), 65–76. http://doi.org/10.2489/jswc.72.1.65

Van Meter, K. J., Basu, N. B., Veenstra, J. J., & Burras, C. L. (2016). The nitrogen legacy: Emerging evidence of nitrogen accumulation in anthropogenic landscapes. *Environmental Research Letters*, *11*, 35014. http://doi.org/10.1088/1748-9326/11/3/035014

Van Meter, K. J., Van Cappellen, P., & Basu, N. B. (2018). Legacy nitrogen may prevent achievement of water quality goals in the Gulf of Mexico. *Science*. Retrieved from http://science.sciencemag.org/content/early/2018/03/21/science.aar4462.abstract

Veith, T. L., & Ghebremichael, L. T. (2009). How To: Applying and Interpreting the SWAT Auto-calibration Tools. In *2009 International SWAT Conference: Conference Proceedings* (pp. 43–50). College Station, Texas: Texas Water Resources Institute.

Veraart, A.J., de Klein, J. J.M., & Scheffer, M. (2011). Warming Can Boost Denitrification Disproportionately Due to Altered Oxygen Dynamics. *PLOS ONE*, *6*(3). https://doi.org/10.1371/journal.pone.0018508

Verma, S., Bhattarai, R., Bosch, N. S., Cooke, R. C., Kalita, P. K., & Markus, M. (2015). Climate Change Impacts on Flow, Sediment and Nutrient Export in a Great Lakes Watershed Using SWAT. *Clean - Soil, Air, Water*, *43*(11), 1464–1474. http://doi.org/10.1002/clen.201400724

Vidon, P., & Cuadra, P. E. (2010). Impact of precipitation characteristics on soil hydrology in tile-drained landscapes. *Hydrological Processes*, *24*(March), 1821–1833. http://doi.org/10.1002/hyp.7627

Vidon, P., & Cuadra, P. E. (2011). Phosphorus dynamics in tile-drain flow during storms in the US Midwest. *Agricultural Water Management*, *98*(4), 532–540. http://doi.org/10.1016/j.agwat.2010.09.010

Vidon, P., Hubbard, L. E., & Soyeux, E. (2009). Seasonal solute dynamics across land uses during storms in glaciated landscape of the US Midwest. *Journal of Hydrology*, *376*(1–2), 34–47. http://doi.org/10.1016/j.jhydrol.2009.07.013

Walker, W. W. (1996). *Simplified Procedures for Eutrophication Assessment and Prediction: User Manual*. *U.S. Army Corps of Engineers*.

Wallace, C. W., Flanagan, D. C., & Engel, B. A. (2017). Quantifying the Effects of Future Climate Conditions on Runoff, Sediment, and Chemical Losses at Different Watershed Sizes. *Transactions of the ASABE, 60*(3), 915-929. http://doi.org/10.13031/trans.12094

Wang, H., Gao, J., Li, X., Zhang, S., & Wang, H. (2015a). Nitrate Accumulation and Leaching in Surface and Ground Water Based on Simulated Rainfall Experiments. *Plos One*, *10*(8), 1–18. http://doi.org/10.1371/journal.pone.0136274

Wang, L., Flanagan, D. C., Wang, Z., & Cherkauer, K. A. (2018). Climate Change Impacts on Nutrient Losses of Two Watershed in the Great Lakes Region. *Water*, *10*(4), 442. http://doi.org/10.3390/w10040442

Wang, X., Huang, G., & Liu, J. (2014). Projected increases in intensity and frequency of rainfall extremes through a regional climate modeling approach. *Journal of Geophysical Research: Atmospheres*, *119*(23), 271–286. http://doi.org/10.1002/2014JD022564.Received

Wang, X., Huang, G., Liu, J., Li, Z., & Zhao, S. (2015b). Ensemble Projections of Regional Climatic Changes over Ontario, Canada. *American Meteorological Society*, *28*, 7327–7346. http://doi.org/10.1175/JCLI-D-15-0185.1

Wang, X., & Melesse, A. M. (2005). Evaluation of the SWAT Model's Snowmelt Hydrology in a Northwestern Minnesota Watershed. *Transactions of the American Society of Agricultural Engineers*, *48*(4), 1359–1376. http://doi.org/10.13031/2013.19194

Wesström, I., Joel, A., & Messing, I. (2014). Controlled drainage and subirrigation – A water management option to reduce non-point source pollution from agricultural land. Agriculture, Ecosystems & Environment, 198, 74–82. http://doi.org/10.1016/j.agee.2014.03.017

Wesström, I., & Messing, I. (2007). Effects of controlled drainage on N and P losses and N dynamics in a loamy sand with spring crops. Agricultural Water Management, 87(3), 229–240. http://doi.org/10.1016/j.agwat.2006.07.005

Wilkes, G., Brassard, J., Edge, T. A., Gannon, V., Gottschall, N., Jokinen, C. C., … Lapen, D. R. (2014). Long-term monitoring of waterborne pathogens and microbial source tracking markers in paired agricultural watersheds under controlled and conventional tile drainage management. *Applied and Environmental Microbiology*, *80*(12), 3708–3720. http://doi.org/10.1128/AEM.00254-14

Williams, M. R., King, K. W., & Fausey, N. R. (2015). Drainage water management effects on tile discharge and water quality. *Agricultural Water Management*, *148*, 43–51. http://doi.org/10.1016/j.agwat.2014.09.017

Williams, M.R., King, K.W., & Penn, C.J. (2018). Integrating Temporal Inequality into Conservation Planning to Improve Practice Design and Efficacy. *Journal of the American Water Resources Association*, 1–16. https://doi.org/10.1111/1752-1688.12662

Wiskow, E., & Van Der Ploeg, R. R. (2003). Calculation of drain spacings for optimal rainstorm flood control. *Journal of Hydrology*, *272*, 163–174. http://doi.org/10.1016/S0022-1694(02)00262-7

Woznicki, S. A., & Nejadhashemi, A. P. (2012). Sensitivity analysis of best management practices under climate change scenarios. *Journal of the American Water Resources Association*, *48*(1), 90–112. http://doi.org/10.1111/j.1752-1688.2011.00598.x

Xiao, Y., Tang, J., Wang, M., Zhai, L., & Zhang, X. (2017). Impacts of soil properties on phosphorus adsorption and fractions in purple soils. *Journal of Mountain Science*, *14*(12), 2420–2431. http://doi.org/10.1007/s11629-017-4545-2

Xiuqing, Z., & Flerchinger, G. N. (2001). Infiltration into freezing and thawing soils under differing field treatments. *Journal of Irrigation and Drainage Engineering*, *127*(3), 176–182.

Yaghi, N., & Hartikainen, H. (2013). Enhancement of phosphorus sorption onto light expanded clay aggregates by means of aluminum and iron oxide coatings. *Chemosphere*, *93*(9), 1879–1886. http://doi.org/10.1016/j.chemosphere.2013.06.059

Ye, L., & Grimm, N. B. (2013). Modelling potential impacts of climate change on water and nitrate export from a mid-sized, semiarid watershed in the US Southwest. *Climatic Change*, *120*, 419–431. http://doi.org/10.1007/s10584-013-0827-z

Youssef, M. A., Abdelbaki, A. M., Negm, L. M., Skaggs, R. W., Thorp, K. R., & Jaynes, D. B. (2018). DRAINMOD-simulated performance of controlled drainage across the U.S. Midwest. *Agricultural Water Management*, *197*, 54–66. http://doi.org/10.1016/j.agwat.2017.11.012

Zabaleta, A., Meaurio, M., Ruiz, E., & Antigüedad, I. (2014). Simulation Climate Change Impact on Runoff and Sediment Yield in a Small Watershed in the Basque Country, Northern Spain. *Journal of Environment Quality*, *43*, 235–245. http://doi.org/10.2134/jeq2012.0209

Zhang, D., Chen, X., Yao, H., & Lin, B. (2015). Improved calibration scheme of SWAT by separating wet and dry seasons. Ecological Modelling, 301, 54–61. http://doi.org/10.1016/j.ecolmodel.2015.01.018

Zhang, T. Q., Tan, C. S., Zheng, Z. M., Welacky, T., & Wang, Y. T. (2017). Drainage water management combined with cover crop enhances reduction of soil phosphorus loss. *Science of the Total Environment*, *586*, 362–371. http://doi.org/10.1016/j.scitotenv.2017.02.025

# APPENDIX A

Calibrated Parameters and Final Values

*Table A.1.* Sensitive SWAT parameters used during calibration of the MCW model with the final fitted value

| Calibrated Parameters | | |
|---|---|---|
| Name | Description | Fitted Value |
| **River Flow** | | |
| v__GW_REVAP.gw | Groundwater revap coefficient | 0.29 |
| v__ALPHA_BF.gw | Baseflow alpha factor | 0.89 |
| v__GW_DELAY.gw | Groundwater delay time (days) | 6.45 |
| v__GWQMN.gw | Threshold depth of water in the shallow aquifer required for return flow to occur (mm $H_2O$) | 490 |
| v__RCHRG_DP.gw | Deep aquifer percolation fraction | 0.38 |
| v__TIMP.bsn | Snow pack temperature lag factor | 0.71 |
| v__SMTMP.bsn | Snow melt base temperature (˚C) | -0.56 |
| v__SFTMP.bsn | Snowfall temperature (˚C) | 0.72 |
| v__SMFMX.bsn | Melt factor for snow on June 21 (mm $H_2O$/˚C-day) | 4.2 |
| v__SMFMN.bsn | Melt factor for snow on December 21 (mm $H_2O$/˚C-day) | 8.9 |
| v__SNOCOVMX.bsn | Minimum snow water content for 100% snow cover (mm $H_2O$) | 23.3 |
| v__SNO50COV.bsn | Fraction of snow volume represented by SNOCOVMX that corresponds to 50% snow cover | 0.13 |
| v__CH_K2.rte | Effective hydraulic conductivity in main channel alluvium (mm/hr) | 268 |
| v__CH_N2.rte | Manning's "n" value for the main channel | 0.15 |
| v__CH_K1.sub | Effective hydraulic conductivity in main channel alluvium (mm/hr) | 106 |
| v__ESCO.hru | Soil evaporation compensation factor | 0.37 |
| v__EPCO.hru | Plant uptake compensation factor | 0.3 |
| r__OV_N.hru | Manning's "n" value for overland flow | 0.18 |
| v__CANMX.hru | Maximum canopy storage (mm $H_2O$) | 49 |
| r__CN2.mgt | Initial SCS runoff curve number for moisture condition II | 0.05 |
| r__SOL_BD().sol | Soil bulk density | -0.37 |
| r__SOL_AWC().sol | Available water capacity of the soil layer (mm $H_2O$/mm soil) | -0.21 |
| v__SOL_EC().sol | Macropore connectivity factor | 0.22 |
| **Suspended Sediment** | | |
| v__ADJ_PKR.bsn | Peak rate adjustment factor for sediment routing in the subbasin | 1.9 |
| v__SPEXP.bsn | Channel re-entrained exponent parameter | 1.4 |
| v__SPCON.bsn | Channel re-entrained linear parameter | 0.0015 |
| v__PRF_BSN.bsn | Peak rate adjustment factor for sediment in the main channel | 0.42 |
| r__USLE_K().sol | USLE equation soil erodibility (K) factor | -0.49 |
| v[a]__USLE_P.mgt | USLE support practice factor | 0.42 |
| v__CH_COV2.rte | Channel cover factor | 0.43 |
| **Nitrate** | | |
| v__CDN.bsn | Denitrification exponential rate coefficient | 1.03 |
| v__SDNCO.bsn | Denitrification threshold water content | 0.85 |
| v__NPERCO.bsn | Nitrate percolation coefficient | 0.6 |
| v__N_UPDIS.bsn | Nitrogen uptake distribution parameter | 12.9 |
| v__BC1_BSN.bsn | Rate constant for biological oxidation of NH4 to NO2 in the reach at 20˚ C in well-aerated conditions (day-1) | 0.69 |
| v__ANION_EXCL.sol | Fraction of porosity (void space) from which anions are excluded | 0.37 |
| v__CH_ONCO.rte | Organic nitrogen concentration in the channel (ppm) | 57.8 |
| **Total P** | | |
| v__BC4.swq | Rate constant for mineralization of organic P to dissolved P in the reach at 20˚ C (day-1) | 0.37 |
| v__ERORGP.hru | Phosphorus enrichment ratio for loading with sediment | 2.12 |
| v__P_UPDIS.bsn | Phosphorus uptake distribution parameter | 96.6 |
| v__PHOSKD.bsn | Phosphorus soil partitioning coefficient (m3/Mg) | 144.9 |

[a] Only calibrated agricultural land use for this parameter

*letters before parameter name represents the replacement method used during calibration

*Table A.2.* SWAT parameter ranges used during calibration of the LON model with the final fitted value

| Calibrated Parameters | | | |
|---|---|---|---|
| Name | Description | Calibration Range | Fitted Value |
| GW_REVAP.gw | Groundwater "revap" coefficient | 0.02 to 0.6 | 0.56 |
| ALPHA_BF.gw | Baseflow alpha factor | 0 to 1 | 0.96 |
| GW_DELAY.gw | Groundwater delay time (days) | 0 to 70 | 47 |
| GWQMN.gw | Threshold depth of water in the shallow aquifer required for return flow to occur (mm $H_2O$) | 0 to 1900 | 447 |
| RCHRG_DP.gw | Deep aquifer percolation fraction | 0 to 0.6 | 0.23 |
| REVAPMN.gw | Threshold depth of water in the shallow aquifer for "revap" to occur | 0 to 400 | 245 |
| TIMP.bsn | Snow pack temperature lag factor | 0 to 1 | 0.315 |
| SMTMP.bsn | Snow melt base temperature (˚C) | -3 to 3 | 1.3 |
| SFTMP.bsn | Snowfall temperature (˚C) | -3 to 3 | -1.6 |
| SMFMX.bsn | Melt factor for snow on June 21 (mm $H_2O$/˚C-day) | -1 to 10 | 2.4 |
| SMFMN.bsn | Melt factor for snow on December 21 (mm $H_2O$/˚C-day) | -1 to 10 | 6.5 |
| SNOCOVMX.bsn | Minimum snow water content for 100% snow cover (mm $H_2O$) | 0 to 100 | 8.8 |
| SNO50COV.bsn | Fraction of snow volume represented by SNOCOVMX that corresponds to 50% snow cover | 0 to 0.9 | 0.17 |
| DEPIMP.bsn | Depth to the impervious layer (mm) | 1500 to 3000 | 2967 |
| DDRAIN.bsn | Depth to the sub-surface drain (mm) | 750 to 900 | 841 |
| DRAIN_CO.bsn | Drainage coefficient (mm/day) | 10 to 51 | 16.5 |
| LATKSATF.bsn | Multiplication factor to determine lateral hydraulic conductivity (mm/h) | 0.01 to 4 | 1.87 |
| SSTMAXD.bsn | Static Maximum depressional storage (mm) | 0 to 25 | 24 |
| ESCO.hru | Soil evaporation compensation factor | 0 to 1 | 0.835 |
| EPCO.hru | Plant uptake compensation factor | 0 to 1 | 0.005 |
| CANMX.hru | Maximum canopy storage (mm $H_2O$) | 5 to 20 | 9.6 |
| SURLAG.hru | Surface runoff lag time in the HRU (days) | 0.01 to 6 | 5.9 |
| CN2.mgt | Initial SCS runoff curve number for moisture condition II | 30 to 85 | 51.2 |
| SOL_BD.sol | Soil bulk density (g/cm$^3$) | ± 25% [a] | 1.57-1.72 |
| SOL_AWC.sol | Available water capacity of the soil layer (mm $H_2O$/mm soil) | ± 25% [a] | 0.15-0.20 |
| SOL_KSAT.sol | Saturated Hydraulic Conductivity (mm/hr) | ± 25% [a] | 2.75-10 |

[a] For each soil parameter and layer the parameter was allowed to vary between ±25 percent of its original value

*Table A.3.* Soil profile details and calibration results. Brackets indicate the value before calibration

| Soil Layer | Cumulative Depth (mm) | Organic Matter (%) | Clay (%) | Sand (%) | Bulk Density (g/cm3) | Available Water Capacity (mm/mm) | Saturated Hydraulic Conductivity (mm/hr) |
|---|---|---|---|---|---|---|---|
| 1 | 300 | 2.1 | 21 | 35 | 1.72 (1.45) | 0.16 (0.15) | 10 (13.1) |
| 2 | 360 | 0.6 | 27 | 33 | 1.59 (1.41) | 0.17 (0.15) | 8 (8.38) |
| 3 | 480 | 0.5 | 38 | 25 | 1.57 (1.36) | 0.15 (0.14) | 4.4 (3.56) |
| 4 | 1100 | 0.1 | 28 | 20 | 1.61 (1.51) | 0.2 (0.16) | 2.75 (2.79) |

# APPENDIX B

Climate Characteristics in the Historic and Future Period

*Table B.4.* Average seasonal temperature and precipitation relative to the baseline period for each forcing scenario, two different periods showing the mean plus standard deviation.

| Variable | Season | Baseline | | RCP 4.5 | | | | RCP 8.5 | | | |
|---|---|---|---|---|---|---|---|---|---|---|---|
| | | 1990-2010 | | 2040-2060 | | 2080-2100 | | 2040-2060 | | 2080-2100 | |
| | | $\bar{x}$ | std | $\bar{x}$ | std | $\bar{x}$ | std | $\bar{x}$ | std | $\bar{x}$ | std |
| Temperature | Winter | -4.0 | 5.6 | -2.4 | 2.8 | -1.7 | 2.8 | -1.7 | 2.7 | 1.5 | 2.3 |
| | Spring | 6.9 | 7.5 | **8.0**[a] | **6.3** | 8.9 | 6.1 | 8.9 | 6.3 | 11.5 | 6.3 |
| | Summer | 19.8 | 3.4 | 21.3 | 2.0 | 22.0 | 2.0 | 22.5 | 2.0 | 25.5 | 2.1 |
| | Fall | 9.8 | 6.6 | 11.4 | 5.6 | 11.9 | 6.0 | 12.4 | 6.1 | 15.2 | 6.2 |
| | **Year** | 8.1 | 5.8 | 9.6 | 4.2 | 10.3 | 4.2 | 10.5 | 4.3 | 13.4 | 4.2 |
| Precipitation | Winter | 234 | 44 | 245 | 17 | **256**[b] | **19** | 248 | 25 | **288**[b] | **20** |
| | Spring | 234 | 45 | 247 | 33 | **260**[b] | **28** | 256 | 31 | **278**[b] | **33** |
| | Summer | 230 | 67 | 236 | 21 | 243 | 34 | 234 | 33 | 242 | 36 |
| | Fall | 264 | 84 | 283 | 31 | 270 | 33 | 264 | 33 | 269 | 44 |
| | ∑ **Year** | 962 | 153 | 1010 | 45 | 1028 | 45 | 1002 | 69 | 1076 | 85 |

[a] Not significantly different relative to the baseline $\alpha>0.05$
[b] Significantly different relative to the baseline $\alpha<0.05$

# APPENDIX C

Historic and Future Water Balance

*Table C.5.* Watershed annual average water balance changes relative to the historic period (1990-2010) for each climate projection in the ensembles future period (2080-2100).

| Scenario | | Precipitation | ET | Surface Runoff | Tile Flow | Interflow | Groundwater Flow | Transmission Loss | Snow Fall |
|---|---|---|---|---|---|---|---|---|---|
| Historic Sim. (1980-2100) | | 963 | 604 | 163 | 105 | 1.3 | 166 | 74 | 181 |
| RCP | GCM | +/- Change from present (2080-2100) | | | | | | | |
| 4.5 | INM-CM4 | 4 | 8 | -36 | 14 | 0.2 | 3 | -12 | -47 |
| | GFDL-ESM2M | 55 | 31 | -6 | 17 | 0.2 | 10 | -1 | -17 |
| | CanESM2 | 41 | 34 | -31 | 20 | 0.3 | 8 | -10 | -46 |
| | MPI-ESM-LR | 99 | 38 | 8 | 30 | 0.2 | 28 | 7 | -41 |
| | ACCESS1.3 | 128 | 61 | -8 | 40 | 0.4 | 28 | -4 | -71 |
| | Average | 65 | 34 | -15 | 24 | 0.2 | 16 | -4 | -44 |
| 8.5 | INM-CM4 | 51 | 37 | -46 | 28 | 0.4 | 13 | -16 | -90 |
| | MPI-ESM-LR | 156 | 71 | -20 | 56 | 0.6 | 36 | -9 | -100 |
| | CanESM2 | 91 | 70 | -45 | 32 | 0.4 | 11 | -19 | -79 |
| | ACCESS1.3 | 205 | 88 | -14 | 70 | 0.7 | 50 | -7 | -102 |
| | BNU-ESM | 70 | 64 | -74 | 34 | 0.6 | 15 | -30 | -145 |
| | Average | 115 | 66 | -40 | 44 | 0.5 | 25 | -16 | -103 |
| **Average All** | | **90** | **50** | **-27** | **34** | **0.4** | **20** | **-10** | **-74** |

# APPENDIX D

Parameter Values from Literature

*Table D.6.* Parameter values reported in the literature.

| Parameter Values Reported in Literature | | | |
|---|---|---|---|
| Name | Description | Fitted Values | Source |
| GW_REVAP.gw | Groundwater revap coefficient | 0.06, 0.19, 0.066 | Zhang et al. (2015), Zabaleta et al. (2014), Merriman et al. (2018) |
| ALPHA_BF.gw | Baseflow alpha factor | 0.64, 0.021 | Zhang et al. (2015), Zabaleta et al. (2014) |
| GW_DELAY.gw | Groundwater delay time (days) | 40, 14, 30 | Zabaleta et al. (2014), Merriman et al. (2018), El-khoury et al. (2015) |
| GWQMN.gw | Threshold depth of water in the shallow aquifer required for return flow to occur (mm $H_2O$) | 700, 618, 987 | Zabaleta et al. (2014), Malagó et al. (2017), Ikenberry et al. (2017) |
| RCHRG_DP.gw | Deep aquifer percolation fraction | 0, 0.09 | Zabaleta et al. (2014), Malagó et al. (2017) |
| REVAPMN.gw | Threshold depth of water in the shallow aquifer for "revap" to occur (mm) | 500, 196, 750 | Merriman et al. (2018), Malagó et al. (2017), Ikenberry et al. (2017) |
| TIMP.bsn | Snow pack temperature lag factor | 0.24, 0.6, 0.77 | Poon (2013), Moriasi et al. (2013), Ikenberry et al. (2017) |
| SMTMP.bsn | Snow melt base temperature (˚C) | 4.9, 0.31 | Merriman et al. (2018), Poon (2013) |
| SFTMP.bsn | Snowfall temperature (˚C) | 1.7, -4.46 | Merriman et al. (2018), Poon (2013) |
| SMFMX.bsn | Melt factor for snow on June 21 (mm $H_2O$/˚C-day) | 3.2, 3.72 | Merriman et al. (2018), Poon (2013) |
| SMFMN.bsn | Melt factor for snow on December 21 (mm $H_2O$/˚C-day) | 2.6, 2.72 | Merriman et al. (2018), Poon (2013) |
| SNOCOVMX.bsn | Minimum snow water content for 100% snow cover (mm $H_2O$) | 48, 102 | Merriman et al. (2018), Poon (2013) |
| SNO50COV.bsn | Fraction of snow volume represented by SNOCOVMX that corresponds to 50% snow cover | 0.05, 0.528 | Poon (2013), Moriasi et al. (2013) |
| DEPIMP.bsn | Depth to the impervious layer (mm) | 1300, 2900, 3100 | El-khoury et al. (2015), Guo et al. (2018), Malagó et al. (2017) |
| DRAIN_CO.bsn | Drainage coefficient (mm/day) | 51, 24, 10 | Moriasi et al. (2013), Malagó et al. (2017), Ikenberry et al. (2017) |
| LATKSATF.bsn | Multiplication factor to determine lateral hydraulic conductivity (mm/h) | 1-1.4, 3.8, 1.22 | Guo et al. (2018), Moriasi et al. (2013), Malagó et al. (2017) |
| SSTMAXD.bsn | Static Maximum depressional storage (mm) | 12 | Guo et al. (2018) |
| ESCO.hru | Soil evaporation compensation factor | 0.81, 0.9, 0.95 | Zhang et al. (2015), Zabaleta et al. (2014), Merriman et al. (2018) |
| EPCO.hru | Plant uptake compensation factor | 0.01-1, 0.001 | Stark and Moriasi (2009), Moriasi et al. (2013) |
| CANMX.hru | Maximum canopy storage (mm $H_2O$) | 8, 216.25 | Zabaleta et al. (2014), El-khoury et al. (2015) |
| SURLAG.hru | Surface runoff lag time in the HRU (days) | 1-6, 1, 0.3 | Stark and Moriasi (2009), Zabaleta et al. (2014), Guo et al. (2018) |
| OV_N.hru | Manning's "n" value for overland flow | 0.6 | Zabaleta et al. (2014) |
| CN2.mgt | Initial SCS runoff curve number for moisture condition II | 47-76, 65, -19% | Stark and Moriasi (2009), Zhang et al. (2015), Merriman et al. (2018) |
| SOL_BD.sol | Soil bulk density (g/cm$^3$) | 0.97 | Zhang et al. (2015) |
| SOL_AWC.sol | Available water capacity of the soil layer (mm $H_2O$/mm soil) | 0.25 | Zhang et al. (2015) |
| CH_K2.rte | Effective hydraulic conductivity in main channel alluvium (mm/hr) | 53.43, 100 | Zhang et al. (2015), Zabaleta et al. (2014) |
| CH_N2.rte | Manning's "n" value for the main channel | 0.03, 0.075 | Zhang et al. (2015), Merriman et al. (2018) |
| CH_K1.sub | Effective hydraulic conductivity in main channel alluvium (mm/hr) | 0.5, 12.8 | Stark and Moriasi (2009), Poon (2013) |
| ADJ_PKR.bsn | Peak rate adjustment factor for sediment routing in the subbasin | 0.5, 1.2 | Merriman et al. (2018), Guo et al. (2018) |
| SPEXP.bsn | Channel re-entrained exponent parameter | 1.5, 1.4 | Zabaleta et al. (2014), Merriman et al. (2018) |
| SPCON.bsn | Channel re-entrained linear parameter | 0.0001, 0.0008 | Zabaleta et al. (2014), Merriman et al. (2018) |

| | | | |
|---|---|---|---|
| PRF_BSN.bsn | Peak rate adjustment factor for sediment in the main channel | 1.8, 1.9 | Merriman et al. (2018), Me et al. (2015) |
| USLE_K().sol | USLE equation soil erodibility (K) factor | 0.35, 0.1 | Zabaleta et al. (2014), El-khoury et al. (2015) |
| USLE_P.mgt | USLE support practice factor | 1, 0.5 | El-khoury et al. (2015), Me et al. (2015) |
| CH_COV2.rte | Channel cover factor | 0.6 | Me et al. (2015) |
| CDN.bsn | Denitrification exponential rate coefficient | 0.317, 0.3, 0.06, 1.24 | Merriman et al. (2018), Me et al. (2015), Moriasi et al. (2013), Ikenberry et al. (2017) |
| SDNCO.bsn | Denitrification threshold water content | 0.991, 0.02 | Merriman et al. (2018), Me et al. (2015) |
| NPERCO.bsn | Nitrate percolation coefficient | 0.161, 0.0003, 0.15, 0.2 | Merriman et al. (2018), Me et al. (2015), Guo et al. (2018), Ikenberry et al. (2017) |
| N_UPDIS.bsn | Nitrogen uptake distribution parameter | 32.4, 0.5 | Merriman et al. (2018), Me et al. (2015) |
| BC1_BSN.bsn | Rate constant for biological oxidation of NH4 to NO2 in the reach at 20˚ C in well-aerated conditions (day-1) | 1, 4.15 | Me et al. (2015), El-khoury et al. (2015) |
| ANION_EXCL.sol | Fraction of porosity (void space) from which anions are excluded | 0.2, 0.50 | Merriman et al. (2018), Ikenberry et al. (2017) |
| CH_ONCO.rte | Organic nitrogen concentration in the channel (ppm) | 0.01 | Me et al. (2015) |
| BC4.swq | Rate constant for mineralization of organic P to dissolved P in the reach at 20˚ C (day-1) | 0.34, 0.3 | El-khoury et al. (2015), Me et al. (2015) |
| ERORGP.hru | Phosphorus enrichment ratio for loading with sediment | 0, 0.1, 2.5 | El-khoury et al. (2015), Malagó et al. (2017), Me et al. (2015) |
| P_UPDIS.bsn | Phosphorus uptake distribution parameter | 98.3, 0.5 | Merriman et al. (2018), Me et al. (2015) |
| PHOSKD.bsn | Phosphorus soil partitioning coefficient (m3/Mg) | 188, 5, 174 | Merriman et al. (2018), El-khoury et al. (2015), Me et al. (2015) |

## APPENDIX E

Water Balance for Two Different HRUs

*Table E.7.* Average annual water balance changes for two HRUs with different soil types in the historic and future period

| | HRU9 (1990-2010) | HRU13 (1990-2010) | HRU9 | HRU13 |
|---|---|---|---|---|
| Soil Texture | SiCL | SiL | Change in water balance component in 2080-2100 | |
| Clay | 29 | 18 | | |
| Sand | 25 | 38 | | |
| Hydrologic group | C | B | | |
| Precipitation (mm) | 964.8 | 964.8 | 91.1 | 91.1 |
| ET (mm) | 628.9 | 624.6 | 53.0 | 53.3 |
| Surface runoff (mm) | 199.3 | 172.3 | -67.7 | -91.0 |
| Tile Flow (mm) | 113.8 | 106.0 | 84.1 | 80.8 |
| Percolation (mm) | 24.0 | 60.8 | 20.4 | 45.5 |
| Transmission loss (mm) | 93.5 | 82.8 | -27.1 | -42.1 |
| Interflow (mm) | 0.0 | 2.5 | 0.0 | 1.2 |
| Groundwater (mm) | 73.3 | 89.5 | -4.2 | 2.2 |